AN EXAMINATION OF THE SNOW AND AVALANCHE HAZARD ON THE MILFORD ROAD, FIORDLAND, NEW ZEALAND

A thesis

submitted in partial fulfilment

of the requirements of the

Degree of

**Doctor of Philosophy in Geography**

in the

University of Canterbury

by

Jordy Hendrikx

University of Canterbury

2005

Frontispiece –Head of the Cleddau Valley on the western side of the Homer Tunnel, showing the Milford Road below the steep avalanche paths

Acknowledgements

In completing this thesis I am aware of all the people who have helped me in some way over the last few years, I will mention a few in particular.

First and foremost, a huge 'thank you' is owed to Associate Professor Ian Owens who inspired me and provided encouragement and guidance along the way. I have really appreciated your support, friendship and patience, especially as you waded through my numerous drafts for papers and chapters. I also want to thank you for believing in me and giving me this opportunity to undertake this research work on the Milford Road, a project that I know is dear to you. Cheers Ian, I owe you one. I would also like to extend a thank you especially to Research Professor Howard Conway a.k.a. 'Twit" and to my other associate supervisors, Dr. Andy Kliskey and Dr. Clive Sabel.

Others in the Geography Department have also been great to me, with help coming from all sides, including, Justin and Nick for finding and building field gear, John, Steven and Graham for technical IT support and data manipulation, Gillian Blackler for proof reading, Jeff Wilson for putting up with me in the office, and all the other staff and PhD students for generating such a great working environment.

A significant amount of my time was spent in Te Anau on or above the Milford Road working alongside the staff of Works Infrastructure. I would like to thank Ann and Wayne Carran for their help and access to data, without their ongoing effort, and the effort of all the other people that have worked on the Milford Road, this data would not be available. A big thank you also to Ian Wilkins, Alistair Pearce and Rosie Pearce who made working and living in Te Anau such a great experience.

On a personal note I would like to thank my family and friends who have always been there for me, especially my mother who always provided encouragement and support and

my partner Sarah Tammik, who in the last year has really supported me after long days in the office.

Abstract

Avalanches pose a significant natural hazard in many parts of the world. Worldwide the hazard is being managed in a number of new and traditional methods. In New Zealand, the Milford Road, Fiordland, has a significant avalanche problem which has been managed by the Transit New Zealand Milford Road Avalanche Programme since 1984. This avalanche programme has generated a database of all avalanche occurrences and associated meteorological parameters for the time period 1985 to 2002. Elsewhere around the world, similar and more extensive data sets have been used to examine a wide variety of aspects in relation to the snow cover, avalanching and avalanche hazard. The availability of the Milford Road database has provided the opportunity use new and traditional approaches to examine many aspects of avalanching including; the trends in and relationships with the snow and avalanche regime, evaluation of the avalanche hazard, statistical forecasting of avalanches and the visualisation of avalanche occurrence information in a GIS.

Statistical and graphical examination of the inter-annual variation in the snow and avalanche regime revealed relationships between the snow depth, avalanche occurrences and atmospheric circulation similar to those found elsewhere around the world, but not previously examined in New Zealand. Furthermore, the analysis resulted in strong correlations despite using a database significantly shorter than those used elsewhere. Atmospheric circulation types that bring strong winds and precipitation were found to be highly significantly correlated with avalanche occurrences and snow depth. Avalanche occurrences were more highly correlated with atmospheric circulation than snow depth was, reflecting the strong maritime avalanche climate.

Risk evaluation was undertaken using two approaches, the avalanche hazard index (AHI) and the probability of death to individuals (PDI) method. The present avalanche risk was compared to a theoretically uncontrolled avalanche regime, using 2002 traffic volumes

for AHI and PDI. The AHI analysis highlighted the reduction in the AHI resulting from the control programme, and the significantly lower AHI when compared to Rogers Pass, B.C., Canada. The PDI analysis using equations modified to allow for a range of consequences indicated that the Milford Road is similar in risk to roads in Switzerland, but is far more accessible, with fewer closed days. A new equation for PDI, which accounted for waiting traffic was derived, and suggested that the calculated risk was high and unacceptable compared to standards applied to other hazards.

Statistical forecasting using classification tree analysis has been successfully applied to avalanche forecasting in other climatic settings. This study has applied an extension to this technique through 10-fold cross validation to permit classification of an avalanche day in this direct action maritime climate. Using varying misclassification costs two classification trees were generated. The tree that used only wind speed and wind speed and precipitation combined in a temperature sensitive wind drift parameter obtained an overall accuracy of 78%, with correct prediction for an avalanche day at 86%. These predictor variables are considered to be the fundamental controls on avalanche forecasting in this climate, and coincide with important variables inferred from the atmospheric circulation analysis.

Following the investigation of various methods for the creation of a high resolution digital elevation model (DEM), a GIS was used for the visualisation and examination of avalanche occurrences. Similar to other studies, qualitative and quantitative analysis of the spatial distribution in terms of aspect of avalanche occurrences was undertaken using the GIS. Colour coding of occurrences highlighted the influence of two storm directions, while an excess ratio showed the clear influence of aspect on avalanche occurrences in relation to two dominant storm directions, avalanche size and avalanche paths. Furthermore, the GIS has many applications for operational forecasting, teaching and the maintenance of institutional memory for the avalanche programme.

Contents

List of Figures

List of Tables

List of symbols

Symbol	Definition	Units
a	Index for aspect of interest	
d	Length of time waiting vehicles are exposed to an avalanche	hours
i	Index for aspect class	
j	Index for avalanche type j_1 to j_5	
k	Index for avalanche type k_1 to k_4	
n	Number of avalanche paths	
t	The waiting period which is the time required for a member of the road crew to react, normally 2 hours.	hours
z	Number of passages per day	
AHI	Avalanche Hazard Index	
B	Mean number of passengers per vehicle	
$C:B$	Ratio of cars to buses	
CR	Collective risk	deaths year^{-1}
CR_w	Collective risk including waiting traffic	deaths year^{-1}
D	Stopping distance on a snow-covered road for a vehicle with the speed V	m
F	Average frequency of avalanche occurrence	year^{-1}
I	Length of record or interval	years
IR	Individual risk	deaths year^{-1}
IR_w	Individual risk including waiting traffic	deaths year^{-1}
L	Average length of the road covered by the avalanche	m or km
L_v	The average length of road each vehicle occupies on a public road, normally 15 m.	m
L_w	Length of a queue of traffic	m
N_w	Number of vehicles in the adjacent avalanche track	
P	Probability of an event with a return period R occurring within a record of length I.	
$P´_s$	Probability of a second avalanche running along a given path	
$P’_w$	Encounter probability for waiting traffic in the same path	
PDI	Probability of Death to Individuals	deaths year^{-1}
P_m	Encounter probability for moving vehicles	year^{-1}
P_s	Probability of a subsequent avalanche in an adjacent or another part of the same path	
P_w	Encounter probability for waiting traffic	year^{-1}
R	Return period of avalanche occurrence	years
R	Return period of an event within a record	years
S	The safe waiting distance between avalanche paths	m
T	Daily traffic volume per 24 hour counted in both directions	vehicles d^{-1}
V	Average speed of the traffic	ms^{-1} or kmh^{-1}
W	Weighting for avalanche type j or k	
β_B	Number of passengers per bus	

β_C	Number of passengers per car
λ	Probability of death in a vehicle hit by an avalanche
Λ	Number of avalanche paths in aspect class i
Φ	Number of avalanche occurrences in aspect class i

1.0 Introduction

1.1 Background

The Milford Road (State Highway-94), New Zealand, which runs between Te Anau and Milford Sound has as severe an avalanche problem as any mountain highway in the world (LaChapelle, 1979). Over approximately the last thirty years the traffic volumes and hence the level of hazard has varied from relatively low in the 1970s to much higher numbers at the present. LaChapelle(1979) considered the hazard to be low to moderate but recommended that the avalanche terrain be mapped and the level of hazard assessed. Fitzharris and Owens(1980) undertook this with funding from the New Zealand Mountain Safety Council, and they also recommended improvements in data gathering, traffic control and avalanche forecasting and control. Following the death of a roading overseer in 1983, authorities initiated a formal programme of weather and snowpack monitoring and avalanche hazard control in 1984 (Weir, 1998). An experienced avalanche forecaster was employed, high level weather stations were upgraded, stricter control of traffic was maintained and helicopter bombing for artificial release of avalanches was introduced. A standardised procedure for recording avalanche occurrences, snow and weather data gathering was adopted and these data have now been loaded into an MS Access relational database (Carran, pers. comm., 2002; Owens, pers. comm., 2002). This was the inception of the Transit New Zealand Milford Road Avalanche Programme, charged with managing the avalanche hazard on the Milford Road.

This thesis will utilise this extensive database of avalanche and meteorological parameters to examine various aspects of avalanching on the Milford Road. While there has been a significant amount of previous work on the Milford Road examining various aspects of avalanching (e.g. Smith, 1947; Conway, 1977; Fitzharris and Owens, 1980; Fitzharris and Owens, 1984; Petrie, 1984; McLauchlan, 1995; Weir, 1998; Föhn, 1999;

Carran et al., 2000; Conway et al., 2000; Conway et al., 2002), there is now an opportunity to use a significant amount of historical data to document and develop further understanding of the snow and avalanche regime. Using the database and new techniques in risk evaluation, statistical avalanche forecasting, and in conjunction with topographic data in a Geographical Information System (GIS), there is further opportunity to re-enumerate the hazard, improve avalanche forecasting and visualise avalanche data under varying meteorological conditions.

Fitzharris et al.(1999) identified the lack of research undertaken on seasonal snow in New Zealand, especially when compared to glaciers. This reflects the lack of long term basic data collection exemplified by the fact that there are only three different snow courses, which are all located far from the main divide, in the low precipitation eastern areas. Fortunately, hourly snow depth has been measured at one location above the Milford Road since 1989. These snow depth data may permit the documentation and examination of temporal snow depth trends at a location, close to, and west of the main divide. Linkages between atmospheric circulation patterns or synoptic classifications have been used to explain changes in glacier behaviour in New Zealand (Clare et al., 2002), or linked directly with snow melt (Grundstein, 2003), snow deposition (Laternser and Schneebeli, 2003) and heavy avalanche seasons (Schneebeli et al., 1997) elsewhere around the world. In New Zealand, other than Kelly(1992) and de Lautour(1999) using modelled snow depth, no work has examined the relationship of seasonal snow depth to atmospheric circulation patterns or daily synoptic classification schemes. Furthermore, except for individual storms the relationship between avalanche occurrences and atmospheric circulation patterns has not been examined in New Zealand.

Risk analyses have been conducted for the Milford Road using the Avalanche Hazard Index (AHI) (Fitzharris and Owens, 1980) and the Probability of Death for an Individual (PDI) method, (Weir, 1998). Fitzharris and Owens(1980) provided a base line for the hazard assessment, estimating magnitudes and frequency of avalanche occurrences from a wide range of sources. Weir(1998) using the PDI method attempted to enumerate the risk to an individual on the Milford Road. Unfortunately, Weir(1998) used rather

subjective, poorly constrained probability assumptions which led to a high PDI, equivalent to those experienced by an individual partaking in white water rafting. Margreth et al.(2003) devised a set of equations to calculate PDI, and applied them to several alpine pass roads in Switzerland. The calculations by Margreth et al.(2003) were then used to examine the acceptability of the risk on those pass roads in Switzerland. With increasing traffic volumes on the Milford Road (URS, 2004), and a database of open road avalanches, the open road PDI and AHI can now more accurately be enumerated and compared to other locations around the world.

With increasing traffic volumes the potential consequences of an avalanche on an open road also increases. Combined with increased pressure to keep the road open for tourism and the fishing industry, there is a clear need to examine options for improving forecasting techniques and accuracy. While physically based models such as SNOSS have been developed by Conway et al.(2000), there has been no attempt at statistical forecasting. Buser(1983; 1989) promoted the nearest neighbour method as a non-parametric approach to forecasting avalanches. However, this requires a very large database of avalanche occurrences. An alternative method using Classification and Regression Trees (C&RT) has been proven to work on smaller data sets, and the interpretations of complex interactions are clearer and often more easily understood than other model constructions (Davis et al., 1999). These properties make C&RT an ideal option for operational avalanche forecasting.

Although the Transit New Zealand Milford Road Avalanche Programme has been managing the avalanche hazard and collecting an ever increasing range of data on avalanche occurrences, there are still some major deficiencies. Most significant among these is the inability of the MS Access database of avalanche occurrences to provide a visual representation of avalanche incidence and extent. An interface to a Geographic Information System (GIS) would go a considerable way towards addressing this deficiency. GIS's have been applied to reconnaissance mapping of avalanche terrain in Europe (Toppe, 1987; Furdada et al., 1995; Ghinoi, 2003) and in New Zealand (Briggs, 1997). However, their application in connection with avalanche hazard management and

visualisation of avalanche data (Marti et al., 1997; Gruber, 2001; Tracy, 2001; Maggioni et al., 2002; McCollister et al. 2002; 2003) is quite recent and often lacks both temporal and spatial resolution. With the development of new methods to obtain high quality topographic data, there is now a clear opportunity to visualise data on avalanche occurrences and relate these to meteorological and topographic data at a very high spatial resolution.

1.2   Research Aims

As outlined above, while there has already been a significant amount of research relating to avalanching on the Milford Road, a review of recent international work reveals that there are some deficiencies that should be addressed. In addition, there is a need to verify results of research on the Milford Road that was completed up to 25 years ago. Consequently, this thesis will:

❋ Examine the intra- and inter-annual variation of snow depth for a high level site along the Milford Road and the year-to-year variation of avalanche activity, investigate their inter-relationships and analyse the possible influence of atmospheric circulation and synoptic patterns on these variables.

❋ Apply and modify previously developed techniques of avalanche hazard estimation to allow comparison with other avalanche affected roads internationally, and with risks associated with other types of hazards.

❋ Use historical data to create a statistical forecasting tool or model to predict avalanche occurrences on the Milford Road.

❋ Create a GIS to visualise spatial historical avalanche data, to obtain an improved understanding of the spatial distribution of avalanching and to contribute to the maintenance of institutional memory.

The underlying aim of the thesis which is embodied in all of these above aims is to document and obtain a better understanding of the avalanche regime on the Milford Road.

1.3 Thesis Outline

As outlined above, the main focus of this thesis is the examination of avalanching on the Milford Road. This focus will be split into various sub foci, addressing the main aims, within the following chapters.

Chapter Two provides a background to the area and a context to the research undertaken. This chapter profiles the history of the Milford Road and highlights recent developments in the research aimed at gaining a better understanding of avalanching on the Milford Road. A summary and outline of the data collected is also provided. Associated factors such as the weather and geomorphology as well as increasing tourist numbers and seasonal timing of tourists are also considered.

Chapter Three investigates and documents the available snow and avalanche data and comments on trends, both intra- and inter-annual. Relationships between avalanche and snow depth are examined, as well as relationships between atmospheric circulation patterns, snow depths, and avalanche occurrences. Trends in avalanche occurrences and snow depth are related to atmospheric circulation patterns, and anthropogenic influences and pressures.

Chapter Four uses the database of avalanche occurrences and traffic statistics to examine the risk on the Milford Road. The risk is enumerated using two methods, the Avalanche Hazard Index (AHI) and the probability of death to individuals (PDI). Following a brief review of these methods, calculations are presented for a theoretically uncontrolled Milford Road and the current day, managed Milford Road. The results of these analyses

are compared to results internationally and a new equation for PDI, which accounts of waiting traffic, is formulated to allow comparison with other hazards.

Chapter Five takes a data mining approach, using classification trees for avalanche forecasting. A statistical analysis of meteorological variables using classification trees is undertaken, with the aim of determining, and potentially forecasting, significant avalanche activity.

Chapter Six links avalanche occurrences, meteorological data, a high resolution digital elevation model (DEM), and spatial distribution information in a GIS, which in turn allows for the visualisation of the spatial distribution of avalanche occurrences under a range of different scenarios. The distribution of avalanches occurrences is examined both qualitatively using the GIS and quantitatively using an excess ratio.

Chapter Seven summarises the main findings from the preceding four chapters. This chapter also highlights the clear linkages between the chapters and suggests the directions of future research into avalanching and hazard management on the Milford Road.

2.0 Setting & avalanche hazard management

2.1 Introduction

This chapter provides a background and context to the Milford Road region and the research undertaken. The history and current day practices are outlined, while the pressures and challenges are highlighted.

2.2 Location, exploration and road building

The Milford Road (State Highway-94) is located in the southwest of the South Island of New Zealand. It is the only public highway with a significant avalanche problem in New Zealand. The road extends for 119km from Te Anau to Milford Sound - *Piopiotahi* through Fiordland National Park which is part of *Te Wāhipounamu* - Southwest New Zealand World Heritage Area (Figure 2.1).

The overland route to Milford Sound via the Hollyford and Cleddau Valleys and the Homer Saddle was discovered in 1889 by William Homer and George Barber (Figure 2.2). They were convinced that this was the best overland route through to Milford Sound, and they began pushing for the construction of a tunnel. This was further supported by increasing numbers of walkers on the Milford Track having to return the same way. The projected tunnel was shelved until almost half a century later when during the depression years large numbers of roads were constructed to provide work for the unemployed (Anderson, 1990). In 1934, parliamentary approval was given to build a tunnel, 7m wide and 5m high, linking the Hollyford Valley on the east and the Cleddau Valley on the west. The danger posed from avalanches was made obvious to the workers on the Milford Road with three fatalities occurring within the first two years of construction. The tunnel was finally completed, following stoppages because of World War Two in 1953. It is 1.25km in length and runs in a downward grade from the eastern portal entrance at 925m to the western portal at 790m (Petrie, 1984) (Figure 2.2).
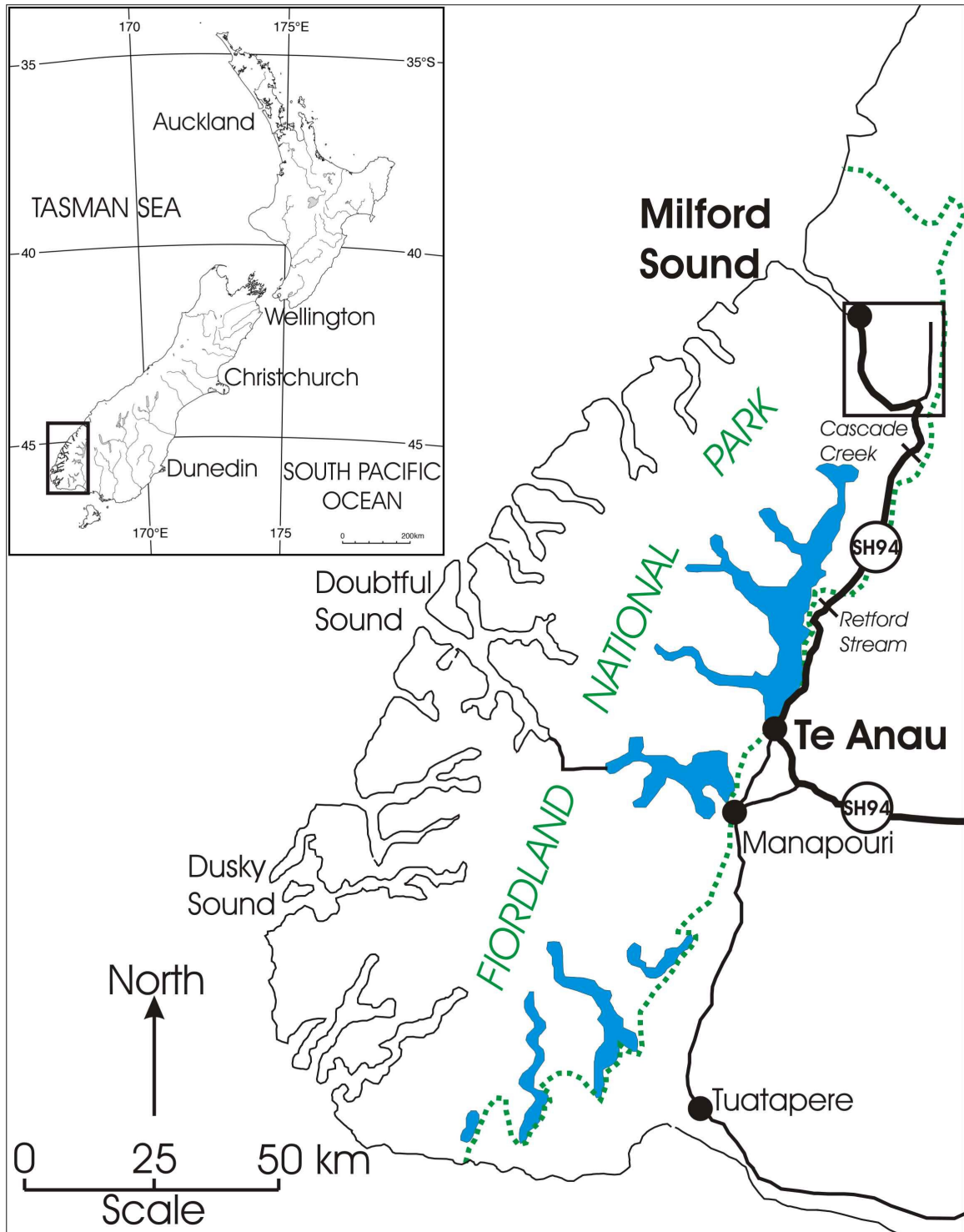
Figure 2.1   Location Map of the Milford Road (SH94) from Te Anau to Milford Sound and the Fiordland National Park. The avalanche area, as denoted by the rectangle north of Cascade Creek and south of Milford Sound, can be seen in more detail in Figure 2.2.
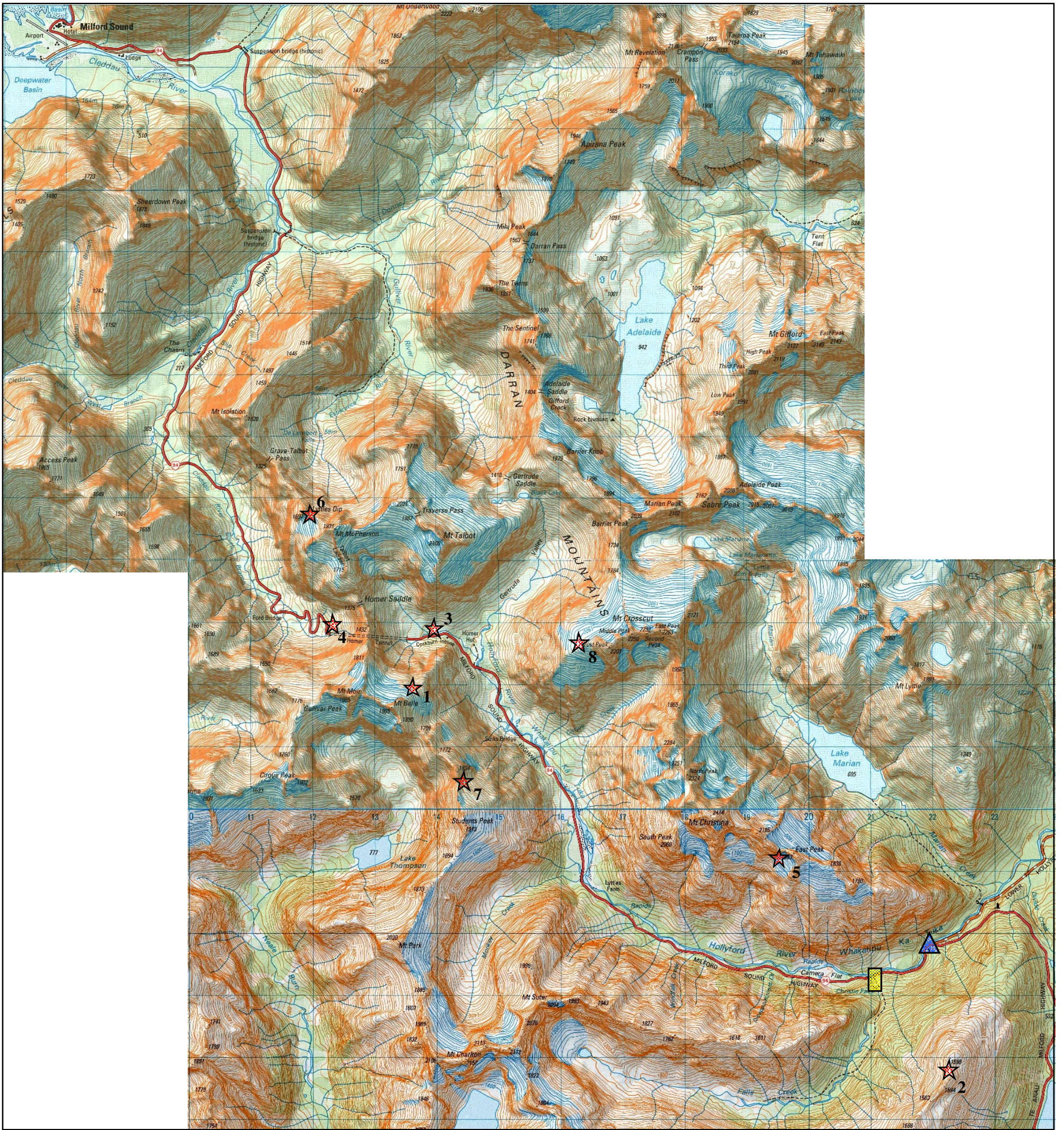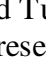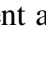
Figure 2.2   The approximate locations of the 8 sites for snow and meteorological measurements, marked with ⭐, on and above the Milford Road. Where: 1 = Mt Belle AWS, 2 = Consolation Peak AWS, 3 = East Homer AWS, 4 = West Homer AWS, 5 = Gates Snow Pole, 6 = Cleddau AWS, 7 = Rover AWS, 8 = Crosscut Hut. The blue triangle 🔺 marks the Hollyford Turnoff, while the Yellow rectangle ▯ marks the Transit New Zealand traffic counter site, Falls Creek. Gridlines on the map represent a 1km x 1km grid, or an approximate scale of 1:75,000. (Source: Land Information New Zealand, 1994; 1995).

From the opening of the tunnel in 1954 until 1961 Milford Sound was considered a summer destination. During the winter the road into Milford was closed at the Hollyford turnoff and no maintenance was undertaken. Snow was allowed to build up, and avalanches released naturally without incident. In 1962, under increasing pressure from the tourism industry the Ministry of Works operated a conservative approach and only opened the road in winters when they considered it safe. At first the tourism industry accepted closures but as the demand for winter tourism grew, the operators became less tolerant of frequent winter closures (Ede, 1988).

2.3   Geology, geomorphology and vegetation

In the Fiordland area, intense heat and pressure about 500 million years ago caused the formation of gneiss, schist and granite rocks. These rocks have been thrust upwards by folding of the crust and fragmented by faulting. Darran diorite of lower Permian to Cambrian in age (Wood, 1960), is the dominant rock type in the avalanche area. The Fiordland region is shaped mainly from the effects of Pleistocene glaciations, with features persisting in the landscape because of the highly erosion resistant bedrock (Owens and Fitzharris, 1989). In the last one million years the Fiordland region has seen three major glaciations, but it is the last, the Otiran from about 70,000 to 15,000 years before present that has the most obvious effect. The Hollyford and Cleddau Rivers occupy valleys excavated by glacier ice during the Otiran Glaciation (Suggate, 1990). The resulting landscape is one of over-steepened valley sides with extensive, occasionally permanent snowfields perched above (Owens and Fitzharris, 1985) (Figure 2.3).

Due to this over steepening caused by the glacial history, avalanche paths have tracks with an average slope of approximately 50°, considerably steeper than that of most other areas (Fitzharris and Owens, 1980). The avalanche track is defined as the area between the starting zone, or area of avalanche initiation, and the run out zone, the area of deposition. These tracks are also unusual because they are steeper than the starting zones (Fitzharris and Owens, 1980). The steep slopes of the avalanche tracks cause the formation of avalanche tarns at the base of the steeper avalanche paths. Due to the rapid

change in slope between starting zone and track, avalanches often become airborne and can free fall over 1000m, from some starting zones of over 2000m a.s.l. down to the valley floors at less than 900m a.s.l. (Figure 2.2). The tarns are formed from avalanche impact where there is an abrupt change of angle with the valley floor (Fitzharris and Owens, 1984).
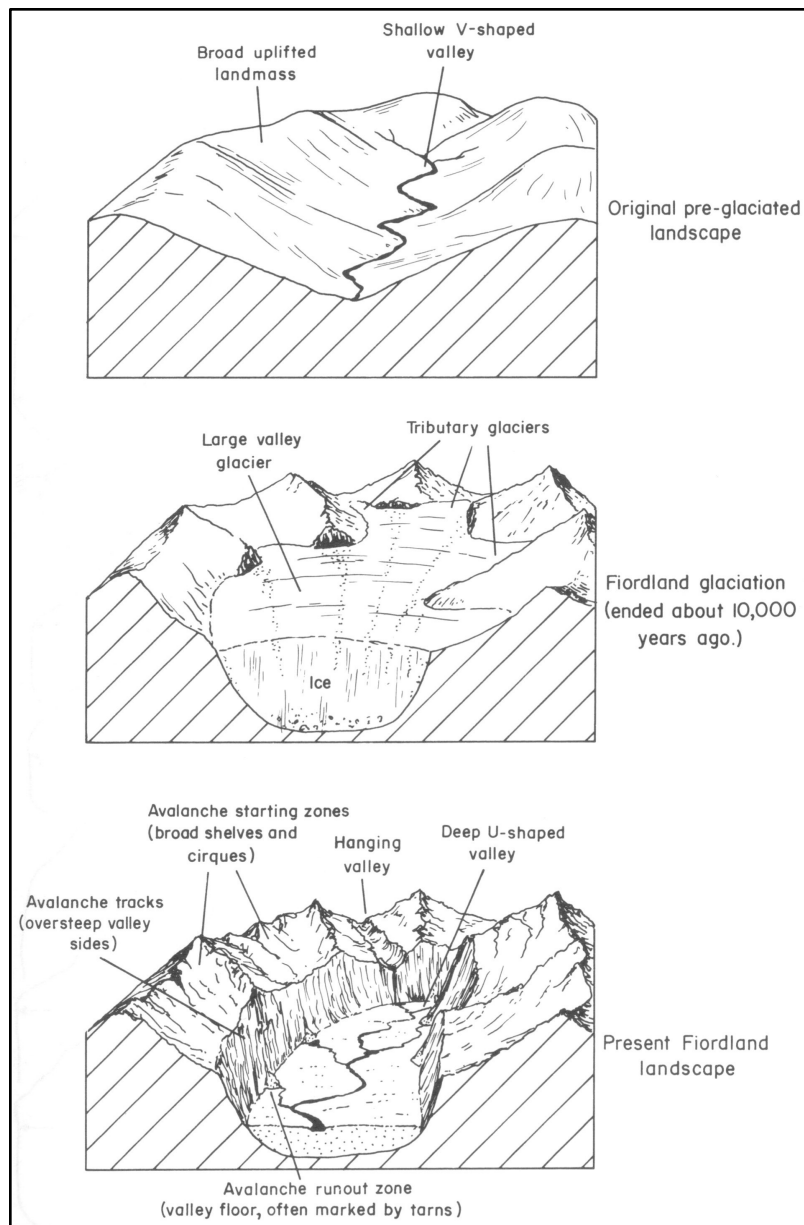
Figure 2.3   Schematic diagram showing how the retreat of ice from the last glaciation has led to the formation of the steep sided U-shaped valleys of Fiordland (Source: Owens and Fitzharris, 1985, p.7).

The vegetation is mainly mountain and silver beech (*Nothofagus solandri* var. *cliffortioides* and *N. menziesii*) with a timber line at approximately 1000m in the east, lowering to about 900m in the west (Owens and Fitzharris, 1989). The timberline elevation restricts vegetation to the valley bottoms, leaving sparsely vegetated avalanche tracks, and tussock and bare rock in avalanche starting zones. The vegetation in the valley bottoms has been used in dendrochronology for extending estimates of size and frequency of past avalanche occurrences (Conway, 1977; Fitzharris and Owens, 1980; McLauchlan, 1995).

2.4   Climate

The climate of Fiordland is dominated by frequent strong moisture laden mid-latitude westerlies from the Tasman Sea. Fiordland is at the southern reaches of the northeast-southwest orientated Southern Alps of New Zealand. The western and central parts of the Southern Alps experience an extreme maritime climate with strong winds and heavy precipitation as they are aligned almost perpendicular to the prevailing westerly winds blowing across a large ocean expanse (Sturman and Tapper, 1996; Sturman and Wanner, 2001).

Fiordland is a region of extremely high, though spatially variable rainfall with high precipitation westerly and low precipitation easterly zones (Figure 2.4). The precipitation ranges from a maximum mean annual rainfall of 10,000mm in the west to 1,000mm in the east (Owens and Fitzharris, 1989) mainly because of orographic forcing of the prevailing westerly winds. This is highlighted when examining the data for Manapouri and Milford Sound for the period 1971 to 2000 (Figure 2.5). Manapouri is 15km south of Te Anau on the eastern side of Fiordland and has an average annual precipitation sum of 1164mm, with on average 129 wet days (greater than 1mm of precipitation) (NIWA, 2003). The wettest month on average is October with 131mm, and the driest is January with 89mm (NIWA, 2003). Milford Sound on the coast on the western side of Fiordland has an average annual precipitation sum of 6749mm, with on average 186 wet days

(greater than 1mm of precipitation) (NIWA, 2003). The wettest month on average is January with 717mm, and driest is July with 418mm (NIWA, 2003). Petrie(1984), analysing earlier records commented on the considerable inter-annual variability in precipitation at Milford Sound, with a maximum annual sum of 8368mm, and a minimum of 4244mm. Maximum 24 hour precipitation at Milford Sound has been recorded at 520mm and on average wettest day at Milford Sound each year is 297mm. Significant avalanching occurs in Fiordland because of the over-steepened terrain combined with this very heavy precipitation (Owens and Fitzharris, 1985), and with winter storms depositing up to 2m of snow in the starting zones (Conway et al., 2000). The ability of precipitation to fall as snow with such high intensity is a very significant component of the Fiordland climate.
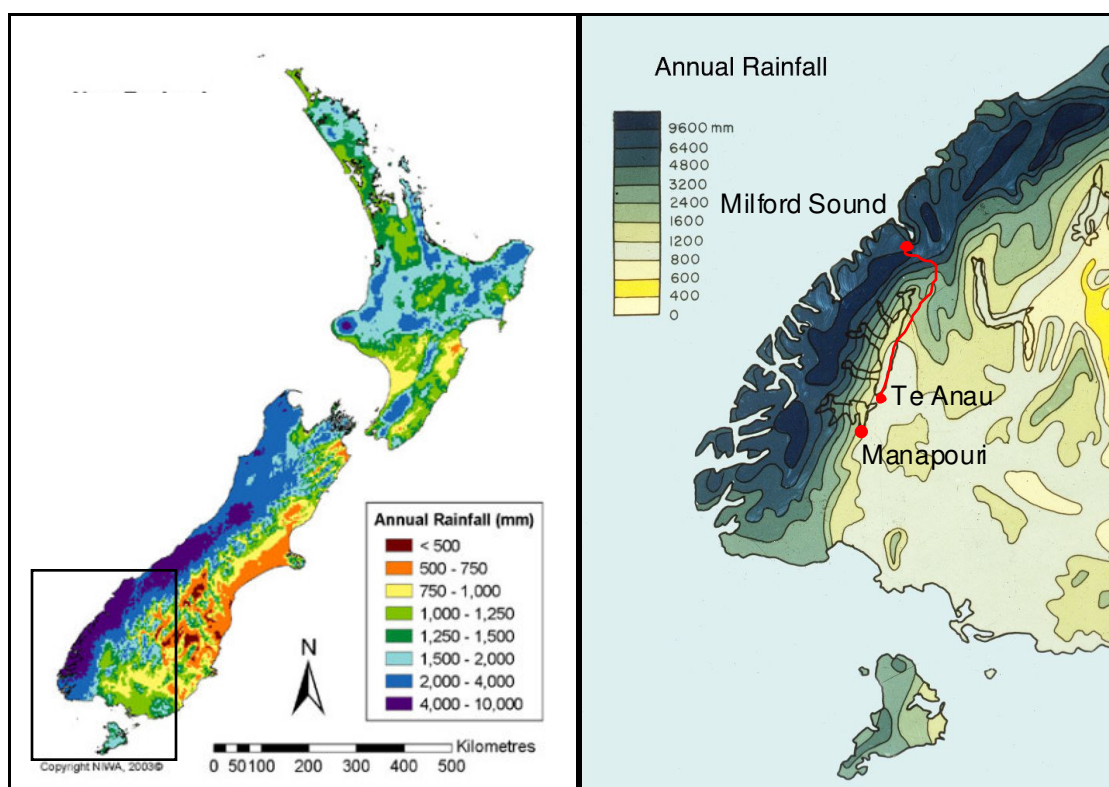
Figure 2.4   Mean annual rainfall (mm) for New Zealand for 1971-2000 (Source: NIWA, 2003) Left, with inset of the Fiordland region mean annual rainfall (mm) (Source: New Zealand Meteorological Service, 1984, p.10) Right.
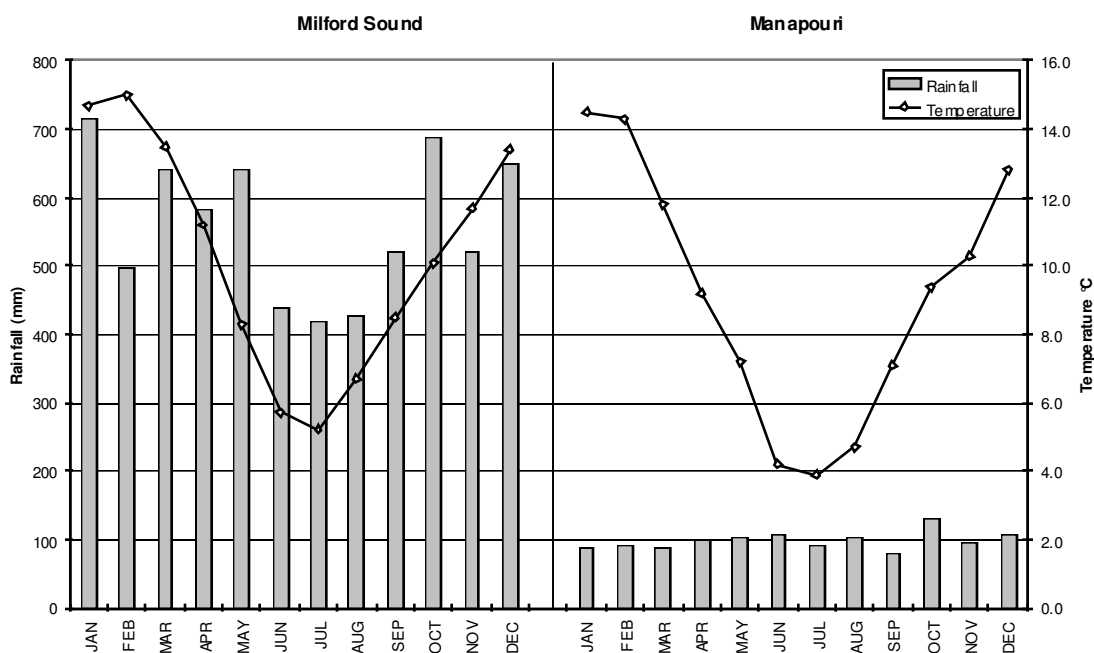
Figure 2.5   Mean monthly rainfall and temperature trends at Milford Sound on the west of Fiordland and on the east at Manapouri (Source: NIWA, 2003).

Temperatures in the starting zones are relatively warm and rain can occur to high levels at any time during the winter, but occurs less frequently in July and August (Fitzharris and Owens, 1980). This produces a relatively deep, dense snowpack with multiple ice layers, because of the fluctuating freezing levels and frequent thick layers of heavily rimed snow or graupel (Owens and Fitzharris, 1989). The snowpack reflects the maritime location, in that winter temperatures are warmer than for similar latitudes and elevations in the northern hemisphere. This results in a winter snowline of approximately 1000m at or close to the timberline elevation.

The Fiordland climate is also characterised by rapid changes associated with cold front onset and passage. A typical storm begins with the approach of a moisture laden westerly or northwesterly airflow preceding a cold front. As the storm progresses the passing of the front is typically marked by a sudden wind change from northwest to south or southwest, strong gusty winds, and a drop in temperature and rise in relative humidity (Sturman and Wanner, 2001). Behind the front there is often cool calm and clear weather

with winds from the south. A typical storm cycle has duration of between two and seven days (Sturman and Tapper, 1996). New Zealand also regularly experiences blocking anticyclones, which can disturb the storm cycle for several days to weeks (Sturman and Wanner, 2001) and lead to calm settled periods.

2.5 Snow and avalanches

2.5.1 Avalanche hazard in New Zealand

Avalanches are common alpine phenomena in New Zealand, with a relatively high proportion of avalanche terrain and seasonal snow on relatively steep slopes covering approximately 35% of the South Island and about 5% of the North Island (Irwin and Owens, 2004). However, as there are no populated settlements in these areas, the actual avalanche hazard and number of fatalities in New Zealand has been relatively low. In recent decades there has been an increase in the number of fatalities, with 12 in the 1960s, 16 in the 1970s, 23 in the 1980s and 17 in the 1990s (Irwin and Owens, 2004). The majority of these fatalities have occurred while participating in alpine climbing, with only a few fatalities occurring in or close by a ski field. Despite providing easy access for climbers to dangerous avalanche terrain (as well as accommodation in the New Zealand Alpine Clubs Homer Hut, near the Homer Tunnel (Figure 2.2)), there has only been one avalanche climbing fatality in 1995, and none on the Milford Road since 1983.

2.5.2 Avalanche path morphology

Smith(1947), Fitzharris and Owens(1980; 1984), Owens and Fitzharris(1985; 1989) and Dingwall et al.(1989), all commented on the steep nature of the avalanche paths in Fiordland. Fitzharris and Owens(1984) highlighted that while starting zones and run outs of Fiordland are similar to elsewhere, the tracks are significantly steeper. Fitzharris and Owens(1980) documented 50 individual avalanche paths, some with multiple starting zones. Starting zones ranged in size from 0.008 to 0.861 km^2, with an average slope of

40°, ranging between 29° to 59° (Fitzharris and Owens, 1980). The elevation of the starting zones range between 1000m a.s.l. to 2500m a.s.l., with a significant grouping at around 1500m a.s.l., reflecting the influence of the edge of the glacial trough (Fitzharris and Owens, 1980). Runout zones have an average slope of 20°, but range between river flats at 0° to steep fans at 40°.

2.5.3 Avalanche characteristics

Supervising engineer on the Homer Tunnel H.W. Smith reported that the Hollyford and Cleddau Valleys "provide optimum conditions for avalanches, with large upper snowfields, steep valley walls and copious moisture saturated winds to keep up the snow supplies; consequently, the total count of avalanches often exceeds 100 per mile per year along sections of the valleys" (Smith, 1947, p.491). Smith(1947) described two types of avalanches on the Milford Road, wet and dry. Wet avalanches result from a thaw event, most commonly from July to November. Dry avalanches, while less frequent, occur from May to November and are normally accompanied by a destructive wind blast (Smith, 1947). The first three fatalities P.L. Overton in July 1936 and D.F. Hulse and T.W. Smith in May 1937 on the Milford Road during its construction, were due to the wind blast (Irwin et al., 2002). Smith(1947) also noted that the dry avalanches can on occasion free fall down the avalanche track landing with explosive impact forces (Figure 2.6). Fitzharris and Owens(1984) later identified avalanche tarns at the base of these tracks as a result of these forces. McLauchlan(1995) assessed impact pressures and velocities, finding velocities up to $83ms^{-1}$ ($288\ kmh^{-1}$) from large avalanches of size 5 on the 5 class Canadian size scale (McClung and Schaerer, 1993). McLauchlan(1995) also recorded high densities in the order of $650kgm^{-3}$ to $775kgm^{-3}$ in avalanche deposits. These are higher than typically recorded elsewhere, and are considered a consequence of the steep terrain and abundant snow (McLauchlan, 1995).
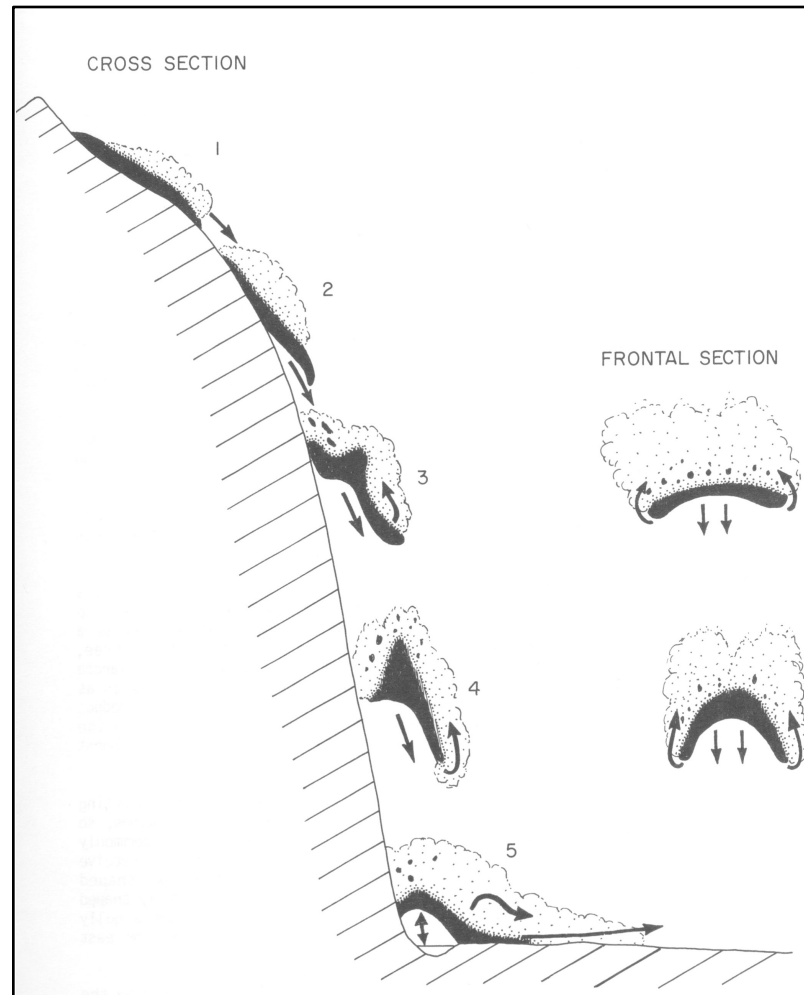
Figure 2.6   Sequence showing the probable fall of a large plunging avalanche in
               Fiordland (Source: Smith, 1947 [In] Owens and Fitzharris, 1985, p.9).

Petrie(1984) examined the spatial distribution of avalanching, considered 16 large events
and related these to synoptic weather records. Three main processes for large avalanches
were distinguished, rain on snow, snow overloading and thaw events. Rain on snow was
found to be associated with a northwesterly air stream on the western limb of an
anticyclone to the east of the South Island. Snow overloading events were associated with
a series of southerly fronts, often followed by a depression moving southwards and thaw
events were associated with a slow moving intense anticyclone crossing the South Island.
Petrie also found slopes with northeast aspects had the greatest amount of lee slope
loading, as they are subject to loading from a wider range of common wind directions.

More recent and ongoing observations show that avalanches on the Milford Road tend to be predominantly direct action avalanches, with the majority of avalanches occurring during or shortly following a storm cycle (Conway et al., 2000). A model known as SNOSS (Conway et al., 2000), which calculates the stress strength balance, works reasonably well because of this direct action nature of the avalanche regime. This is also observed in the examination of available fracture line profiles, where the weakness is most often found to be in the new snow. Climax avalanches do occur, but far less frequently, and predominantly towards the end of the avalanche season. Fitzharris(1979) working in the Mt Cook region to the east of the divide, suggested that approximately 90 percent of all avalanches occur during or shortly after a storm. In common with other maritime mountainous areas (e.g. Floyer and McClung, 2003), there is a lack of distinct wet and dry avalanche seasons (Smith, 1947; Fitzharris and Owens, 1980). While less frequent in July and August, rain can occur to high levels at any time during the winter. Rain on snow events can cause widespread avalanching (Conway and Raymond, 1993), and have been given special attention on the Milford Road with the development of a lysimeter to enable the measurement of percolation to the base of the snowpack (Carran et al., 2000).

2.6   Tourism and traffic

Fiordland National Park is part of the *Te Wāhipounamu* – Southwest New Zealand World Heritage Area. It is one of approximately 400 outstanding natural and cultural sites world wide which have been recognised by UNESCO (Department of Conservation, 2002). World heritage areas are designated under the World Heritage Convention because of their outstanding universal value (World Heritage Convention, 1972). In recent years Fiordland National Park has experienced a steady increase in visitor numbers and growth in both domestic and international tourism is forecast to continue (Department of Conservation, 2002).

Some of the most striking features of *Te Wāhipounamu* - Southwest New Zealand World Heritage Area are revealed along the Milford Road and in Milford Sound, the end point of the road. According to the Department of Conservation(2002) visitor use of the road has increased at a rate of about 7% annually and approximately 75% of road users are international visitors. The vast majority of visitors, almost 90%, travel the full length of the road from Te Anau to Milford Sound - *Piopiotahi* (Department of Conservation, 2002). The main reasons people use the road is to undertake a scenic cruise on Milford Sound - *Piopiotahi*, which is an internationally recognised icon tourist destination. In 2002, more than 410,000 people visited Milford Sound - *Piopiotahi*, up from 247,000 in 1992 (Department of Conservation, 2002). This is reflected in the traffic count data from the Department of Conservation(2002) of 230 return vehicle trips per day in 1992 to 370 return vehicle trips per day in 2002. Transit New Zealand(2002) also conducts traffic counts along the Milford Road (Figure 2.7), but it has been noted that there are some discrepancies in their data (URS, 2004). Foremost among these discrepancies is that the volume at Falls Creek / Cascade Creek site (Figure 2.1 and 2.2) is on an annual basis consistently much greater than at the Retford Stream site (Figure 2.1), which is closer to Te Anau. The reverse trend in traffic volumes would be expected. URS(2004) calculated an Average Annual Daily Traffic (AADT) value of 635 for 2003 with a mean growth of 5.3%. This equates to approximately 317 return vehicle trips per day, which is lower than the counts obtained by The Department of Conservation(2002). Calculations for the winter avalanche period, defined as mid June to mid December were 381 for 2003.
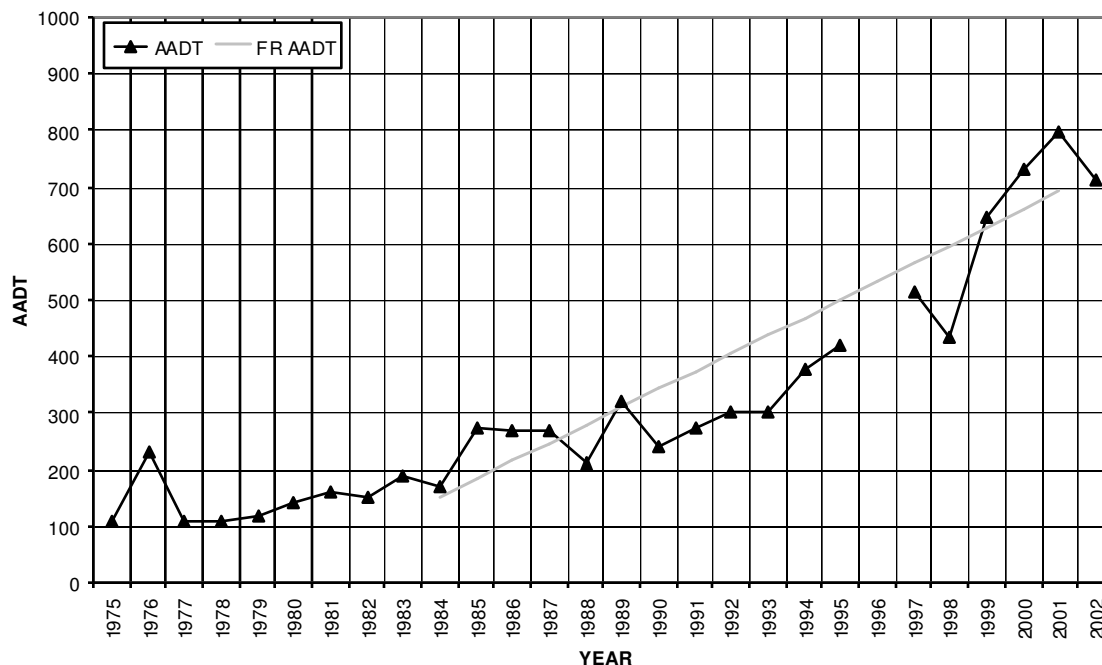
Figure 2.7   Transit New Zealand (2002) AADT for Falls Creek / Cascade Creek site on the Milford Road for the period 1975 to 2002. Forecasted (FR) AADT is calculated only for the period 1985 to 2002, and shows a growth rate of 5.3%.

The main visitor season for Fiordland National Park occurs from mid October until the end of April, peaking between January and March. This season may extend or contract dependent upon prevailing weather conditions (Department of Conservation, 2002). The Department of Conservation(2002) has noted a moderate increase in visitation to the major attractions of Fiordland National Park outside of the traditional visitor season, and have realised that the prominence of these shoulder periods may have implications for future visitor management. Kerr et al.(1990) suggested the need to encourage more tourism into the shoulder seasons, and this seems to have occurred. When examining the monthly Transit New Zealand AADT values for several years there is also a noticeable increase in numbers during the shoulder seasons (Figure 2.8). Of most concern from an avalanche safety viewpoint, is the increase in AADT from October onwards, as this often coincides with maximum snow accumulation, large rain on snow events, and the occurrence of the large climax type avalanches. Of further concern is the draft management plan for Fiordland National Park (Department of Conservation, 2002) in

which there is a suggested recommendation to set a limit of 4000 visitors per day to Milford Sound. If this limit were implemented it would increase and extend the high AADT values further into the shoulder seasons.
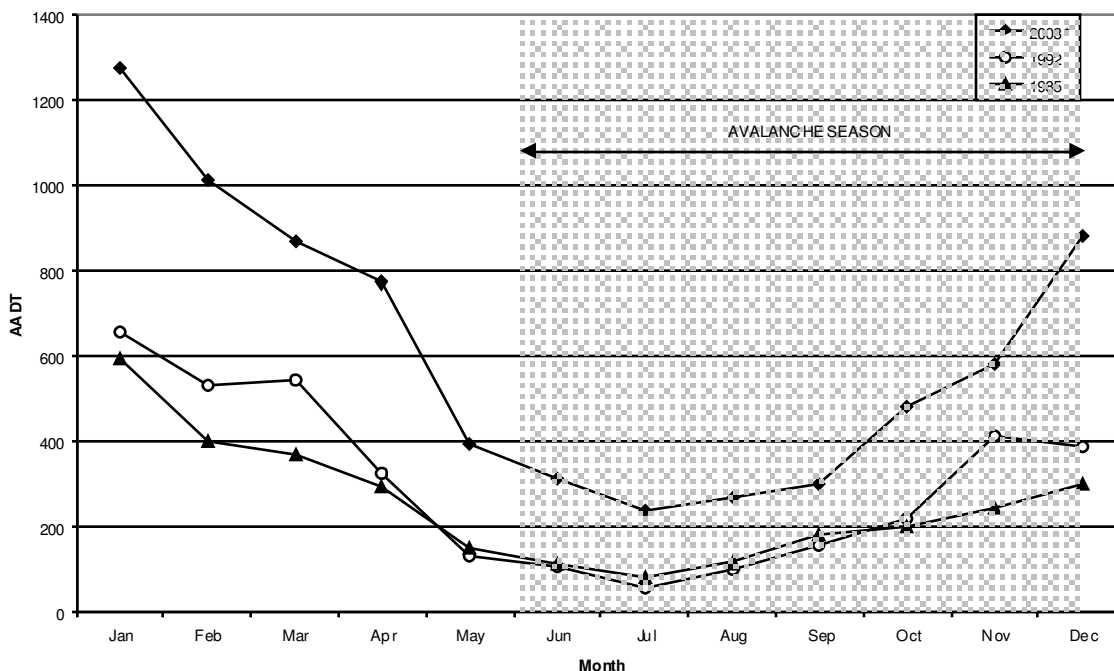
Figure 2.8   Monthly trends in Transit New Zealand AADT at Falls Creek / Cascade Creek site on the Milford Road, clearly showing the increased use of the shoulder seasons. Of greatest concern is the spring shoulder season, at the end of the avalanche season. *2003 data from Retford Stream site.

Travers Morgan(1995) noted that the effect of completing the sealing of the road in 1995 has caused a shift in independent travellers from using buses to cars. This has resulted in changing the types of vehicles on the road, as well as the total number. However, in 2003 there was still approximately 14% of the total traffic as buses, with over 100 buses per day during summer (URS, 2004). With the proposed alternative forms of transport from Queenstown, including the development of a gondola or monorail to the lower Of most concern from an avalanche safety and risk viewpoint, is that the daily traffic flow is strongly bimodal, causing periods of very high traffic concentrations in the mornings and the evenings. In the case of an incident, the resulting number of waiting vehicles

endangered by avalanches would be significantly greater than the AADT would suggest. This has been shown to be an important contributor to avalanche risk (Schaerer, 1989).

Tourism is now considered vital to New Zealand's economy, directly and indirectly contributing almost 10% of New Zealand's GDP and supporting one in ten jobs (Ministry of Tourism, 2005). Tourism is also very significant for the local and regional economy of Te Anau and Fiordland. Closure of the Milford Road disrupts tourist traffic and fishermen from Milford Sound, and has very serious financial implications for businesses in Milford and in Te Anau. In 1980, closure of the Milford Road was estimated to have cost $750,000 in lost revenue alone (Dingwall et al., 1989). Furthermore, an incident involving one or more tourist buses on the Milford Road has the potential to do severe medium term damage to New Zealand's tourism industry (Weir, 1998).

2.7   Avalanche hazard management

Professor Ed LaChapelle was invited by the New Zealand Mountain Safety Council to New Zealand in 1978 and noted that the Milford Road has as severe an avalanche problem as any other mountain highway in the world (LaChapelle, 1979). Following LaChapelle's recommendations the avalanche terrain was mapped and the level of hazard assessed by Fitzharris and Owens(1980) (Figure 2.9 and Table 2.1). They recommended that the roading authorities make improvements in data gathering, traffic control and avalanche forecasting and control on the Milford Road.

Table 2.1   1980 AHI for paths that effect the Milford Road (Source: Fitzharris and Owens, 1980, p 19).
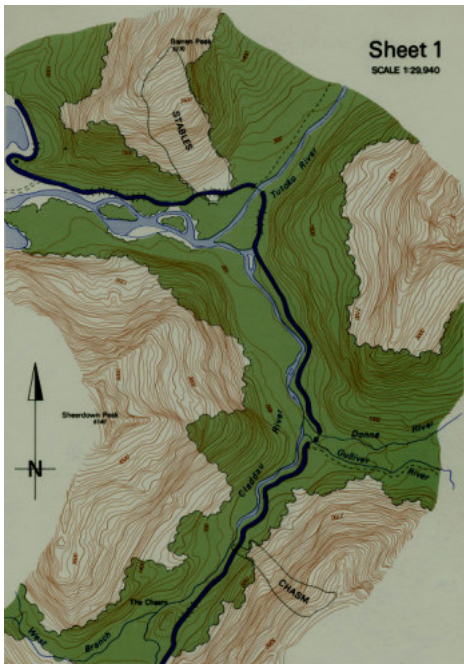
Path Name	Pm	Pw
Turnoff	0.001	0
Gates	0.086	0
Camera 1	0.001	0
Camera 2	0.001	0
Camera 3	0.001	0
East Peak 2	0.001	0
Christina 2	0.001	0.04
Windfall 1	0.008	0.36
Windfall 2	0.040	0.67
Powerhouse 1	0.001	0.05
Powerhouse 2	0.001	0.05
Powerhouse 3	0.006	0
Students Peak	0.400	4.98
North Peak 2	0.008	0.60
North Peak 3	0.010	0.83
Bakehouse	0.024	1.05
Crosscut 1	0.001	0.01
Crosscut 2	0.001	0.01
Crosscut 3	0.001	0
The Sinks	0.110	6.00
Raspberry Patch	0.520	2.20
Forks	0.002	0
Talbot	0.001	0
Homer Tunnel	0.400	11.60
Portal	0.006	0
Homer Saddle	0.004	0.10
Loop 1	0.016	12.00
West Tunnel	0.016	1.25
Moir	0.012	0.87
Gulliver 1	0.001	0.15
Gulliver 3	0.001	0
Gulliver 4	0.001	0
Loop 2	0.004	0
Cleddau	0.010	0
Morels	0.014	0.52
Dip 1	0.001	0
Dip 2	0.001	0
Big Rock	0.018	0
Schaerer	0.001	0
Chasm	0.001	0
Stables	0.016	0
TOTALS	**2**	**44**
TOTAL HAZARD INDEX = 46		

Figure 2.9   All avalanche paths mapped for the Milford Road (Source: Fitzharris and Owens, 1980, p.29-31).

On 23 September, 1983 Ministry of Works and Development overseer Robert "Pop" Andrew was killed by an avalanche when the bulldozer he was working by was pushed on top of him. Following his death authorities upgraded and formalised a programme of weather and snowpack monitoring and avalanche hazard control (Weir, 1998). An experienced avalanche forecaster was employed, high level automatic weather stations (AWS) were upgraded, stricter control of traffic was maintained and helicopter bombing for artificial release of avalanches was introduced. Standardised procedures for avalanche occurrence, snow and weather data gathering were adopted and these data have been archived since 1985. This was the inception of what is currently known as the Transit New Zealand Milford Road Avalanche Programme which is responsible for the safety of people on the Milford Road.

2.7.1 Avalanche data 1936 - 1984

Historical avalanche data for the Milford Road before 1984, the start of the avalanche programme, is of a mixed quality and not always reliable. Smith(1947) and an internal report by Paisley(1946) provides information from 1936 to 1945. Construction work was suspended from 1942 to 1951 because of World War Two so no avalanche reports are available for the period 1947-1951. From 1953 to 1964 it was not normal to use the road in winter, so recording of avalanches was infrequent and unreliable (McLauchlan, 1995). From 1963 onwards records are largely continuous, but are in the form of highway snow reports until 1971, and road condition / closure until 1983, so only larger avalanches are well documented (McLauchlan, 1995). Therefore, in the past, estimates of the size and frequency of all the avalanche paths were based on a mixture of field evidence and discussion with long term employees and available historical records (Fitzharris and Owens, 1980).

2.7.2 Avalanche data 1985 - present

Since the inception of the Transit New Zealand Milford Road Avalanche Programme in 1984, data has been collected and archived. As the programme has developed the amount and quality of the data recorded has increased. A standardised procedure has been adopted for the recording of avalanche occurrence and these data have now been loaded into an MS Access relational database. Snow data in the form of snowpits and crown wall profiles are gathered and archived. Weather data are also gathered, and these are archived and sent directly to the New Zealand Meteorological Service to provide additional input for their meso-scale forecasts for the Milford Road. Weather data are gathered from a number of weather stations, at road level and above the Milford Road. These data are currently telemetered from the avalanche area back to Te Anau, where it can be viewed, stored and sent through to the New Zealand Meteorological Service. Since 1985 the array of weather stations has been constantly increased and improved (Table 2.2 and Figure 2.2). Hourly observations are available from all weather stations, except for Mt Belle and Consolation Peak before 1989. These two stations have only daily observations for the time period 1986 to 1988 for Consolation Peak and 1985 to 1988 for Mt Belle. While each station measures an array of snow and weather variables, only Mt Belle and East Homer AWS have been fully described in this thesis (Table 5.1).

Table 2.2   Table of weather station with hourly data on and above the Milford Road, with approximate elevations, and the date of the data availability. * Daily observations only for the time period 1985 or 1986 to 1988 for Mt Belle and Consolation Peak respectively.

Weather Station	Date	Elevation (m)
Mt. Belle	1985*	1600
Consolation Peak	1986*	1570
East Homer	1993	920
West Homer	1995	790
Gates Snow Pole	1998	1800
Lysimeter added to Mt Belle	1999	1600
Cleddau (includes Lysimeter)	2000	1680
Rover	2001	1800
Crosscut Hut	2001/2	1880

All avalanches are recorded in the avalanche database in a two part process. The first part of this process is the recording of an avalanche occurrence in the logging atlas. The logging atlas is a series of oblique air photographs on which the avalanche paths are drawn. Many of the paths are made up of several starting zones, and these are also labelled. When recording an avalanche the spatial extent is drawn on the laminated photograph in the logging atlas and a range of parameters are recorded along side in text form (Figure 2.10 and Table 2.3). The second part of the process involves entering this field data from the logging atlas into the database. The text data are checked, corrected and clarified before being entered following the convention shown in Table 2.3. The photographic spatial data are currently not entered into the database, but the logging atlas pages are photocopied and archived at the end of each season.
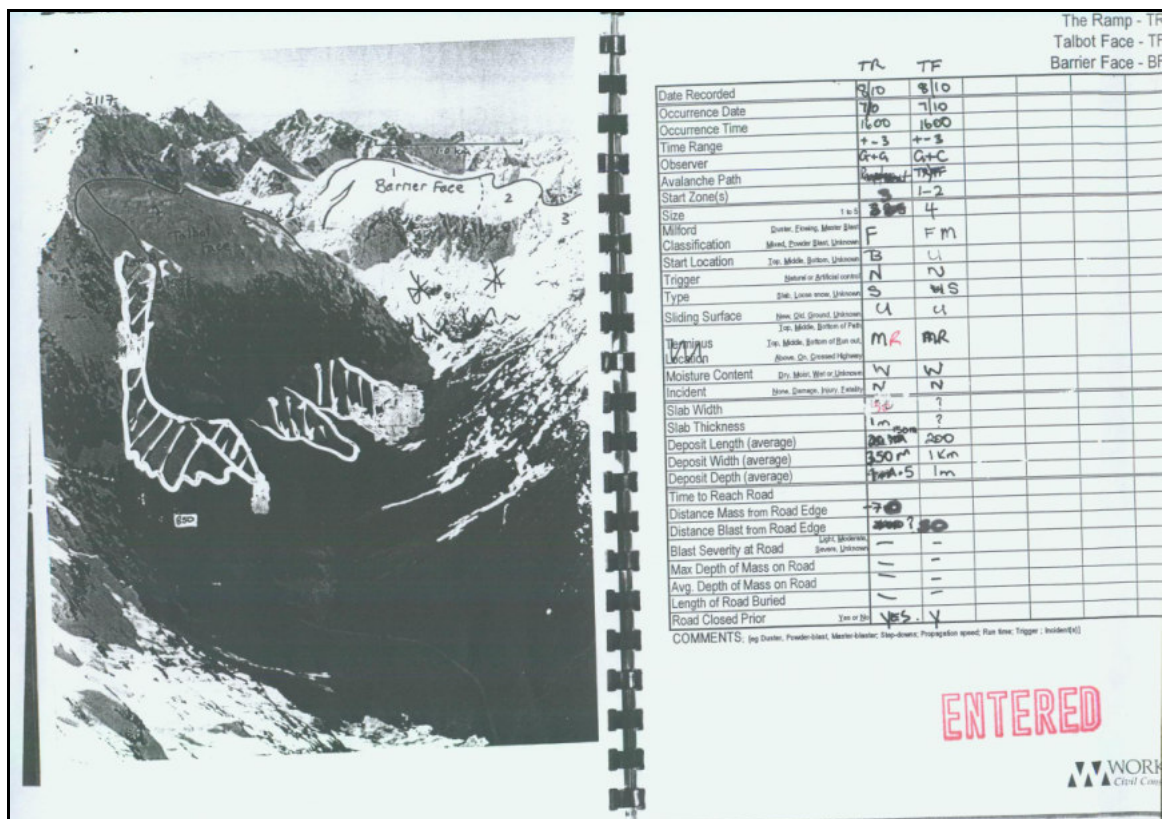
Figure 2.10   An example of the Milford Road avalanche logging atlas, showing the photo where the spatial extent can be entered and a table for the avalanche details in text form.

Table 2.3   Information ideally collected for each avalanche for the Milford Road avalanche database. Underlined letters are used where available.

Date of Occurrence	dd/mm/yyyy
Time of Occurrence	hh:mm
Avalanche Event Number	4 digit number (Unique identifier)
Date Recorded	dd/mm/yyyy
Time Range	hh:mm
Avalanche Path	Name according to logging atlas
Starting Zone(s)	Number according to logging atlas
Observer Initials	2 or 3 letters
Road Closed Prior To Occurrence	Yes or No
Start Location	Top, Middle, Bottom, Unknown
Sliding Surface	New, Old, Ground, Unknown
Trigger	Natural or Artificial control
Size	1 to 5 including ½ sizes
Milford Classification	Duster, Flowing, Master Blast, Mixed, Powder Blast, Unknown
Release Type	Slab, Loose snow, Unknown
Slab Width	X m
Slab Thickness	X m
Incident	None, Damage, Injury, Fatality
Moisture Content	Dry, Moist, Wet, Unknown
Terminus Location	Top, Middle, Bottom of Path Top, Middle, Bottom of Run out Above, On, Crossed Highway
Distance of Mass From Edge Of Road	X m
Distance of Snowdust from edge Of Road	X m
Maximum Depth Of Mass On Road	X m
Average Depth Of Mass On Road	X m
Length Of Road Buried	X m
Deposit Length (Maximum)	X m
Deposit Length (Average)	X m
Deposit Width (Maximum)	X m
Deposit Width (Average)	X m
Deposit Depth (Maximum)	X m
Deposit Depth (Average)	X m
Density	XXX kgm^{-3}
Time to Reach Road	X s
Blast Severity	Light, Moderate, Severe, Unknown
Comments	

Snow profiles are also undertaken when conditions allow access into the starting zones. Due to the nature of the topography, helicopter access is the only feasible means of accessing the starting zones safely. This has meant that snowprofiles have only been undertaken during spells of fine weather when the helicopter could fly safely. In the summer of 2001/2002 Crosscut Hut was built, thereby allowing avalanche technicians to observe the snow pack in the starting zones during storm periods. This has lead to a huge increase in the number of snowprofiles obtained during a season, from approximately 15 to well over 80 in 2004. Every season the Transit New Zealand Milford Road Avalanche Programme collects an ever increasing amount of information on avalanche occurrences, snowpack properties and an increasing array of meteorological parameters.

2.7.3 Avalanche risk management

The Transit New Zealand Milford Road Avalanche Programme currently manages the avalanche risk on the Milford Road through forecasting and control by artificial avalanche control. Constant winter monitoring of high alpine weather stations, field work to assess the snowpack structure and stability, and expert judgement of local forecasters are used to estimate the potential of an avalanche crossing the road. Avalanche forecasting is undertaken using a traditional approach (LaChapelle, 1980) where the forecast for each day is initially determined from the previous conditions, with observational evidence from avalanche events and weather data supporting or refuting this. When the avalanche risk is high, the road is closed and avalanches are released through helicopter bombing using 25kg bags of Amex (ammonium nitrate and oil) (Weir, 1998). Following the successful release of avalanches the road is cleared of avalanche debris and the road re opened to the public.

2.8   Conclusion

The Milford Road is situated in a unique environment subjected to a combination of climatic and topographic extremes. The starting zones high above the road receive large

quantities of snow annually, which combined with the over steepened glacial terrain results in very large powerful, dense and destructive avalanches.

With ever increasing annual visitor numbers to Milford Sound and of more concern the increasing numbers during the early spring shoulder season, the potential consequences of an avalanche on an open road are increasing. Despite this the Transit New Zealand Milford Road Avalanche Programme has managed the avalanche risk effectively, maintaining a clean slate, and successfully collecting an ever increasing amount of data pertaining to the avalanche and weather regime of the Milford Road. This comprehensive data set will become the focus of this thesis, as it can be used to examine, understand and validate existing and previous work regarding the avalanching on the Milford Road.

3.0 Snow and avalanche regime

3.1 Introduction

The snowfields and glaciers of the Southern Alps of New Zealand are the most significant in the Southern Hemisphere outside of Antarctica and South America (Fitzharris et al., 1999). While there is an extensive body of literature regarding the glaciers of the Southern Alps (e.g. Chinn, 1991; Chinn, 1996; Fitzharris et al., 1999), their inter-annual variability (e.g. Chinn and Whitehouse, 1980; Fitzharris et al., 1997; Tyson et al., 1997; Chinn, 1999), and their response to climate variability (e.g. Chinn, 1996; Hooker and Fitzharris, 1999; Lamont et al., 1999; Clare et al., 2002; Chinn et al., 2005), there is comparatively very limited research undertaken on seasonal snow (Fitzharris et al., 1999). This is despite the extensive seasonal snow cover in the Southern Alps, often covering a total of 55,000 km^2 or 35% of the South Island (Fitzharris et al., 1999) (Figure 3.1). Seasonal snow often exceeds 4000 mm water equivalent close to the main divide, lowering to less than 1000 mm further east, mirroring the precipitation rates of 12000 mm year^{-1} a few kilometres west of the main divide, receding to 1000 mm year^{-1} or less further to the east (Griffiths and McSaveney, 1983).

Research undertaken on seasonal snow in New Zealand has focussed on two main aspects, the snowpack as a water resource and snow avalanche hazards. Works examining the snowpack as a water resource have attempted to quantify the amount of snow in a catchment through measurement or modelling (Morris and O'Loughlin, 1965; Harrison, 1986; Garr and Fitzharris, 1996; Kerr, 2005), or across the Southern Alps as a whole (Fitzharris and Garr, 1995; Fitzharris and McAlevey, 1999). Unfortunately, there are only three snow course data sets from which annual variability of the snowpack depth and water equivalence can be estimated (Fitzharris et al., 1999). The three different snow courses are located far from the main divide, in the low precipitation eastern areas, but do show similar patterns to one another. The work of Morris and O'Loughlin(1965) and

O'Loughlin(1969) at an elevation of 1750m in the Craigieburn Range of Canterbury shows snow accumulation ranging from 230mm to 1030mm water equivalence with a standard deviation of 240mm and a coefficient of variation of 44% over a 12 year period (Moore and Prowse, 1988). Chinn(1981) working at an elevation of 1300m further south in the Two Thumb Range, showed a coefficient of variation of 52% over a 19 year period, while Harrison(1986) examining 17 winters in central Otago found the driest winter to have 40% lower water equivalence than that of the heaviest snow cover winter. In New Zealand more recently, new data are becoming available with the expansion of the snow sport industry and with ski fields improving their record keeping. However, these records are as yet to be collated, are unpublished and only cover the period of ski field operation, rather than the entire seasonal snow cover duration.

Figure 3.1   The Southern Alps of New Zealand viewed from Space Shuttle Atlantis, showing the typical winter scene, with lowlands free of snow and a well defined winter snow line. (Source: Geocarta International, 1999).

Elsewhere around the world, there have been many successful attempts to relate the spatial and temporal distribution and variability of snow cover or snow depth to large scale atmospheric circulations. One of the atmospheric circulations that has been related to snowfall is the El Niño-Southern Oscillation (ENSO) phenomenon. The ENSO phenomenon has two phases, warm or El Niño and cold or La Niña in respect to the ocean water off the coast of Peru (Sturman and Tapper, 1996). El Niño events result in the reduction of up welling off the coast of Peru, and result in changes to the intensity of the Walker circulation, thereby changing mean sea level pressures across the Pacific. The Southern Oscillation Index (SOI), is an index of the strength and phase of the ENSO phenomenon. It is calculated from the sea level pressure difference between Tahiti and Darwin. An anomalously low (negative) value of this index represents El Niño conditions, while anomalously high (positive) values represent the La Niña episodes. In the past, El Niño and La Niña events have occurred about every 3 to 7 years, typically becoming established around April or May and persisting for about a year thereafter (Heydenrych et al., 2001). ENSO has been related to snowfall events in northwest Missouri USA, with fewer snowfall events during El Niño years (Berger et al., 2002), and in the Pacific Northwest of the United States where there has been an increase in the occurrence of light, moderate and heavy snowfalls during the cold phase ENSO winter (Patten et al., 2003). Berger et al.(2002) also showed that snowfall variability related to ENSO was superimposed on longer term North Pacific Oscillation (NPO) related variability. The work of Changnon(1999), focussing on the economic losses and benefits from the 1997-1998 El Niño event, explains how the warmer than average air temperatures over the northern two thirds of the United States caused less snow, and therefore resulted in fewer deaths and lower energy consumption rates over the winter period. There have also been significant positive correlations with warm ENSO events and modelled snow depth anomalies over northern Europe and Siberia (Corti et al., 2000) and strong relationships with ENSO and precipitation fluctuations in Nepal, where warm El Niño years have been shown to reduce the strength of the monsoon (Shrestha et al., 2000). Furthermore, Lee et al.(2004) showed spatially highly variable results of snow water equivalence in the Rio Grande River basin in relation to ENSO, with eastern locations showing a strong ENSO signal.

ENSO is known to be modulated by the Interdecadal Pacific Oscillation (IPO) (Salinger et al., 2001). The IPO is associated with decadal climate variability over parts of the Pacific, and there have been three main phases identified; a positive phase from 1922-1944, a negative phase from 1946-1977 and another positive phase from 1978-1998 (Salinger et al., 2001). The positive phase of the IPO has been characterised by strong westerly circulation over the South Island, and a period of more frequent El Niño events (Salinger et al., 2001; Chinn et al., 2005). The phase change of the IPO is coincident with an increased mass balance of glaciers in New Zealand, and increased snowfall during the accumulation season (Chinn et al., 2005). Moore and McKendry(1996) working in British Columbia, noted a shift in spatial and temporal snowpack patterns following 1976, with snow lighter than average over the whole province, or heavier than average in the north and lighter in the south in the period 1977 to 1992. Brown and Braaten(1998) also note the changes in snow depth and snow cover extent in Canada, which has been associated with a shift in atmospheric circulation over the North Pacific in 1976.

Another atmospheric circulation pattern that has been related to the variability of snow cover or snow depth is the North Atlantic Oscillation (NAO). The NAO is measured by an index of sea level pressure measured at the Azores and in Iceland. A high NAO index tends to mean relatively warm conditions in northern Europe, while a low or negative index usually means weaker westerly winds, resulting in a colder continental climate which is dominated by cold air from the north and east (Hurrell, 1995). Hurrell(1995) examined correlations between the NAO index and climate parameters, such as temperature and precipitation with the conclusion that the NAO explained up to 34% of inter-annual variability in non equatorial parts of the northern hemisphere. Beniston(1997) showed that increased snow depth and duration in Switzerland is correlated with the negative phase of the NAO. Clark et al.(1999) when considering Eurasian snow extent also found that a negative NAO resulted in more snow cover in central Europe, while Morinaga et al.(2003) found that January snow depth in parts of Mongolia is highly correlated with the NAO for November. In Poland, Bednorz(2002) reported that during negative phases of the NAO there was an increase in the probability of severe snowy winters in western Poland, while Falarz(2004), also in Poland, showed a

statistically significant negative correlation between maximum snow depth and the NAO. Recently, Scherrer and Appenzeller(2003) and Scherrer et al.(2004) have noted smaller scale regional differences, with the northern parts of the Swiss Alps inter-annual snow days being unaffected by the NAO, in contrast to the southern alpine regions. Laternser and Schneebeli(2003) noted a change from a persistent period of negative NAO indices from 1950 to 1974 (resulting in mainly cold and snowy winters), to a period of positive NAO indices from 1974 to 1995 (resulting in record warm temperatures, and low snow years). Further south, in the Central Spanish Pyrenees measurements from snow stakes over a 14 year period related winter precipitation to a positive trend in the NAO (López-Moreno, 2005).

While the relationships between snow depth, snow cover and duration and large scale atmospheric circulation patterns have received much attention, so too have the related fluctuations of synoptic scale anomalies. Grundstein and Leathers(1998) and Grundstein(2003) related snow melt and decreased snow depth on the great northern plains to the frequency of air masses. A distinct difference in the frequency of air masses was found during high Snow Water Equivalence (SWE) and low SWE years. Hartley and Keables(1998) related snowfall in New England from 1950 to 1992 to a negative NAO index and negative 700-mb height anomalies over eastern USA, while Frei and Robinson(1999) examined the snow extent over eastern North America for the period 1972-1994 and suggested that the meridional oscillation of the 500 mb geopotential height field is the main control on snow extent. Work in the Colorado River basin (McGinnis, 2000) related snowfall to atmospheric variance in the Pacific Northwest and the resulting changes in synoptic systems and Berger et al.(2002) noted that heavy snowfall events during neutral ENSO years were the result of synoptic scale variability. In the former Soviet Union, Rikiishi and Sakakibara(2004) examined snow depths, and have related this to the migration of synoptic disturbances from the Arctic Ocean.

While snow cover and snow depth have received much attention, there has also been research examining the intensity of avalanche winters in relation to shifts in synoptic circulation patterns. Fitzharris and Bakkehøi(1986) working in Norway found that while

no one synoptic type explains all large avalanche winters, winters with more meridional and less mixed weather types, combined with a cold December and or January resulted in large avalanche seasons. In a similar study in Western Canada, Fitzharris(1987) again found that more than one climatology is needed to explain large avalanche winters, but noted the major avalanche winters tend to be cold in December and or January. Schneebeli et al.(1997) noted that a single weather situation is responsible for most avalanches in the eastern and southern parts of Switzerland, while western and central parts of Switzerland needed several different weather situations. Mock(1995) and Mock and Birkeland(2000) have related the avalanche variability in the Southern Rocky Mountains and shift between continental and maritime conditions in the Western United States mountain ranges to the height anomalies at 500 mb. Anomalies at the 500 mb level have also been related to extreme avalanche events across the western United States (Birkeland and Mock, 2001; Birkeland et al., 2001). While snow depth, snow cover and duration in Switzerland has been well documented and related to the NAO (e.g. Beniston, 1997; Laternser and Schneebeli, 2003), Laternser and Schneebeli(2002) have been unable to detect a long-term change in avalanche activity, which is in contrast to the significant increases in winter precipitation in Switzerland.

The effect of recent and potential future climate change on snow amounts and avalanche activity has also been examined by Föhn(1992), Schneebeli et al.(1997), Beniston et al.(2003a), Beniston et al.(2003b) in Switzerland, Martin et al.(2001) in the European Alps, and Glazovskaya(1998) and Glazovskaya and Seliverstov(1998) globally. Glazovskaya(1998) and Glazovskaya and Seliverstov(1998) suggested that global warming will result in moderation of avalanche activity, with increased occurrence in continental areas, and a decreased occurrence in maritime areas. Martin et al.(2001) suggested an overall decrease in avalanche activity, with an increase in wet snow avalanche activity, when using a climate scenario of increased precipitation and temperature. Beniston et al.(2003a) and Beniston et al.(2003b) under modelled climate change, note the altitudinal differences with more snow at higher elevations in the Swiss Alps, and significantly less below 1500m. Schneebeli et al.(1997) examined historical

avalanche records, and highlighted that large destructive avalanches are not primarily a product of slow climatic changes, but are the result of extraordinary weather situations.

In New Zealand, however, because of data set limitations, limited work has looked at the relationship between snow depth and atmospheric circulation patterns for a series of years. Burrows(1976) examined exceptional snow storms to low levels in the South Island, while Neale and Thompson(1977) looked at the synoptic circulations associated with ten low level snowfall events. The only works in New Zealand to examine the relationship between snow depth and a number of circulation indices and synoptic patterns was that by Kelly(1992) and de Lautour(1999). Kelly(1992) examined the relationship between snow depth at Treble Cone, Wanaka, east of the divide, and atmospheric circulation indices. Unfortunately, the snow depth used was only an index calculated from valley precipitation and temperature records. However, a very weak negative correlation was found between the SOI and snow depth. Kelly(1992) also determined that 78% of all days with more than 10cm of new snow at this location, were days with a northwest synoptic circulation pattern. Using modelled snow depth from SnowSim (Fitzharris and Garr, 1995), de Lautour(1999) examined the relationship between seasonal snow storage in the main hydro catchments and atmospheric circulation patterns for the period 1930 to 1993. His analysis showed that there was no statistically significant difference in mean circulation patterns between the eight highest snow years and eight lowest snow years. When de Lautour(1999) examined the relationship between SOI and modelled snow storage a weak correlation (-0.43) was found. No works examine the relationship between actual measured snow depth and atmospheric circulation patterns. Furthermore, there has been no work examining the relationship between avalanches and synoptic circulation or atmospheric circulation patterns in New Zealand. Fortunately, snow depth data obtained from Mt Belle AWS, and avalanche data from the Transit New Zealand Milford Road Avalanche Programme, while short in duration compared to many other studies worldwide, are among the best data sets available in New Zealand, with respect to their duration, accuracy and consistency. This chapter will examine the 14 year data set from 1989 to 2002, obtained from a location more westerly, and closer to the main divide than previous work.

3.2 Aims

This chapter aims to document and examine the annual snow depth variability and avalanche regime in the Milford Road region. Once the snow depth and avalanche regime have been described they will be related to indices that represent various forms and scales of atmospheric circulation, including the Trenberth circulation indices (Trenberth, 1975; 1976), Kidson(2000) synoptic typing and the SOI.

3.3 Data description

The data used for this chapter are from a range of sources. Hourly snow depth data are obtained from the Mt Belle AWS located at 1600 m a.s.l., above the Milford Road (Figure 2.2 and Figure 3.2). Snow depth has been measured in a number of ways over this period, with the majority and most recent data measured using a downwards facing sonic ranger. Mt Belle AWS is at an elevation representative of the starting zones above the Milford Road. The snow depth data, along with a large array of other climate data are telemetred back to Te Anau via a radio link. For various reasons, including sensor and data transmission malfunction, the data are incomplete and contain many erroneous values. The majority of these errors have been removed from the data using filters that identified data points above a threshold value of 5 m or negative values. Despite this, some errors such as spikes remain, but these are small and insignificant to the results of the analysis. Hourly snow depth data was then averaged into daily snow depth data for the historical duration of the avalanche season. Using the daily snow depth data, an average snow depth curve was generated for the 13 seasons of snow depth data. Avalanche data were obtained from the Transit New Zealand Milford Road Avalanche Programme and are in the form as described in chapter two. In this chapter, only the size and date of the avalanche occurrence were used. These avalanche data are of a very high quality and consistency, as they have been manually entered at the completion of each season.

Two sets of regional climate data were obtained from the National Institute of Water & Atmospheric Research (NIWA). Updated Trenberth circulation indices as used by (Salinger, 1980a, 1980b; Salinger and Mullan, 1999; Heydenrych et al., 2001) were obtained from Dr. Brett Mullan through assistance from Dr. Jim Salinger. Daily synoptic type data, using the scheme outlined by Kidson(2000) were obtained directly from Dr. Jim Renwick also at NIWA. ENSO data, in the form of the SOI, were obtained from the Australian Bureau of Meteorology(2005).
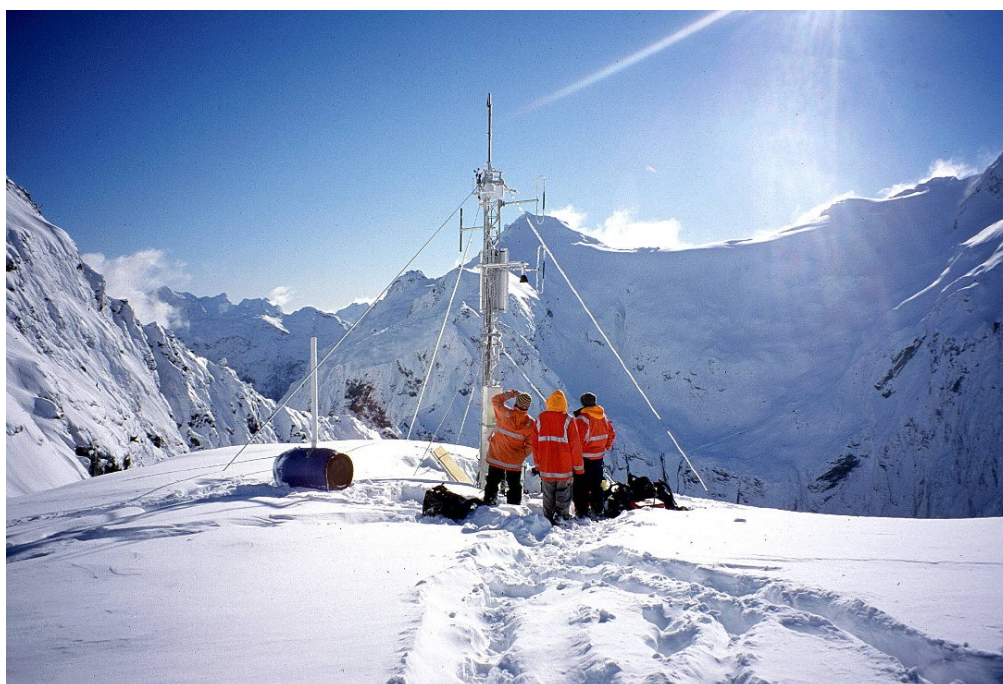
Figure 3.2   Mt Belle AWS situated above the Milford Road at 1600m a.s.l., the sonic ranger can be seen shielded by the black cone, level with lowest aerial on the right. (June, 2003)

The Trenberth circulation indices were first developed by Trenberth(1975, 1976) and later added to by Salinger and Mullan in 1992 (Heydenrych et al., 2001). The first seven indices in Table 3.1 were defined by Trenberth(1975, 1976) and the remaining four (MZ1, MZ2, MZ3 and MZ4) were added to enumerate aspects of New Zealand's circulation that are neither directly zonal or meridional. Trenberth circulation indices have been used to successfully explain variance in inflow to the Clutha lakes (Trenberth, 1977), spatial precipitation patterns (Salinger, 1980a; Salinger and Mullan, 1999),

temperature patterns (Salinger, 1980b; Salinger and Mullan, 1999), ENSO (Kidson and Renwick, 2002) and severe fire seasons (Heydenrych et al., 2001).

Table 3.1   Zonal and Meridional indices of the New Zealand circulation

Index	Pressure difference	Type of circulation	Region
Z1	Auckland-Christchurch	Westerlies	36.5 – 43.5°S near 170°E
Z2	Christchurch-Campbell Island	Westerlies	43.5 – 52.5°S near 170°E
Z3	Auckland-Invercargill	Westerlies	36.5 – 52.5°S near 170°E
Z4	Raoul Island- Chatham Island	Westerlies	29 – 44°S near 175°E
M1	Hobart-Chatham Islands	Southerlies	147.5°E-176°W near 43°S
M2	Hokitika-Chatham Island	Southerlies	171°E-176°E near 43°S
M3	Hobart-Hokitika	Southerlies	147.5°E-171°W near 43°S
MZ1	Gisborne-Hokitika	North-westerly flows	Near 170°E and 43°S
MZ2	Gisborne-Invercargill	North-westerly flows	Near 170°E and 43°S
MZ3	New Plymouth-Chatham Island	South-westerly flows	Near 170°E and 43°S
MZ4	Auckland-New Plymouth	WNW flows	Near 170°E and 43°S

The indices are a way of characterising the predominant weather patterns for the New Zealand region on monthly time-scales. A monthly index number is generated from a pair of climate stations using the monthly mean pressure difference between the stations, minus the long-term mean monthly pressure difference calculated over a 30-year normal period from 1971 to 2000. An index other than zero implies an anomalous pressure gradient between the stations and hence an anomalous windflow perpendicular to this gradient. Therefore, a north-south pressure difference between stations indicates the strength of the wind in the west-east direction, while an east-west pressure difference between stations indicates north-south wind strength (Table 3.2). The indices can therefore be interpreted as a measure or indicator of the prevalent monthly wind speed and direction (Heydenrych et al., 2001).

The synoptic circulation types used are those as described by Kidson(2000) are shown in Figure 3.3 and are described in Table 3.3. These 12 types are generated from clusters obtained from composite patterns of 1000 hPa height and frequency of occurrence from the twice-daily NCEP:NCAR reanalyses from January 1958 to July 1997 (Kidson, 2000). The 12 types are presented in terms of three interrelated groups, or regimes, i.e. Trough,

Zonal or Blocking (Kidson, 2000). Kidson's synoptic typing has been successfully used to explain variance in the stock of southern gemfish (*Rexea solandri*) in New Zealand waters (Renwick et al., 1998), severe fire seasons (Heydenrych et al., 2001), and ENSO (Kidson and Renwick, 2002).

Table 3.2   Typical flow patterns associated with circulation index anomalies
             (Heydenrych et al., 2001)

Index	Positive anomaly	Negative anomaly
Z1	Stronger westerlies over NZ	Stronger easterlies (weaker westerlies)
Z2	Stronger westerlies south of NZ	Easterlies south of NZ
Z3	Stronger west-northwest flow over NZ	East-southeast flow over NZ
Z4	Stronger westerlies northeast of NZ	Easterlies to northeast of NZ
M1	Stronger southerly flow NZ/Tasman	Northerlies over NZ/Tasman
M2	Enhanced southerlies east of NZ	Northerly airflow east of NZ
M3	Stronger southerlies in Tasman	Northerlies in Tasman
MZ1	Stronger NNW esp. over central NZ	SSE airflow especially over central NZ
MZ2	Stronger north-westerlies over NZ	South-easterly winds over NZ
MZ3	Stronger south-westerlies over NZ	North-easterlies over NZ
MZ4	Stronger WNW over NZ	ESE winds over NZ

Compared with Australia, New Zealand is not usually affected as strongly by phase changes in ENSO, but there is however a significant influence. During a negative SOI phase (El Niño years), New Zealand tends to experience stronger and more frequent winds from the west in summer, leading to more rain in the west and drought in east. In winter, the winds are more from the south, bringing colder conditions to both the land and the surrounding ocean (Gordon, 1985; Sturman and Tapper, 1996). During a positive SOI phase (La Niña years), there is a much weaker impact on New Zealand's climate. New Zealand generally experiences more northeasterly winds bringing warmer and moister conditions to the northeast parts of the North Island. In winter the winds are more from the north, bringing warmer conditions to both the land and sea surrounding the North Island (Gordon, 1985; Sturman and Tapper, 1996).
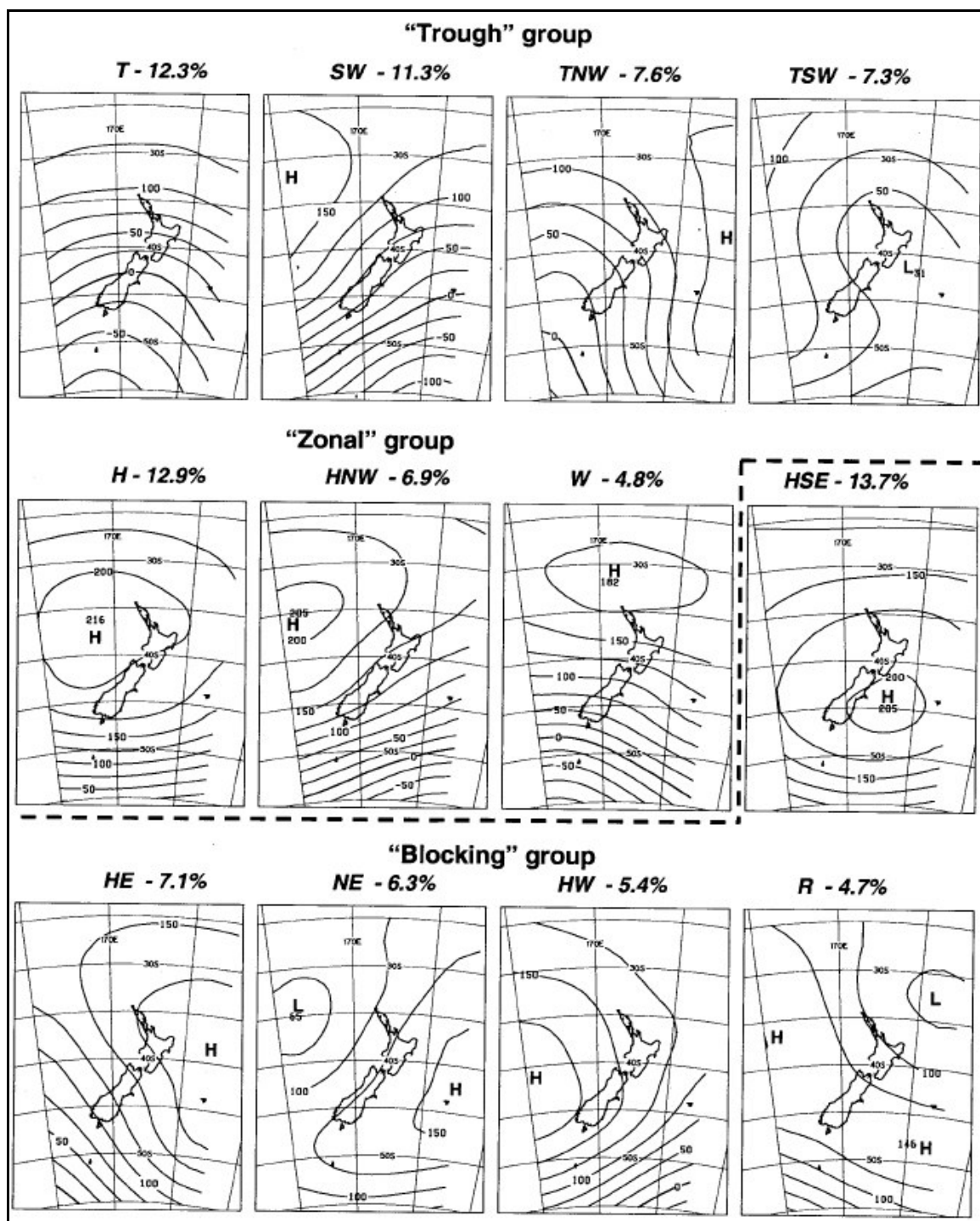
Figure 3.3   Mean 1000 hPa heights associated with the 12 daily synoptic classes used to categorise daily weather patterns. Percentage values represent the frequency of occurrence from January 1958 to July 1997. (Kidson, 2000)

Table 3.3   Synoptic types descriptions and associated windflows (Kidson, 2000)

Index	Synoptic type description	Wind flow
TSW	Trough in southwest flow crossing New Zealand	Westerly flows – North Island Easterly flows – South Island
T	Trough in westerly flow crossing New Zealand	Westerly flows – All NZ
SW	Southwesterly flows	Southwesterly flows- All NZ
NE	Northeasterly flows	Northeasterly flows – All NZ
R	Ridge – light winds	Easterly flows – North Island Light winds –South Island
HW	High to west of the South Island	Southwesterly flows –South Island
HE	High to the east with developing northwesterly flow	Light winds – North Island Northwesterly flows – South Island
W	Westerly flow	Westerly flows – All NZ
HNW	High west of the North Island	Southwesterly flows – All NZ
TNW	Trough to the west preceded by northwesterly flow	Northwesterly flows –All NZ
HSE	High east of the South	Easterly flows – North Island Light winds – South Island
H	High – North Island	Light winds – North Island Southwesterly flows – South Island

Annual Trenberth circulation indices were generated from monthly values, by averaging across the winter months, June to November. Annual synoptic types were generated from twice daily data and expressed by type as a percentage of all occurrences for the historical avalanche period, 30 May (Julian Day 150) to 20 December (Julian Day 355). The annual SOI index (SOI 12) was generated from monthly values, averaged for the calendar year, while the winter SOI was averaged for only the June to November period inclusive (SOI 6).

3.4   Methods

Snow depth and avalanche data were examined using graphical and regression methods to identify trends. Spearman R rank order correlation coefficients were used to examine relationships between snow depth, snow depth variability and avalanche occurrences in relation to a range of atmospheric circulation indices. It is suspected that many of the

atmospheric circulation indices are correlated and are not completely independent. Therefore, circulation indices were first examined for high correlation coefficients, before relationships between the variables were sought. In summary, the predictors investigated in the study were:

* ❊ The Southern Oscillation Index for twelve and six month periods (SOI 12 and SOI 6)
* ❊ The Trenberth circulation Indices: Z1, Z2, Z3, Z4, M1, M2, M3, MZ1, MZ2, MZ3
* ❊ Frequency of occurrence of the Kidson (2000) synoptic circulation patterns: TSW, T, SW, NE, R, HW, HE, W, HNW, TNW, HSE, H
* ❊ Frequency of occurrence of the Kidson (2000) synoptic circulation pattern groupings: Zonal, Trough and Blocking

Following Heydenrych et al.(2001) Pearson product-moment correlation coefficients were initially used. However, unlike Heydenrych et al.(2001) this initial analysis was discarded because of the small sample size and some parameters showing violations to the normality assumptions when examined on bi-variate plots. Consequently, Spearman R rank order correlations were used with p-value $\leq$ 0.05 (two-tailed) considered significant and p $\leq$ 0.01 (two-tailed) considered highly significant for this study.

3.5   Results and Discussion

3.5.1 Snow depth variability

Daily snow depth data from Mt Belle AWS are examined for the period from Julian Day 150 to Julian Day 355, for the years 1989 to 2002 inclusive. Unfortunately, data for 1995 are completely missing from the data set because of sensor failure, and the data for 1991 must be treated with extreme caution as they are of very poor quality. Using the remaining 12 years; 1989, 1990, 1992, 1993, 1994, 1996, 1997, 1998, 1999, 2000, 2001,

2002, a daily average snow depth was calculated. This average surface was then plotted against daily snow depth for a given year, to illustrate seasonal snow depth deviations from the average snow depth curve (Figure 3.4a-c). In addition, the average daily snow depth was subtracted from the daily snow depths, to show absolute deviations from the average (Figure 3.5).
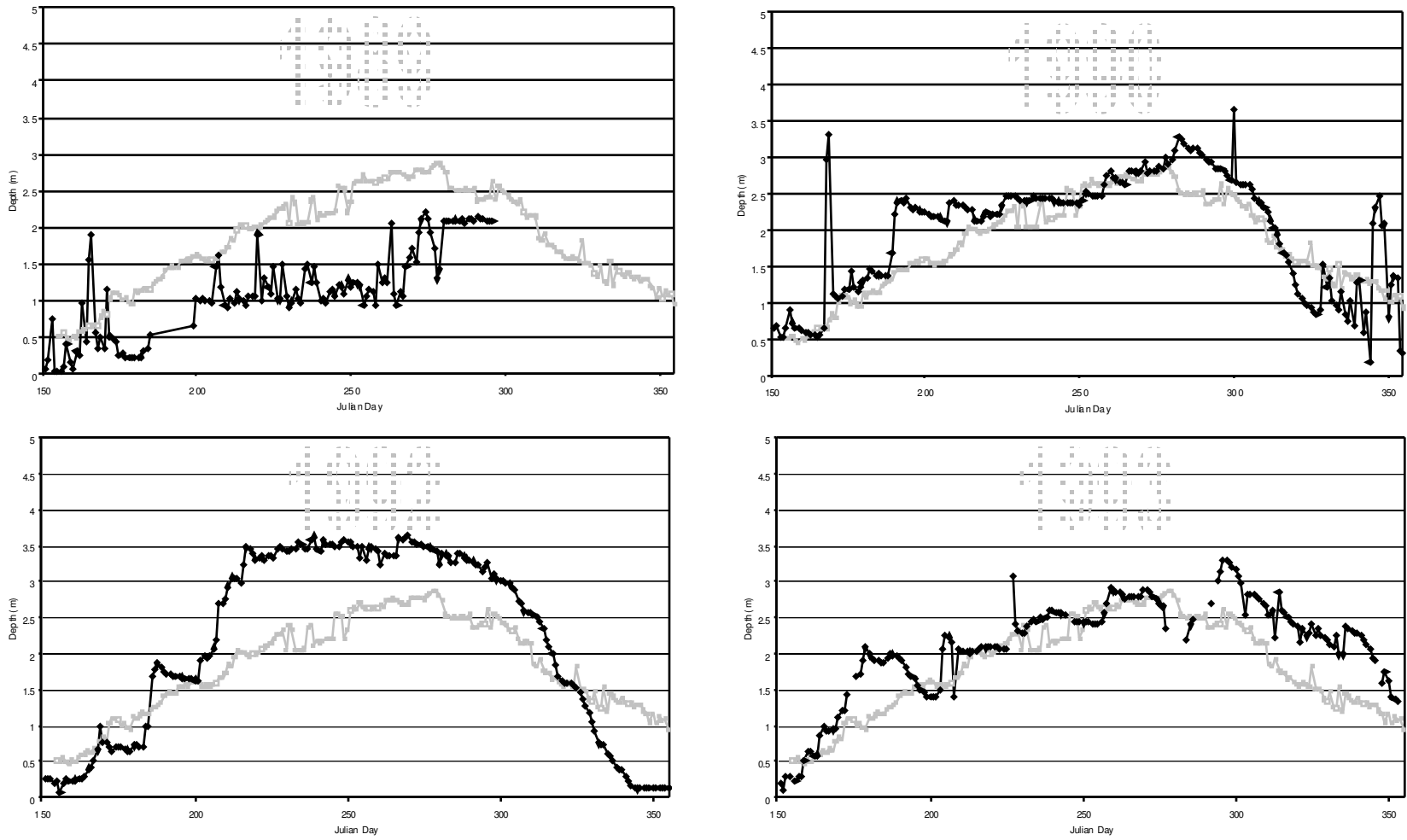
Figure 3.4a 1989, 1990, 1992 and 1993 daily snow depths in black with the average daily snow depth, calculated from the 12 year dataset, shown in grey
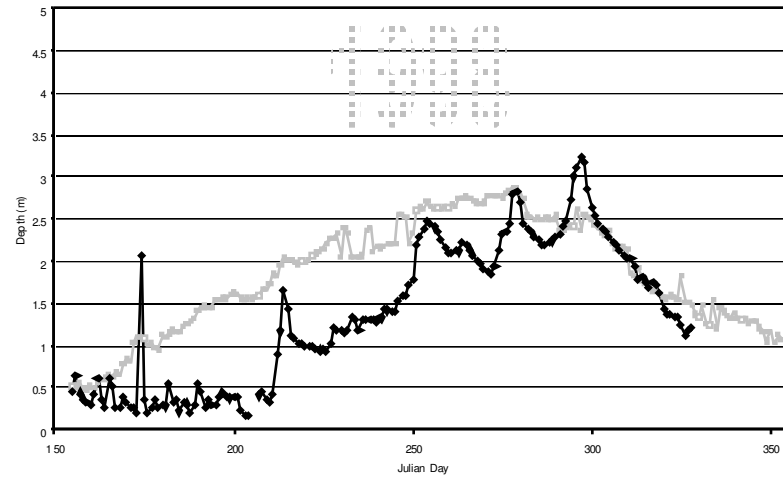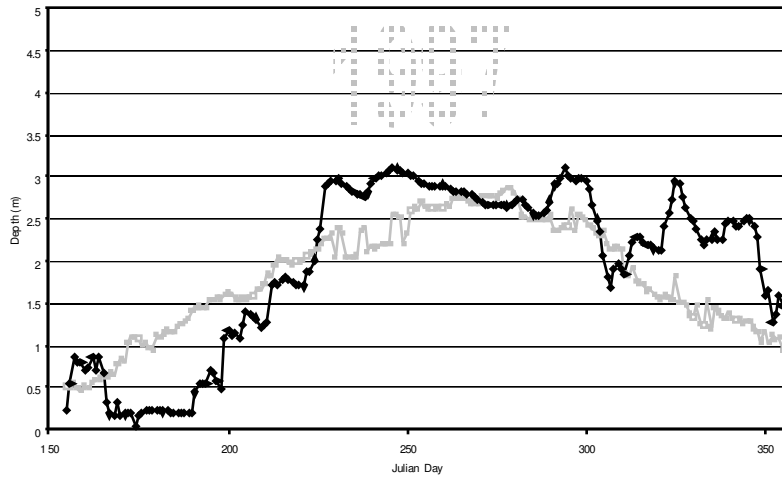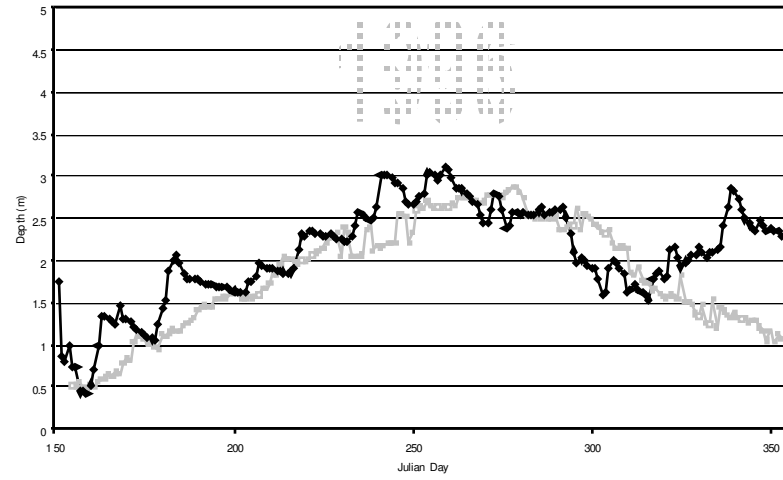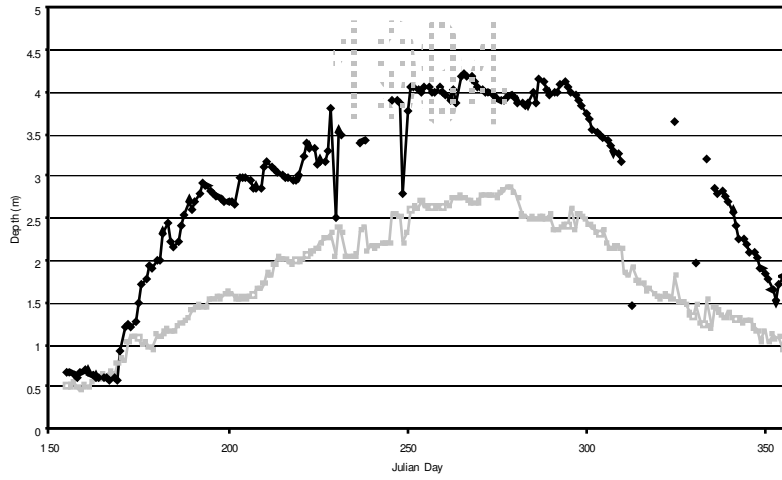
Figure 3.4b   1994, 1996, 1997 and 1998 daily snow depths
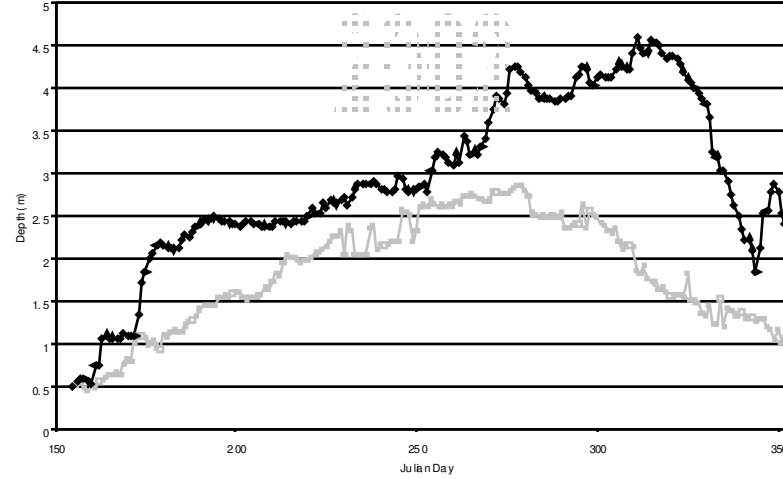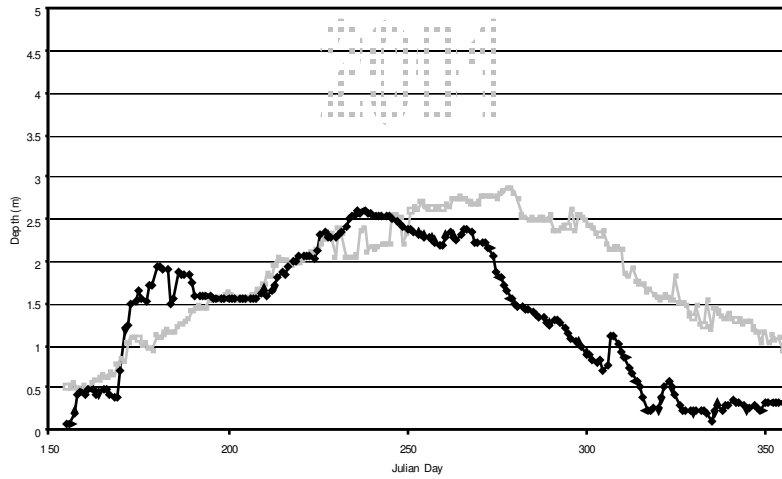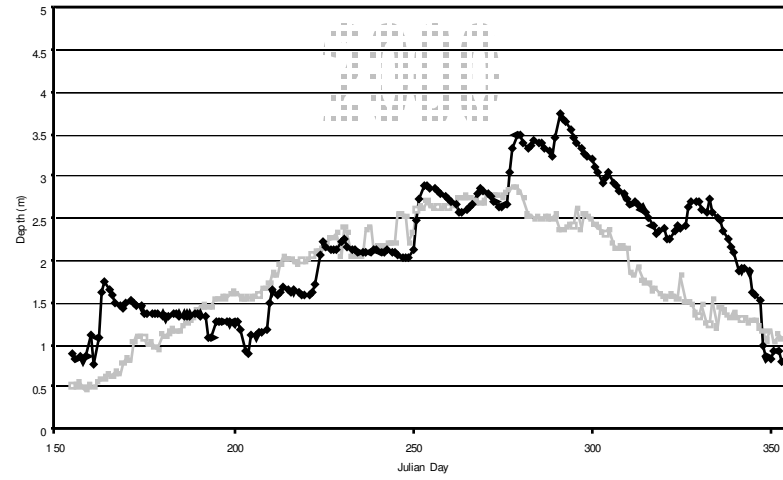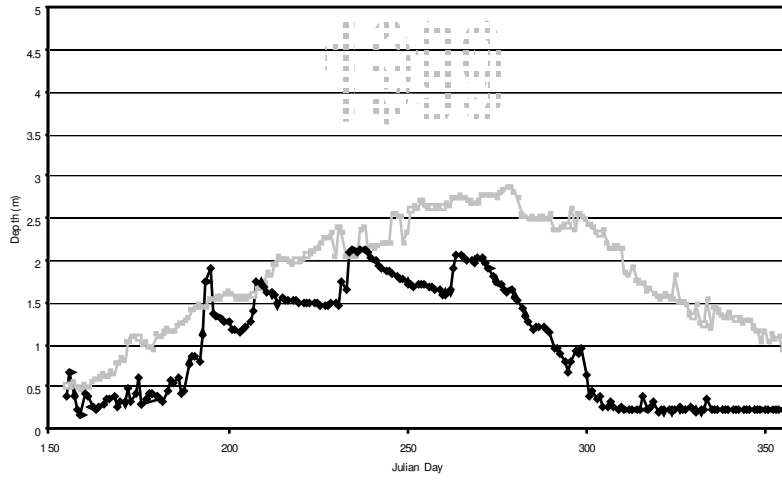
Figure 3.4c   1999, 2000, 2001 and 2002 daily snow depths
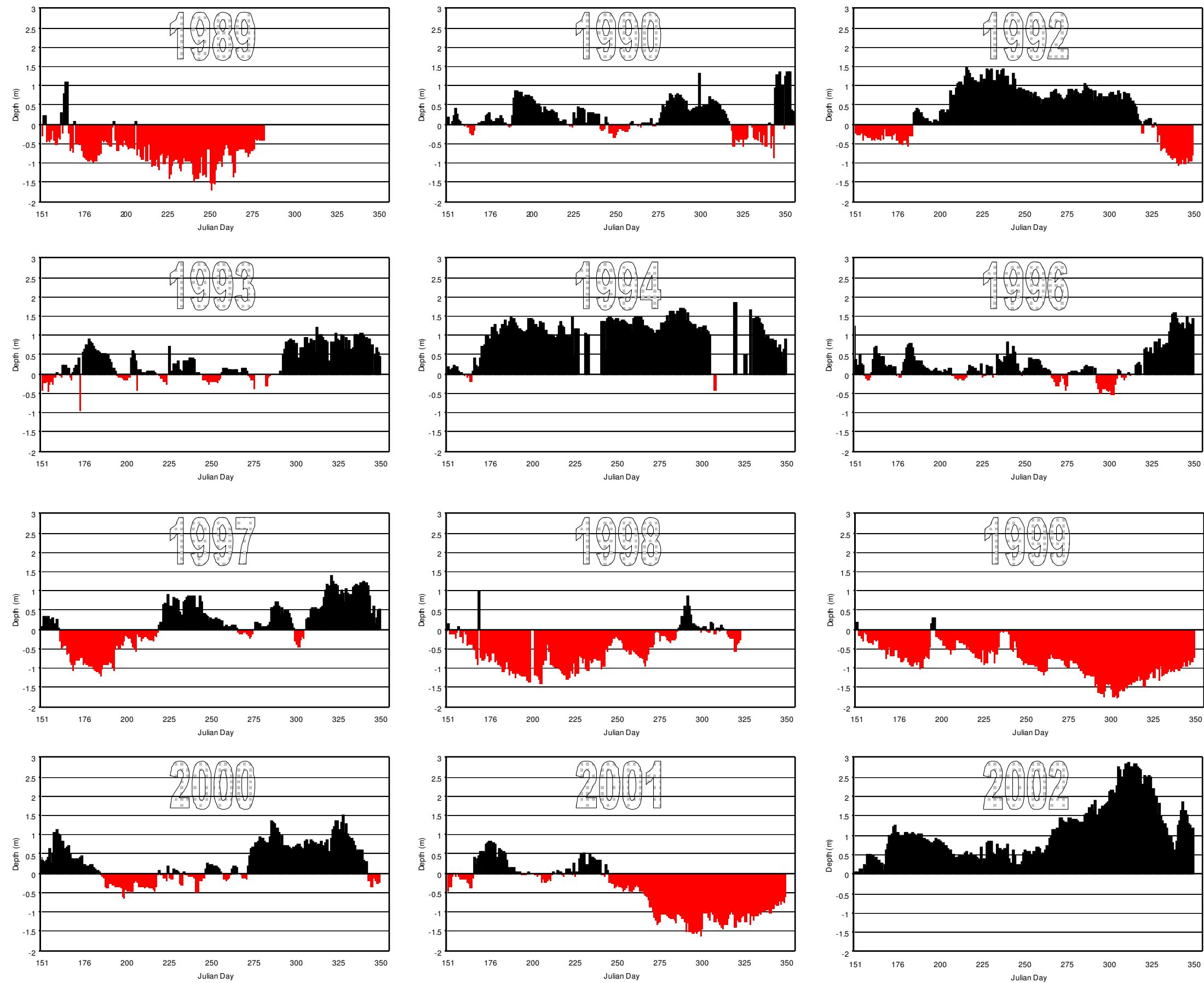
Figure 3.5   Daily snow depth deviations from the average for the 12 years of record, where the average daily snow depth is represented by the line X=0, and surplus snow is shown in black above this line, and deficits of snow is shown in red, below this line

Examination of the graphed daily snow depth data for the 12 years of record (Figures 3.4a-e and 3.5) reveals some interesting features that would otherwise not be obvious in the results of many standard measures of a data set. In qualitative terms, the most notable in chronological order are:

❋ Daily snow depth in 1989 was mostly well below the average snow depth, though the data are only slightly better in quality than the omitted 1991 data set

❋ Daily snow depth in 1992 was above the average around the middle of the season from Julian Day 200 to 320, but below the average at the beginning and the end of the season

❋ Daily snow depth in 1993 was about average, but had some higher values towards the end of the season

❋ Daily snow depth in 1994 started about average, but by Julian Day 165 onwards was significantly above average

❋ Daily snow depth in 1996 was about average most of the season, but above towards the late season from Julian Day 325 onwards

❋ Daily snow depth in 1997 was about average, but the early season was well below average from Julian Day 160 to 220, while the late season was well above (Julian Day 310 onwards)

❋ Daily snow depth in 1998 was below average much of the season, but reached and slightly exceeded the average by the middle to late season from Julian Day 280 onwards

❋ Daily snow depth in 1999 started slightly below the average, but by the middle of the season (Julian Day 240 onwards), dropped away rapidly

❋ Daily snow depth in 2000 was about average most of the season, but above average towards the middle of the season from Julian Day 285 onwards

❋ Daily snow depth in 2002 was very far above average in the late season from Julian Day 280 onwards, while the rest of the season is only slightly above average

As shown in Figure 3.6, annually averaged daily snow depth data for the period from Julian Day 150 to 355, have a range in their means from 0.99m in 1999 up to 2.92m in 2002. The annual coefficients of variation for each year also range greatly from 27.5% in 1996 up to 68.7% in 1999. When all daily snow depth data available are considered they have a mean depth of 1.94m, with a standard deviation of 1.04m, thus placing all annual averaged daily snow depth means within one standard deviation of the overall mean, as shown by the shaded area in Figure 3.6.
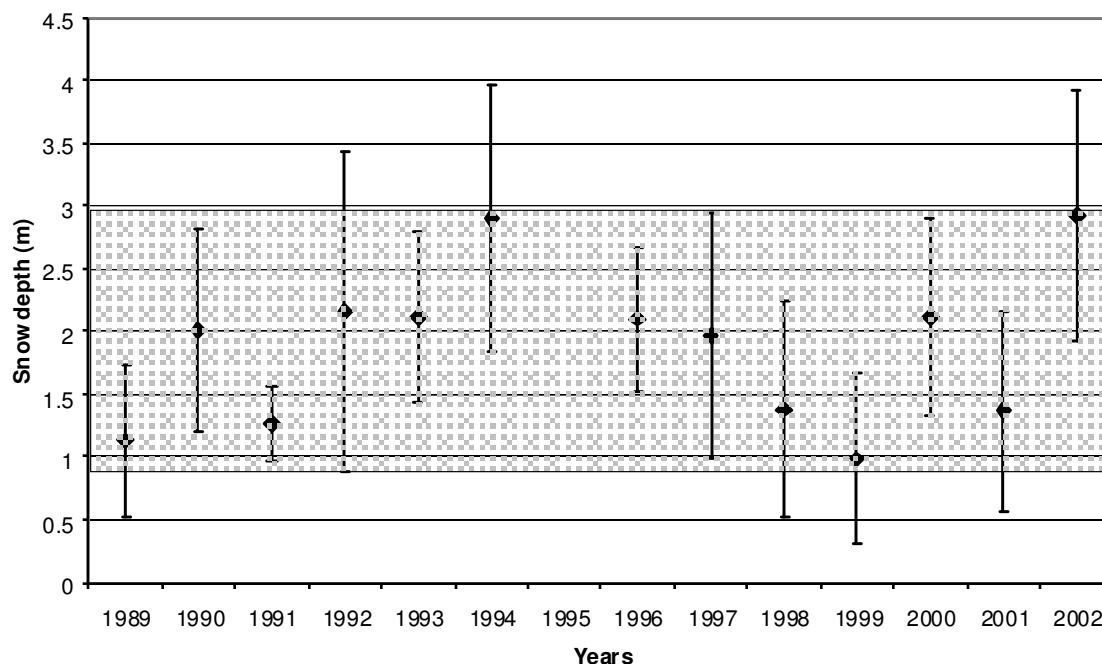
Figure 3.6   Annually averaged daily snow depth at Mt Belle AWS for each of the 13 years, where the dimamonds represent the annual mean and the bars are ± one standard deviation within that year. Shaded area represents the average of all daily snow depth data ± one standard deviation for the entire data set.

The coefficient of variation calculated for the mean annual snow depth for the 13 seasons is 36%, significantly lower than those published by previous work in New Zealand (Morris and O'Loughlin, 1965; O'Loughlin, 1969; Chinn, 1981). It is thought the lower coefficient of variation reflects the maritime climate of the area and the proximity to the ocean, resulting in a reliable minimum amount of snow in any given season.

3.5.2 Avalanche occurrence variability

The avalanche regime on the Milford Road has been significantly modified since the Transit New Zealand Milford Road Avalanche Programme was initiated in 1984. With the introduction of artificially released avalanches (using helicopter bombing), the size and nature of subsequent avalanches on bombed slopes, may have changed. Examination of the total avalanche record from 1985 to 2002 shows that natural avalanche occurrence has high annual variability ranging from 9 in 1989 to 161 in 1988. However, regression analysis indicates that that there is no statistical trend in natural avalanche frequency. The coefficient of variation calculated for all avalanche occurrences for the total record, from 1985 to 2002 is 52%. When calculated for the same period as the snow depth is examined for (1989 to 2002) it is 53%. Artificial avalanche occurrence also has a large annual variability ranging from 6 in 1989 to 170 in 2002 but the increasing trend of 4.6 avalanches year^{-1} is marginally significant with p-value=0.052 and R^2=0.22. This trend reflects the increased pressure to maintain tourist access to Milford Sound and the much larger traffic flows (Figure 3.7a).

The avalanche database confirms that the avalanche season may start as early as May and can last until the middle of December. The majority of the avalanches occur from July to October, with a maximum in the middle of August (Figure 3.7b). Artificially released avalanches are slightly less common at the beginning of the winter and more common than natural avalanches toward the end of the winter, in October and November. Avalanches are recorded on the Milford Road using the Canadian size classification (including half sizes), based on estimates of mass and destructive potential (McClung and Schaerer, 1993; Floyer and McClung, 2003). The size class distribution shows a significant lack of smaller size classes, and a slight bias to recording whole number sizes (Figure 3.7c). The smaller size cases are possibly under-recorded because of their insignificance for road safety and limited observational possibilities during storms. The threshold on avalanches that affect road safety is operationally set at a size class 2.5. Avalanches equal to, or greater than this size, while not necessarily affecting the road, are

considered to be an incident if the road is open. Therefore avalanches at and above this size class are very well recorded in the database.
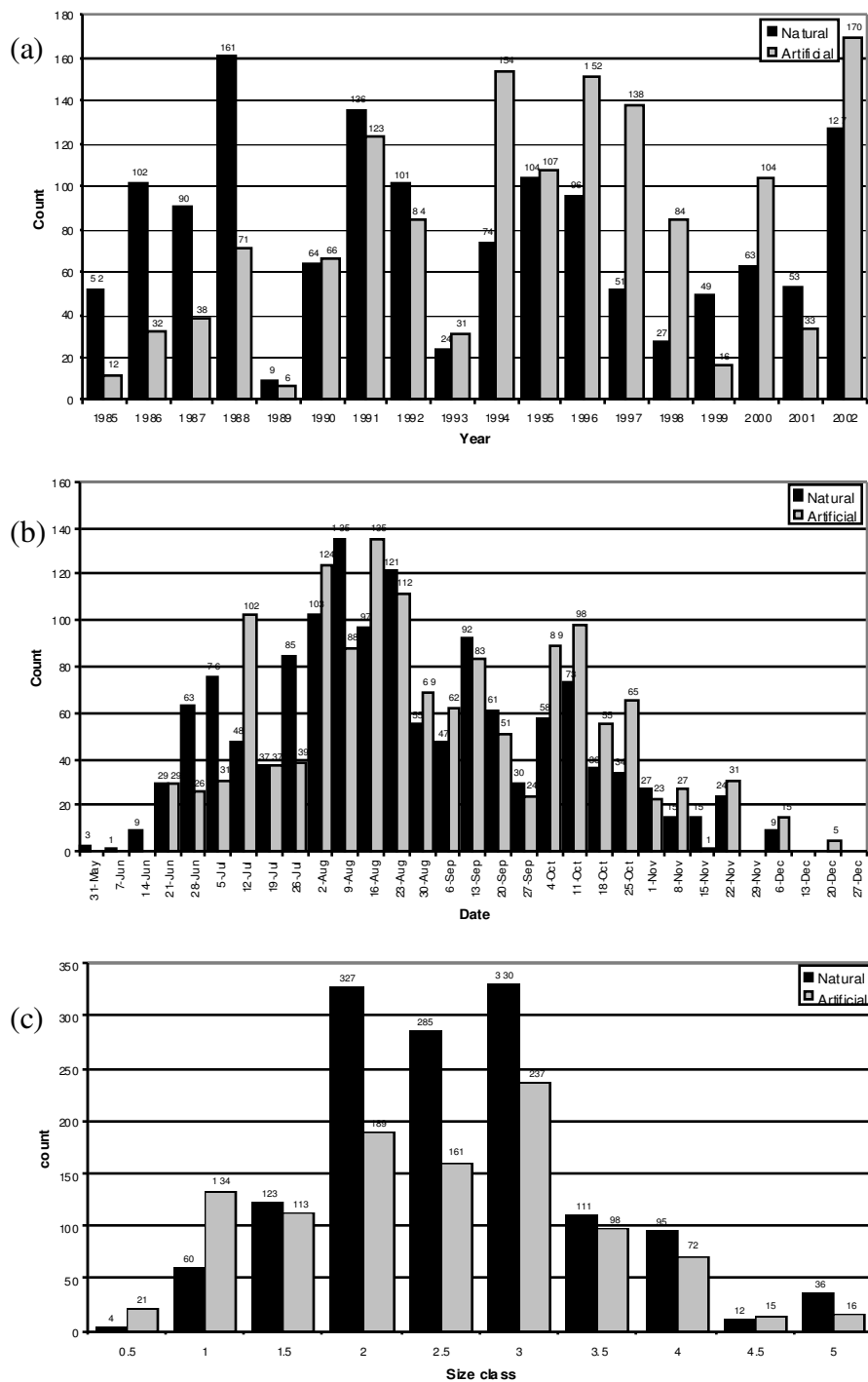
Figure 3.7   The historical data available for the Milford Road avalanches from 1985 to 2002 showing the (a) Inter-annual variability of all avalanche occurrences (b) Time of year of all avalanche occurrences (c) Size frequency of all avalanche occurrences

3.5.3 Correlation between snow depth and avalanche occurrences

In a maritime climate avalanche occurrences are often related to new snowfalls (e.g. LaChapelle, 1966; Fitzharris, 1979; Conway, et al., 2000) and consequently an increase in avalanche occurrence might be expected in years with greater snow depth (mean, median, maximum), or highly variable snow depth (standard deviation). Therefore, the relationships between annual snow depth variables:

❋ Mean snow depth

❋ Median snow depth

❋ Standard deviation (Std. Dev)

❋ Maximum depth (Max depth)

and annual avalanche variables:

❋ All avalanches (All Avo)

❋ Artificial avalanches (X Avo)

❋ Natural avalanches (N Avo)

were examined. Significant correlation coefficients are shown in Table 3.4.

Table 3.4   Spearman rank order correlation coefficients between snow depth variables and avalanche occurrences

Variable	Mean	Median	Std. Dev	Max depth	N Avo	X Avo	All Avo
Bolded correlations are significant at p <.05 / Shaded correlations are significant at p <.01, n=13							
Mean	■	**0.90**	**0.64**	**0.93**	0.47	**0.64**	0.52
Median		■	**0.78**	**0.86**	0.45	**0.60**	0.49
Std. Dev			■	**0.66**	0.18	0.36	0.23
Max depth				■	0.34	0.53	0.38
N Avo					■	**0.71**	**0.89**
X Avo						■	**0.94**
All Avo							■

Table 3.4 shows that there are high correlations between the snow depth variables and between the avalanche occurrence variables. The highest correlation coefficients between

snow depth variables and avalanche occurrence variables are between artificial avalanches and mean snow depth (0.64) and median snow depth (0.60), indicating that years with greater snow depth receive more active control. The lack of other significant correlations suggests that the annual averaged snow depth variables are not the main controller on avalanche occurrences, and that other factors (e.g. the rate of snowfall) may be more influential.

3.5.4 Correlation between synoptic types and atmospheric circulation indices

It is expected that because of the selection, location and obvious interaction of the atmospheric circulation indices selected, many will be highly correlated with each other. Therefore, before relating these measures of atmospheric circulation to snow depth and avalanche occurrences, the association between these indices will be highlighted. Table 3.5 shows that the zonal indices over New Zealand of Z1, Z3, Z4 and MZ3 and MZ4 are all highly positively correlated with each other, as are the meridional indices, M1, M2 and MZ3. This is to be expected as they respectively measure the zonal or meridional flow over New Zealand. Interestingly, despite the documented influence of the SOI on the New Zealand climate (Salinger, 1980a, 1980b; Salinger and Mullan, 1999; Sturman and Tapper, 1996), in this analysis only the Blocking group and the NE synoptic type are highly significantly correlated with the SOI 6, while the MZ1 index is only significantly correlated. The SOI 12 is highly significantly correlated only to the Blocking grouping of the synoptic types, and significantly correlated to the SW synoptic type. Examining the synoptic types there are many significant and highly significant correlations with the Trenberth indices, e.g. the SW synoptic type is highly correlated with Z1, Z3, Z4, M1, MZ3 and MZ4 indices. The large number of highly correlated synoptic types with the Z2 index highlight the connection between the strong pressure gradient from west to east across the South Island, and the related synoptic types. These inter relations must be considered when examining trends between atmospheric circulation and snow depth and avalanche occurrences.

Table 3.5   Spearman rank order correlation coefficients between the predictors

Bolded correlations are significant at p <.05
Shaded correlations are significant at p <.01, n=14

Variable	T	SW	TNW	TSW	H	HNW	W	HSE	HE	NE	HW	R	Trough	Zonal	Blocking	SOI 12	SOI 6	Z1	Z2	Z3	Z4	M1	M2	M3	MZ1	MZ2	MZ3	MZ4
T	■	0.66	0.20	0.09	-0.68	-0.44	0.12	-0.03	-0.73	-0.42	-0.46	0.01	0.90	-0.61	-0.65	-0.48	-0.44	0.41	-0.39	0.30	0.67	0.41	0.18	0.38	0.03	0.05	0.54	0.53
SW		■	-0.21	-0.54	-0.19	0.14	0.35	-0.51	-0.58	-0.49	-0.34	-0.32	0.51	0.00	-0.85	-0.65	-0.50	0.81	0.26	0.68	0.85	0.70	0.53	0.64	0.12	0.43	0.72	0.81
TNW			■	0.61	-0.56	-0.40	-0.43	0.20	-0.20	0.22	-0.20	0.29	0.45	-0.67	0.09	0.20	0.17	-0.29	-0.67	-0.29	-0.24	-0.31	-0.51	0.04	0.33	-0.28	-0.44	0.02
TSW				■	-0.43	-0.56	-0.41	0.47	0.03	0.44	-0.26	0.41	0.30	-0.65	0.35	0.30	0.25	-0.68	-0.83	-0.72	-0.44	-0.45	-0.61	-0.26	-0.10	-0.65	-0.57	-0.40
H					■	0.49	-0.01	-0.42	0.67	-0.23	0.32	0.08	-0.81	0.82	0.22	-0.00	-0.11	-0.17	0.67	-0.14	-0.43	-0.13	0.07	-0.19	-0.25	-0.10	-0.19	-0.26
HNW						■	0.40	-0.17	0.25	0.02	0.27	-0.41	-0.62	0.82	-0.04	-0.13	-0.06	0.25	0.80	0.27	0.03	0.28	0.32	0.17	0.02	0.40	0.15	-0.12
W							■	-0.31	-0.44	-0.25	-0.14	-0.52	-0.05	0.42	-0.50	-0.38	-0.35	0.63	0.57	0.57	0.48	0.66	0.79	0.32	-0.24	0.60	0.66	0.24
HSE								■	0.13	0.52	0.04	0.16	0.02	-0.37	0.58	0.45	0.50	-0.50	-0.44	-0.34	-0.31	-0.49	-0.52	-0.42	0.15	-0.09	-0.39	-0.59
HE									■	0.23	0.54	0.11	-0.76	0.38	0.78	0.51	0.45	-0.63	0.12	-0.53	-0.73	-0.57	-0.49	-0.44	0.11	-0.37	-0.61	-0.65
NE										■	0.00	-0.28	-0.16	-0.17	0.59	0.60	0.83	-0.39	-0.35	-0.30	-0.23	-0.34	-0.40	-0.22	0.27	-0.06	-0.41	-0.34
HW											■	0.11	-0.58	0.30	0.51	0.17	0.11	-0.23	0.19	-0.19	-0.25	-0.06	0.01	-0.07	-0.04	-0.16	-0.17	-0.39
R												■	0.03	-0.29	0.15	-0.21	-0.40	-0.52	-0.32	-0.54	-0.51	-0.41	-0.41	-0.23	-0.41	-0.61	-0.59	-0.32
Trough													■	-0.80	-0.57	-0.28	-0.22	0.35	-0.60	0.26	0.56	0.20	-0.01	0.24	0.18	0.04	0.34	0.60
Zonal														■	0.00	-0.08	-0.14	0.18	0.93	0.20	-0.10	0.23	0.43	0.02	-0.21	0.30	0.16	-0.13
Blocking															■	0.70	0.71	-0.80	-0.24	-0.64	-0.74	-0.68	-0.61	-0.53	0.13	-0.38	-0.71	-0.81
SOI 12																■	0.86	-0.50	-0.31	-0.37	-0.47	-0.53	-0.40	-0.50	0.31	-0.14	-0.38	-0.44
SOI 6																	■	-0.37	-0.31	-0.20	-0.31	-0.50	-0.47	-0.39	0.53	0.05	-0.37	-0.33
Z1																		■	0.46	0.95	0.81	0.64	0.67	0.42	0.20	0.79	0.79	0.83
Z2																			■	0.50	0.13	0.36	0.58	0.12	-0.17	0.55	0.35	0.08
Z3																				■	0.68	0.43	0.56	0.20	0.29	0.92	0.69	0.70
Z4																					■	0.81	0.67	0.62	0.05	0.46	0.89	0.75
M1																						■	0.85	0.83	-0.26	0.24	0.81	0.53
M2																							■	0.47	-0.44	0.43	0.83	0.41
M3																								■	0.03	0.02	0.45	0.53
MZ1																									■	0.37	-0.11	0.31
MZ2																										■	0.51	0.43
MZ3																											■	0.61
MZ4																												■

3.5.5 Correlations between snow depth and atmospheric circulation indices

Snow depth has been shown to have a large annual variability. The reasons for this variability are unknown, but changes in atmospheric circulation patterns may explain some or all of this variability. Correlations between SOI and Trenberth circulation indices and snow depth variables are examined in Table 3.6.

Table 3.6   Spearman rank order correlation coefficients between snow depth variables vs. SOI and Trenberth circulation indices

	Bolded correlations are significant at p <.05 Shaded correlations are significant at p <.01, n=13												
Variable	SOI 12	SOI 6	Z1	Z2	Z3	Z4	M1	M2	M3	MZ1	MZ2	MZ3	MZ4
Mean	-0.50	-0.30	0.47	0.06	0.44	0.44	0.29	0.21	0.30	-0.04	0.41	0.25	0.47
Median	**-0.70**	-0.55	0.37	0.15	0.31	0.38	0.33	0.19	0.43	-0.18	0.21	0.19	0.42
Std. Dev	**-0.59**	-0.34	0.13	0.27	0.14	0.23	0.25	0.15	0.39	-0.30	0.13	-0.01	0.04
Max depth	-0.37	-0.16	0.40	0.10	0.42	0.26	0.11	0.08	0.20	0.09	0.45	0.06	0.37

Table 3.6 shows that there is only one significant, and one highly significant correlation, which are with SOI 12 and the standard deviation (Std. Dev.) of snow depth and median snow depth respectively. Kelly(1992) using an empirically calculated snow depth also found this negative correlation with the SOI, though it was only significant at the p<0.1 level. de Lautour(1999) using modelled snow accumulation in the South Island hydro catchments also found a weak negative correlation with SOI. Gordon(1985) using a much larger dataset, examined the relationships between the SOI vs. precipitation and temperature found a significant positive correlation with air temperature for the west coast as a whole.

In this study no significant correlations could be found between the Trenberth indices and the snow depth variables. In contrast, Salinger(1980a) when examining precipitation, found that weather stations in the south and south west of the South Island correlated positively with the Z2 index. These results suggest that while precipitation is an implicit

component of the snow depth at Mt Belle, the processes which control snow depth are different or only part of those that form precipitation in this region. Furthermore, the negative correlation with the SOI and the work of Gordon(1985), Salinger and Mullan(1999) and Salinger et al.(2001) suggests that the temperature shifts associated with the SOI may be more important for snow depth than the precipitation shifts. However, as noted earlier, this study only considers a short record of snow depths, which is confined mainly to one positive phase of the IPO with a high frequency of El Niño years.

Correlations between synoptic type, groupings and snow depth variables in Table 3.7 indicate that anticyclones to the west (HW), resulting in light winds over New Zealand have highly significant negative correlations with mean, median and maximum snow depths. Anticyclones to the east (HE), resulting in moderate northwesterly flow over the South Island has a highly significant negative correlation with mean snow depth and significant negative correlation with median snow depth. These two synoptic types are normally associated with calm clear weather, with moderate winds at most, resulting from the low horizontal pressure gradient and descending air mass. This type of weather has been associated with high measured snowmelt rates (Neale and Fitzharris, 1997), and negative mass balance years for glaciers, when it has occurred anomalously in the accumulation season (Fitzharris et al., 1997). As the blocking group is comprised of these two synoptic types and three others, it is not surprising that there is a significant and highly significant negative correlation with the mean and median snow depth respectively.

Table 3.7   Spearman rank order correlation coefficients between snow depth variables and synoptic types

| | Bolded correlations are significant at p <.05
Shaded correlations are significant at p <.01, n=13 | | | | | | | | | | | | | |
Variable	T	SW	TNW	TSW	H	HNW	W	HSE	HE	NE	HW	R	Trough	Zonal	Blocking
Mean	0.40	0.46	0.02	-0.02	-0.31	-0.07	0.34	0.02	**-0.69**	-0.09	**-0.80**	-0.02	0.45	-0.13	**-0.62**
Median	0.42	**0.59**	-0.01	-0.09	-0.11	0.04	0.21	-0.16	**-0.59**	-0.34	**-0.72**	0.21	0.37	-0.03	**-0.69**
Std. Dev	0.04	0.36	-0.19	-0.19	0.09	0.31	0.06	0.01	-0.25	-0.03	-0.27	0.26	-0.05	0.18	-0.26
Max depth	0.24	0.42	0.09	-0.05	-0.21	0.05	0.22	0.03	-0.50	-0.01	**-0.76**	0.00	0.32	-0.07	-0.49

Table 3.7 also shows a significant positive correlation with median snow depth and the SW synoptic type, resulting in southwesterly flow. This can be attributed to this synoptic type being associated with the passage a cold front, or several fronts, which bring cooler air from the south west, and cause frontal precipitation which is often compounded by orographic lifting against the Southern Alps. In contrast to the work of Kelly(1992), synoptic types with strong west to northwest flows such as TNW and W had no significant positive correlation with snow depth.

3.5.6 Correlations between avalanches and atmospheric circulation indices

Avalanche occurrences, like snow depth, have been shown to have large annual variability. The reasons for this variability are unknown, but as seen in section 3.5.3 there is a significant correlation between some snow depth variables and avalanche occurrence variables. Changes in atmospheric circulation patterns may better explain some or all of this variability. Correlations between SOI and Trenberth circulation indices and avalanche occurrences variables are examined in Table 3.8.

Table 3.8   Spearman rank order correlation coefficients between avalanche occurrence variables and Trenberth circulation indices

Variable	SOI 12	SOI 6	Z1	Z2	Z3	Z4	M1	M2	M3	MZ1	MZ2	MZ3	MZ4
Bolded correlations are significant at p <.05
Shaded correlations are significant at p <.01, n=14
N Avo	-0.33	-0.23	0.48	-0.35	0.33	**0.78**	**0.54**	0.30	0.53	0.05	0.09	**0.55**	**0.69**
X Avo	-0.48	-0.32	**0.72**	0.13	**0.67**	**0.85**	**0.62**	0.47	0.49	0.14	**0.55**	**0.77**	**0.59**
All Avo	-0.43	-0.30	**0.67**	-0.09	**0.57**	**0.91**	**0.65**	0.46	**0.53**	0.10	0.38	**0.78**	**0.67**

Table 3.8 shows that there are highly significant positive correlations between Z1, Z3, Z4, MZ3, MZ4 and avalanche occurrence variables. Significant positive correlations also exist between Z3, M1, M3, MZ2, MZ3, MZ4 and avalanche occurrence variables. Interestingly, the Z4 index has a very high correlation coefficient, higher than the Z3 index, which is centred more closely to the Milford Road region. This is also the case for

the indices MZ3 and MZ4 having higher correlations than the index MZ2, which uses a station closer to the Milford Road region. This suggests that the indices measured to the north, are very sensitive to the circulation patterns and hence the avalanche occurrences on the Milford Road, further to the south. This may be because off the effect of the Southern Alps disturbing the pressure field over the land area of New Zealand. This would affect the pressure differences between Auckland and Christchurch, Z1, more strongly than the pressure difference between Raoul Island and Chatham Island, Z4. The Z4 index is also measured across a larger area, from 29° to 44°S, thereby capturing more zonal flows across the New Zealand region as a whole, but also capturing more of the southwesterly airflow, and resultant pressure difference because of the more northerly location of Raoul Island. This idea is strongly supported by the high correlation coefficient for the MZ3 index, which measures the strength of the southwesterly airflow, and the MZ4 index which measures the strength of the westerly airflow. These three indices are highly correlated in Table 3.5. These results of this short record are in contrast with the correlations examined for snow depth, where SOI 12 was significant, while the Trenberth indices were not, further suggesting that snow depth is not the only control on the number of avalanche occurrences.

The correlations between synoptic type and synoptic groupings and avalanche occurrence variables are shown in Table 3.9. The frequencies of a trough over New Zealand (T), resulting in strong westerly to south westerly winds over the west coast of the South Island, and of southwesterly flows (SW) synoptic type both have highly significant positive correlation with all avalanche occurrence variables (Table 3.9). Anticyclones to the east (HE), resulting in moderate northwesterly flow over the South Island has highly significant negative correlation with all avalanche occurrence variables. Anticyclones centred over the North Island (H), resulting in light southwesterlies over the South Island have a highly significant negative correlation with natural avalanches (N Avo) and a significant negative correlation with all avalanche occurrences (All Avo). This also means that the trough grouping has highly significant positive correlations with natural avalanche (N Avo) and all avalanche occurrences (All Avo) and a significant positive

correlation with artificial avalanche occurrences (X Avo). The blocking group has highly significant negative correlations with all avalanche occurrence variables.

Table 3.9   Spearman rank order correlation coefficients between avalanche occurrence variables and synoptic types

Variable	T	SW	TNW	TSW	H	HNW	W	HSE	HE	NE	HW	R	Trough	Zonal	Blocking
	Bolded correlations are significant at p <.05 Shaded correlations are significant at p <.01, n=14														
N Avo	**0.78**	**0.67**	0.30	0.08	**-0.68**	-0.28	0.09	-0.19	**-0.80**	-0.05	-0.51	-0.22	**0.84**	-0.52	**-0.68**
X Avo	**0.76**	**0.81**	-0.11	-0.35	-0.50	0.11	0.47	-0.05	**-0.75**	-0.28	-0.49	-0.44	**0.60**	-0.14	**-0.72**
All Avo	**0.85**	**0.81**	0.03	-0.20	**-0.62**	-0.09	0.35	-0.13	**-0.81**	-0.23	-0.48	-0.40	**0.76**	-0.34	**-0.75**

The significant negative correlations with HE and H are expected. These synoptic types are normally associated with calm clear weather, with moderate winds at most, delivering large amounts of energy into the snowpack (Neale and Fitzharris, 1997). This is likely to consolidate and strengthen the snowpack, through increased sintering and melt freeze metamorphism, reducing the avalanche occurrence potential. As the blocking group is comprised of these two synoptic types and three others, it is not surprising that there is a significant negative correlation there also. The highly significant positive correlations with T and SW synoptic types are also expected. The SW synoptic type has also been shown to be significant for snow depth, suggesting that this synoptic type brings new snow which is associated with the passage of a cold front, followed by cooler air from the south west. This also suggests that while new snow is an important parameter for avalanche occurrence, increased wind speed and precipitation is also very important for the formation of high avalanche potential. The T synoptic type, having no significant correlation with snow depth, suggests that it either brings small amounts of snowfall, or rainfall, probably from frontal precipitation, enhanced by orographic lifting against the Southern Alps. As the trough group is comprised of four synoptic types, including these two, it is not surprising that there is a significant positive correlation there also.

Unfortunately, Kidson(2000) in comparing temperature and precipitation patterns to synoptic groupings noted that while departures in temperature and precipitation patterns around New Zealand had high statistical significance, they are small in comparison with monthly standard deviations of around 0.9^{o}C and 46% of normal respectively. Therefore,

while the correlation coefficients are high for the grouped synoptic types and avalanche occurrences, there is an opportunity to further develop these groupings and slightly modify them for use for the Milford Road region. Kidson(2000) grouped the synoptic types in terms of windflow for all of New Zealand. However, these do not all apply well to the Milford Road region. Therefore, the synoptic types were arranged into new groups, to better account for conditions in Fiordland and two new classification schemes were created, Groups_B and Westerly/Not westerly (Table 3.10).

Table 3.10   Synoptic type grouping, with the first three groups, marked with a *, as outlined in Kidson(2000), the next five constitute a modified classification redefined for the Milford Road region

Grouping	Synoptic Types
Trough group *	T, SW, TNW, TSW
Zonal group *	H, HNW, W
Blocking group *	HSE, HE, NE, HW, R
Trough_B group	T, SW, TNW, TSW
Zonal_B group	HNW, W, HE
Blocking_B group	H, HSE, NE, HW, R
Westerly	T, SW, HNW, W, HE
Not Westerly	TNW, TSW, H, HSE, NE, HW, R

Group_B, rearranges the Kidson(2000) zonal and blocking groups so that the H synoptic type moves from the Zonal group to Blocking_B and the HE synoptic type moves from the Blocking group to Zonal_B. The Trough grouping remains unchanged. The Westerly, or Not Westerly grouping arranges all synoptic types with any resultant westerly airflow into Westerly, and the remainder into Not Westerly. This separation into Westerly and Not Westerly flow was undertaken as anecdotal evidence from the forecasters' observations suggested that the presence or strength of these flows may control the intensity of an avalanche season (Wilkins, pers. comm., 2004). This rearrangement of synoptic types into Milford Road specific groupings in terms of windflow, significantly increases the correlations as shown in Table 3.11.

Table 3.11   Spearman rank order correlation coefficients between avalanche occurrence
variables and synoptic type groupings

	Bolded correlations are significant at p <.05 Shaded correlations are significant at p <.01 Underlined correlations are significant at p <.001, n=14							
Variable	Trough	Zonal	Blocking	Trough_B	Zonal_B	Blocking_B	Westerly	Not
Natural Avo	**0.84**	-0.52	**-0.68**	**0.84**	-0.44	**-0.88**	0.49	-0.49
Art Avo	**0.60**	-0.14	**-0.72**	**0.60**	-0.06	**-0.79**	**0.88**	**-0.88**
All Avo	**0.76**	-0.34	**-0.75**	**0.76**	-0.26	**-0.89**	**0.78**	**-0.78**

Table 3.11 shows that the new grouping, Blocking_B, has increased the correlation coefficients from highly significant to very highly significant with correlation coefficients for all avalanche occurrence variables significant at the $p \leq 0.001$ (two tailed) level. This supports the idea that the H synoptic type is more similar to the other types in the blocking group while the HE is more similar to the others in the zonal group for the Milford Road region. The Westerly or Not Westerly grouping also has very highly significant correlation coefficients for X Avo and All Avo. This suggests that the westerly windflow and associated precipitation, or absence thereof, is critical for avalanche occurrences. This is further supported by the high correlation coefficients obtained using the Z1, Z4, MZ3, and MZ4 Trenberth circulation indices. These results are similar to those of Fitzharris and Bakkehøi(1986) and Fitzharris(1987) who suggested that not one climatology is responsible for large avalanche winters in Norway and Canada, but rather a grouping or a range of synoptic types. Schneebeli et al.(1997) also noted this for western and central parts of the Swiss Alps, which needed several different weather situations for large avalanche winters. In the examination of longer, 50 year, records in Switzerland, Laternser and Schneebeli(2002) were unable to detect long term changes in avalanche activity, though serious concerns with their data quality were expressed.

3.6 Conclusions

Graphical and statistical analysis of the snow depth showed that large variability exists both inter-annually and intra-annually, though snow depth was less variable than for other sites east of the main divide in the South Island. Graphical and statistical analysis of the snow avalanche regime was also undertaken, revealing large inter-annual variability. A marginally significant trend in artificial avalanche occurrence increasing at 4.6 avalanches year^{-1} was found and thought to relate to an increasing level of avalanche control. However, correlation analysis showed that there is a positive relationship between snow depth and artificial avalanche occurrence, suggesting that years with greater snow receive more active control.

Annual snow depth was not correlated to any of the Trenberth circulation indices, but had a highly significant negative correlation with the SOI. Highly significant negative correlation coefficients were also found with synoptic types that produce clear settled weather, melting snow, and highly significant positive correlation coefficients with synoptic types that bring strong wind, cold air, and precipitation, resulting in snowfall.

Avalanche occurrences showed highly significant positive correlations with Trenberth indices that measure the strength of the airflow from the westerly quarter. This was further supported by the highly significant positive correlations with the SW and T synoptic types, and the highly significant negative correlations with the H and HE synoptic types and avalanche occurrences. Grouping and regrouping the synoptic types further supported these ideas with highly significant positive correlations between Troughs and Westerly groups with avalanche occurrence variables, and highly significant negative correlations between Blocking, Blocking_B and Not Westerly groups with avalanche occurrence variables. Despite the influence of the westerly circulation to snow depth and avalanche occurrence, no significant correlation with avalanche occurrences and the SOI could be uncovered.

These results concur with anecdotal observations and local experience, which has suggested that because of the location of the Milford Road the westerly flow is a critical controller on the snow depth, and thereby avalanche occurrences to some extent. It is encouraging that a relatively short time series of snow depth and avalanche occurrence, despite being confined mainly to one phase of the IPO with a high frequency of El Niño years, has yielded positive results compared to other studies.

4.0 Avalanche risk evaluation

4.1 Introduction

As shown in Chapter Two and Chapter Three the Milford Road has a severe avalanche regime and an increasing volume of traffic. This chapter examines the application of two risk assessment methods, the Avalanche Hazard Index (AHI) and the probability of death to individuals (PDI), to examine the present avalanche risk on the highway. This will be compared to the risk of a theoretical uncontrolled avalanche regime, as estimated by Fitzharris and Owens(1980), but with traffic at 2002 levels. The difference between the present controlled and theoretically uncontrolled regime will then be estimated to give a measure of the effectiveness of the Transit New Zealand Milford Road Avalanche Programme. Firstly, this chapter will review how the AHI has changed since its inception in 1974 (Avalanche Task Force, 1974) and since its application to the Milford Road in 1980 (Fitzharris and Owens, 1980). The method for calculating PDI is also reviewed and modifications are suggested. Furthermore, the sensitivity of these methods to the various assumptions made in the analysis are examined and the results are compared to other commonly accepted levels of risk for other hazards, including avalanches, both in New Zealand, and elsewhere around the world. Finally, the level of risk on the Milford Road is compared to other roads in Switzerland in terms of collective risk and with Rogers Pass, B.C., Canada in terms of the AHI.

4.2 Methods of avalanche risk assessment

4.2.1 Avalanche Hazard Index

The AHI was first developed in 1974 for use on highways in British Colombia, Canada (Avalanche Task Force, 1974). It was designed as a numerical expression of damage and loss as a result of the interaction between vehicles on a road and a snow avalanches

(Schaerer, 1989). Since then it has been used on other roads, elsewhere in Canada (e.g. Schaerer, 1989; Stethem et al., 1995), the United States of America (e.g. Armstrong, 1981) and on the Milford Road, New Zealand (Fitzharris and Owens, 1980). The AHI is used to determine how serious avalanche problems are to allow comparisons of the hazard of different highways to establish priorities and determine the appropriate level of avalanche safety management and to show where control measures have the greatest effect (Schaerer, 1989). The AHI considers both moving and waiting traffic, and is a function of:

* ❋ The size and type of avalanche
* ❋ The frequency of avalanche occurrences
* ❋ The number of avalanche paths and the distance between them
* ❋ The total length of highway exposed
* ❋ The traffic volume
* ❋ The traffic speed
* ❋ The type of vehicle

Fitzharris and Owens(1980), using the Avalanche Task Force(1974) approach, calculated the AHI for the Milford Road using the encounter probability for moving traffic according to the following equation:

$$P_m = \frac{T(L+D)F}{V.3600.24} \qquad (4.1)$$

where:

$P_m =$ encounter probability for moving vehicles to be hit by avalanches (year^{-1})

$T =$ average daily traffic volume per 24 hour counted in both directions (vehicles d^{-1})

$V =$ average speed of the traffic (ms^{-1})

$L =$ width of avalanche = average length of the road covered by the avalanche (m)

$D =$ stopping distance on a snow-covered road for a vehicle with the speed V (m)

$F =$ average frequency of avalanche occurrence (year^{-1})

This encounter probability is for an individual vehicle, regardless of whether it is a car, bus, truck, maintenance vehicle, travelling in a group or alone. Moving vehicles are exposed to the avalanches for only a few seconds, and the chances of being hit are low. However, the exposure time is much longer for vehicles that have stopped in the avalanche tracks. Waiting traffic has proven to be a significant cause of avalanche accidents (Schaerer, 1989). Vehicles may be stopped or waiting because of previous avalanche activity, fitting snow chains, or taking photographs (Fitzharris and Owens, 1980). The probability of encounter for waiting traffic depends on the probability of a subsequent avalanche in an adjacent or another part of the same path, frequency of avalanche occurrence and the number of vehicles waiting. Fitzharris and Owens(1980) calculated the AHI for the Milford Road using the encounter probability for waiting traffic according to the following equation:

$$P_w = P_s.F.N_w \qquad\qquad (4.2)$$

where:

$P_w =$ encounter probability for waiting traffic to be hit by avalanches (year^{-1})

$F =$ average frequency of avalanche occurrence (year^{-1})

$N_w =$ number of vehicles in the adjacent avalanche track ($=L/15$m)

$L =$ width of avalanche = average length of road covered by the avalanche (m)

$P_s =$ probability of a subsequent avalanche in an adjacent or another part of the same path. Fitzharris and Owens(1980) used 0.15.

Fitzharris and Owens(1980) undertook the assessment of the AHI on the Milford Road, by estimating the frequency and size of avalanches from historical information (e.g. Smith, 1947), local knowledge (e.g. Andrews pers. comm., 1979 [In] Fitzharris and Owens, 1980) as well as topographical and botanical field investigations. Estimates were made for the size and frequency of the three different types of avalanches, powder snow (k_1), light snow (k_2) and deep snow (k_3). Smith(1947) found that because of the very steep

terrain certain snow conditions result in airborne avalanches. Therefore Fitzharris and Owens(1980) introduced an additional avalanche type, plunging avalanches (k_4). These different avalanche types have weightings that consider the relative cost and consequence of an encounter, as seen in Table 4.1.

Table 4.1   Avalanche type and weighting (Source: Fitzharris and Owens, 1980, p.13)

Avalanche type	Weighting
k_1 Powder snow	1
k_2 Light snow	4
k_3 Deep snow	10
k_4 Plunging avalanche	12

Using these weightings, and the different frequencies and avalanche widths associated with each, Fitzharris and Owens(1980) calculated the AHI for the Milford Road using the encounter probability for moving and waiting traffic according to the following equation:

$$AHI = \sum_{k=1}^{4} W_k (P_m + P_w)$$ (4.3)

where:

$k =$ index for avalanche type k_1 to k_4

$W =$ weighting for avalanche type

$P_m =$ encounter probability for moving traffic

$P_w =$ encounter probability for waiting traffic

The 1980 AHI on the Milford Road was calculated at 46 for a winter traffic volume of 80 vehicles per day, where $P_m = 2$ and $P_w = 44$. According to the North American practice to group highways with respect to the avalanche hazard the Milford Road rated at a moderate hazard in 1980 (Table 4.2).

Table 4.2   Hazard level, AHI, and minimum management. Modified from Fitzharris and Owens(1980)

Hazard	AHI	Minimum management level
Very Low	< 1	Post signs in avalanche paths
Low	1 to 10	Warnings and road closures
Moderate	10 to 100	Avalanche control, selected sites
High	> 100	Full avalanche control, artificial release, structures

Moderate hazard was suggested to require avalanche control at selected sites, and be supplemented by warnings and occasional closures (Fitzharris and Owens, 1980). This was the normal practice on the Milford Road through the early 1980s. However, as the traffic volumes have increased the avalanche management has become more rigorous with the implementation of a full avalanche control programme, including the employment of experienced avalanche forecasters in 1984.

Schaerer(1989) modified the descriptions of the avalanche types and their weightings (Table 4.3), which has resulted in any subsequent calculations of AHI to be about 0.7 to 0.9 times the indices calculated with the original weightings.

Table 4.3   Avalanche type, description and weighting. Modified from Schaerer(1989)

Avalanche type	Avalanche description	Weighting
j_1 Powder snow	Less than 0.1m deep deposit and crosses the road at speeds less than 20ms^{-1}. Conditions similar to those from blowing snow.	0
j_2 Slough	Less than 0.3m deep deposit, covers only part of the road, and often originates from a road cutting. Able to drive over or around the deposit.	0
j_3 Light snow	Between 0.3 and 1.0m deep deposit and flowing beyond the road. Cars would be pushed off the road but would not be buried	3
j_4 Deep snow	More than 1m deep deposit, and	10
j_5 Plunging avalanche	High speed dry snow falling long distances over cliffs or steep slopes. Extremely destructive due to their high wind speeds air blasts.	12

Schaerer(1989) also standardised the method for calculating the AHI, provided some examples, and thereby made the process more repeatable. In doing so he restated the equations for moving traffic as:

$$P_{m_{ij}} = \frac{T(L_{ij} + D)}{R_{ij}.V.24000}$$

(4.4)

where:

$T =$ average daily traffic volume counted in both directions (vehicles d^{-1})

$L_{ij} =$ average length of road covered by avalanches of type j at avalanche path i (m)

$D =$ stopping distance for a vehicle with speed V on a snow covered road (m)

$R_{ij} =$ return period of occurrence of avalanches of class j at the avalanche path i (years)

$V =$ average speed of traffic (kmh^{-1})

Compared to the previous equation of P_m, changes are observed in the units of traffic speed (from ms^{-1} to kmh^{-1}) and the use of return period of avalanche occurrences, the reciprocal of frequency.

Schaerer(1989) also restated the equations for waiting traffic as:

$$P_{w_{i+1j}} = P_s . \frac{N_{wi+1j}}{R_{i+1j}}$$

(4.5)

where:

$P_s =$ probability that an avalanche will run along path $i+1$ while the traffic is waiting

$N_{wi+1j} =$ number of vehicles exposed to adjacent avalanche path, $i+1$

$R_{i+1j} =$ return period of occurrence of adjacent avalanches of type j at the avalanche path i (years)

P_s values ranging from 0.05 and 0.3 have been determined from observations at Rogers Pass, Canada (Schaerer, 1989). Fitzharris and Owens(1980), with no information about how an avalanche occurrence would be related to another avalanche at an adjacent site used a value of 0.15 for P_s. Armstrong(1981) suggested a lower value of P_s at 0.03-0.05 for Red Mountain Pass in Colorado. Schaerer(1989) related the P_s value to the characteristics of the avalanche starting zones, noting that a high P_s value would be appropriate for avalanche paths with similar aspects and terrain characteristics.

Compared to the previous equation of P_w, changes can be observed with the use of the return period of avalanche occurrences, the reciprocal of frequency of avalanche occurrences per year. Otherwise the equation is the same; however a more thorough method of calculating the number of exposed vehicles (N_{wi+1j}), is used. To calculate the number of exposed vehicles Schaerer(1989) provided a series of equations that take into account the following factors:

* ❋ The average length of road each vehicle occupies (L_v) on a public road, normally 15m
* ❋ The waiting period (t), which is the time required for a road crew to react, normally 2 hours
* ❋ The safe waiting distance (S) between avalanche paths
* ❋ Average daily traffic volume (T)

Schaerer's(1989) equations work out the length of a queue of traffic (L_w), based on average traffic volume. The safe waiting distance between each avalanche path, combined with the queue length, will determine how many vehicles are then exposed in an adjacent avalanche path, in both directions. However, in this analysis queues have not been calculated using the average daily traffic volume, but rather the peak volume as flow is distinctly tidal, with traffic flow predominantly into Milford in the morning and out in the afternoon (Figure 4.1). While using the June peak flow rate to determine the queue length for waiting traffic could lead to an overestimation at times, there are also

times when this may in fact still be an underestimation e.g. the final two hours preceding road closure for avalanche hazard during the spring shoulder season.
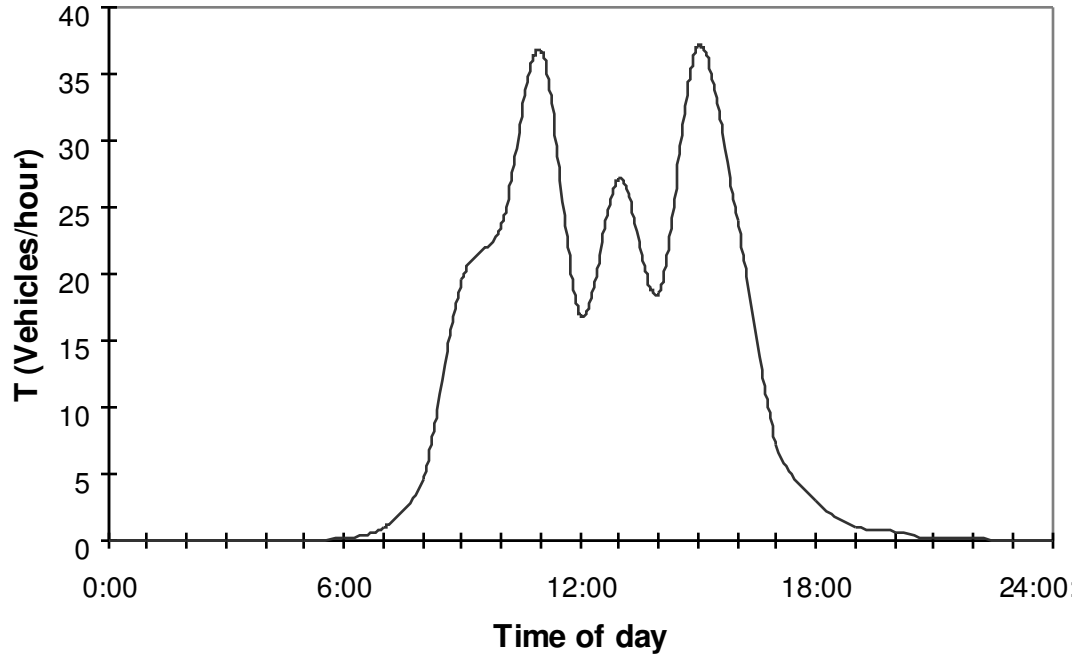
Figure 4.1   Daily winter flow distribution at Falls Creek, June 2003 (Source: URS, 2004).

Schaerer(1989) also considered the case of a second avalanche on a path which is already blocking the traffic. The probability that traffic is likely to be hit by another avalanche in path i is represented as:

$$P'_{w_{ij}} = 0.5P'_s \frac{N_{wij}}{R_i}, N_{wij} \le \frac{L_{ij}}{L_v} \qquad (4.6)$$

where:

P'_s =   probability of a second avalanche running along path i once one avalanche has already occurred.

Schaerer(1989) suggested that values for P'_s can range from 0 to 0.5 and must be chosen from a study of the terrain and for most avalanche paths with a single starting zone $P'_s=0$. In this analysis P'_s has been set at 0 as avalanches need to be substantial to reach the road, and will usually clear instabilities in a given starting zone.

Finally, the resultant AHI was expressed as the weighted expected frequency of encounters of moving (P_m) and waiting (P_w) vehicles with j type avalanches, summed over a road with n avalanche paths in the following equation:

$$AHI = \sum_{i=1}^{n}\sum_{j=1}^{5}W_j(P_{mij} + P_{wij}) \qquad\qquad (4.7)$$

where:

$n =$ number of avalanche paths

$j =$ index for avalanche type j_1 to j_5

$W_j=$ weighting for type j avalanche

$P_{mij} =$ probability of encounter for a moving vehicle in path i with avalanche type j.

$P_{wij} =$ probability of encounter for a waiting vehicle in path i with avalanche type j.

The equations proposed by Schaerer(1989) have been used to calculate both the controlled and theoretically uncontrolled avalanche regime on the Milford Road for the present (2002) situation. Hereinafter, the parameters, length of waiting queue L_w, probability of an adjacent avalanche path avalanching P_s, length of road a vehicle occupies L_v, average speed V, and stopping distance D have been varied to examine the sensitivity and the influence of changes to these parameters to the final AHI. T has expressly not been varied, as it is the effect of the other assumptions on the AHI with present day traffic flow that is to be examined.

4.2.2 Probability of Death to an Individual

The PDI is a method used to express risk. It has been widely used for hazard assessment for a range of natural (e.g. landslides) and anthropogenic (e.g. dams) hazards. Weir(1998) undertook an assessment of risk on the Milford Road using a PDI and Fatal Accident Rate (FAR) methods, where FAR is expressed as the probability of a fatality per 100 million person hours of exposure. Weir(1998) postulated that it might be reasonable to expect a fatal accident every 20 years ± 10 years, based on accounts of two near misses (while the road was closed), and the road maintenance contract being tendered every three years. This assumption was then used in combination with exposure time to calculate FAR. However, to date, there has only been one fatality on the Milford Road since 1983 (on a closed road), and while the contract has been re-tendered on a three to five year basis, the contract has remained with what is now called Works Infrastructure since the programs inception. The probability assumptions of Weir(1998) are rather subjective, poorly constrained and based on too many broad intuitive assumptions with limited numerical basis. Therefore, it was deemed necessary to re-evaluate the PDI of the Milford Road more rigorously using some more stringent controls on the variables used, and following a less subjective, more repeatable methodology.

There have been some recent attempts to standardise a method to express the risk in terms of a PDI for a road with an avalanche hazard (Wilhelm, 1998; Kristensen et al., 2003; Margreth et al., 2003; Norwegian Geotechnical Institute (NGI), 2003). This chapter uses the methods described by Wilhelm(1998) and Margreth et al.(2003) as they are based on fewer assumptions, the variables considered are more clearly explained, they have a large data set of road traffic avalanche fatalities and they have also been applied to several pass roads in Switzerland.

According to Wilhelm(1998) and Margreth et al.(2003), the collective risk (expressed as deaths per year) on a road crossed by *n* avalanche paths is given by:

$$CR = \frac{T.\beta}{24} \sum_{i=1}^{n} \frac{L_i}{R_i.V} \lambda_i \qquad\qquad (4.8)$$

where:

$CR =$ collective risk (deaths year^{-1})

$T =$ average traffic volume for avalanche period (vehicles d^{-1})

$\beta =$ mean number of passengers per vehicle

$n =$ number of avalanche paths

$L_i =$ width of avalanche = average length of road covered by avalanche i (km)

$R_i =$ return period for avalanche i (years)

$V =$ speed in (kmh^{-1})

$\lambda_i =$ probability of death in a vehicle hit by an avalanche

While the parameters, T, β, n, L_i, V and λ_i can be measured on site or determined from historical records, Margreth et al.(2003) estimate R_i from slope angle in the starting zones and track. Slope angle and return period has been plotted for the available avalanche information from four pass roads with the remaining paths having their R_i extrapolated based on this relationship.

The risk, or probability of death to an individual (PDI) can be calculated according to Wilhelm (1998) and Margreth et al.(2003) using:

$$IR = \frac{z}{24} \sum_{i=1}^{n} \frac{L_i}{R_i.V} \lambda_i \qquad\qquad (4.9)$$

Where:

$IR =$ individual probability of death (year^{-1})

$z =$ number of passages per day of that person (i.e. commuter passengers z = 2, road crew z = 6)

The number of passages for the road crew depends on the condition of the road, and Wilhelm(1998) suggested that it be set at 6. For a daily commuter (e.g fishermen, bus drivers and helicopter pilots) the number of passes is 2. In Switzerland it has been found that on pass roads the mean number of passengers per vehicle β is normally 1.6 (Margreth et al., 2003). In the Swiss Alps between 1946 and 1999, 167 passengers were buried by avalanches in their vehicles, of whom 30 persons or 18% died. Therefore $\lambda_i = 0.18$ in equations (4.8) and (4.9). Kristensen et al.(2003), despite lacking data, suggested a higher death rate of 40% or 0.40 because of Norway's topographic characteristics, remoteness and long rescue time. Schaerer(1989) however, provided a range of probabilities of death depending on avalanche type, from 0.05 for light snow to 0.25 for deep snow avalanches. To better enumerate the PDI, the following improvements to the calculation to account for different avalanche types and resulting probabilities of death are suggested, for collective risk:

$$CR = \frac{T.\beta}{24} \sum_{i=1}^{n} \sum_{j=3}^{5} \frac{L_{ij}}{R_{ij}.V} \lambda_{ij} \qquad (4.10)$$

and individual risk:

$$IR = \frac{z}{24} \sum_{i=1}^{n} \sum_{j=3}^{5} \frac{L_{ij}}{R_{ij}.V} \lambda_{ij} \qquad (4.11)$$

where:

$j =$ avalanche type j_3 to j_5

Margreth et al.(2003), while not specifying different avalanche types, use 0.18 as the probability of death for an avalanche that can bury a vehicle, which may be approximately equal to the deep snow avalanche type of Schaerer(1989). However, Schaerer(1989) has a higher probability of death for this avalanche type at 0.25. In the absence of fatality data, plunging snow has been set at a high probability of death of 0.50 because of the continued evidence of the destructive nature of these avalanches on the Milford Road. Light snow avalanches were assigned a probability of death of 0.05 by Shearer(1989). As there is limited data available on the probability of death for each

avalanche type, this study uses numbers on the upper limit for avalanche type j_3 and j_4 as suggested by Schaerer(1989) and shown in Table 4.4.

Table 4.4   Avalanche type, probability of death and AHI weighting

Avalanche type	Probability of death	AHI weighting
j_1 Powder snow	0.00	0
j_2 Slough	0.00	0
j_3 Light snow	0.05	3
j_4 Deep snow	0.25	10
j_5 Plunging avalanche	0.50	12

Table 4.4 indicates that the AHI weightings are not uniformly proportional to the probability of death values. Most significant among these discrepancies is the difference between deep snow and plunging avalanches represented by an increase of 10 to 12 in the AHI, but 0.25 to 0.5 for the probability of death. This could suggest that either the probability of death for a plunging avalanche may be too high when compared to the AHI weightings, or that the AHI weightings do not sufficiently account for the destructive nature of plunging avalanches.

Unfortunately, one significant component of the risk that the PDI method as described by Wilhelm(1998) and Margreth et al.(2003) does not consider, is that to waiting traffic. This is because of the extensive model assumptions needed to make these calculations (Margreth et al., 2003). Kristensen et al.(2003) and NGI(2003), have described a series of complex calculations which attempt to enumerate the increased risk for waiting traffic with increasing queues, while simultaneously decreasing the risk over time, as the probability of a second avalanche reduces. Unfortunately, the calculations were based on cumulative assumptions that were considered unrealistic for application on the Milford Road. However, waiting traffic has been shown to be extremely important in applications of the AHI (Fitzharris and Owens, 1980; Schaerer 1989). In the case of the Milford Road, waiting traffic contributed over 95% to the AHI (Fitzharris and Owens, 1980). Therefore,

calculations of PDI using the Wilhelm(1998) and Margreth et al.(2003) method are likely to be lower than the actual PDI would be during periods involving waiting traffic. This makes the direct comparison of the PDI for avalanche risk difficult to compare with other hazards. However, the modified PDI method of Wilhelm(1998) and Margreth et al.(2003) does allow for easy comparisons between different roads, though this could be compromised if there were significant differences in the path configuration, e.g. single well spaced paths compared to clusters of paths.

The modified equations of Wilhelm(1998) and Margreth et al.(2003) have been used to calculate both the controlled and theoretically uncontrolled avalanche regime on the Milford Road for the present (2002) situation. Hereinafter, the ratio of cars to buses $C:B$, number of passengers per bus β_B number of passengers per car β_C, speed of the vehicles V, and the probability of death for each avalanche type λ_{ij} have been varied to examine the sensitivity and the influence of changes to these parameters to the final PDI. T has expressly not been varied, as it is the effect of the other assumptions on the PDI with present day traffic flow that is to be examined.

4.3   Results and Discussion

4.3.1 Avalanche Hazard Index Results

Using the equation 4.7, and modified weightings proposed by Schaerer(1989) the AHI of the controlled and theoretically uncontrolled avalanche regime on the Milford Road for the present (2002) situation has been calculated. Both of these analyses have been undertaken using the same input parameters:

$T =$ 381 estimated average daily winter traffic volume (URS, 2004)

$V =$ 11 ms^{-1} (Fitzharris and Owens, 1980)

$D =$ 20 m (Fitzharris and Owens, 1980)

$L_v =$ 15 m (Fitzharris and Owens, 1980)

$t =$ 2 h (Schaerer, 1989)

$L_w =$ 525m (Calculated using L_v and a peak winter flow of 35 vehicles h^{-1})

$P_s =$ 0.15 (Fitzharris and Owens, 1980)

Based on the database of all avalanche occurrences on an open road (Appendix I) and using the above parameters, the current controlled avalanche regime was calculated to have a AHI of 2.76, comprised of a P_m of 0.57 and P_w of 2.19. This must be viewed as an absolute maximum, as in practice queues are never allowed to become as long as 525m, the average speed of traffic is often greater than 11 ms^{-1} (40 kmh^{-1}), and stopping distances are often shorter because of snow free roads. Furthermore, the current road operators are very aware of times of increasing hazard while the road is open, and use mitigating strategies as appropriate e.g. convoys during windows of safety. In the opinion of the author, the true AHI on the Milford Road is closer to 0.5 to 0.35 of the calculated value, at approximately 0.97 to 1.38. This opion is based on observations of the current contractor's practices during times of increasing hazard. The contractor maintains regular road patrols, reducing the possible waiting times to less than 1 hour, and maintains a snow free road, increasing averge speed of vehicles while reducing the stopping distances, which were based on snow covered roads. Elimination of all hazard can be expensive, and complete control of avalanches and of traffic movement is not possible. A minimum avalanche hazard must therefore be tolerated. Schaerer(1989) noted that experience showed that people can accept an AHI of 1. Further reduction of the AHI would usually require control measures that are economically not justified, or would demand unacceptably long traffic delays because of extended closure (Schaerer, 1989). Schaerer(1989) suggested that an avalanche hazard of 1 represents a risk that is 4-6 times lower than other risks to traffic.

Using the estimated frequencies of avalanche occurrence and size from Fitzharris and Owens(1980) (Appendix II) and the values given above, the theoretically uncontrolled avalanche regime was calculated to have an AHI of 186.3, comprised of a P_m of 5.2 and P_w of 181.1. This value must be seen as a minimum, as waiting times on an uncontrolled road could easily exceed 2 hours, and vehicles would likely stop more frequently for

photo opportunities. According to the North American practice to group highways with respect to the avalanche hazard, the Milford Road would now rate at a high hazard if uncontrolled. High hazard is suggested to require full avalanche control, artificial release, avalanche protection structures and an avalanche forecaster. A full avalanche control programme, with artificial release of avalanches, and an avalanche forecaster has been in place since 1984, since the inception of the avalanche programme. An avalanche protection structure was build at the eastern end of the Homer tunnel, but a 100m section was destroyed by an avalanche in 1945 and an event in October, 1996 damaged the remaining section (Conway et al., 2000). The high hazard rating is reflected in the recent work undertaken for a scoping exercise for an extension to the Homer tunnel, thereby eliminating risk from the East Homer and McPherson avalanche paths (URS, 2004). The AHI analysis suggests that the Transit New Zealand Milford Road Avalanche Programme is responsible for the reduction of at least 183 in the AHI.

Using the theoretically uncontrolled avalanche regime, the following parameters were varied: length of waiting queue L_w, probability of an adjacent avalanche path avalanching P_s, length of road a vehicle occupies L_v, average speed V, and stopping distance D. Only one parameter was changed at a time, leaving the remaining parameters unchanged as listed earlier, thereby allowing the examination of the sensitivity of the AHI to each parameter. The parameters were graphed against AHI as a ratio of the maximum value tested for each parameter (Figure 4.2), where:

$L_w =$ 100 m to 1500 m (based on an L_v of 15m and t of less than 1h to 3h)

$P_s =$ 0.05 and 0.3 (range as described for Rogers Pass (Schaerer, 1989)

$L_v =$ 5 m to 25 m (range dependent on ratio of cars to busses)

$V =$ 6 ms^{-1} to 22 ms^{-1} (minimum and maximum road speed)

$D =$ 10 m to 80 m (dependent on speed and road snow cover)
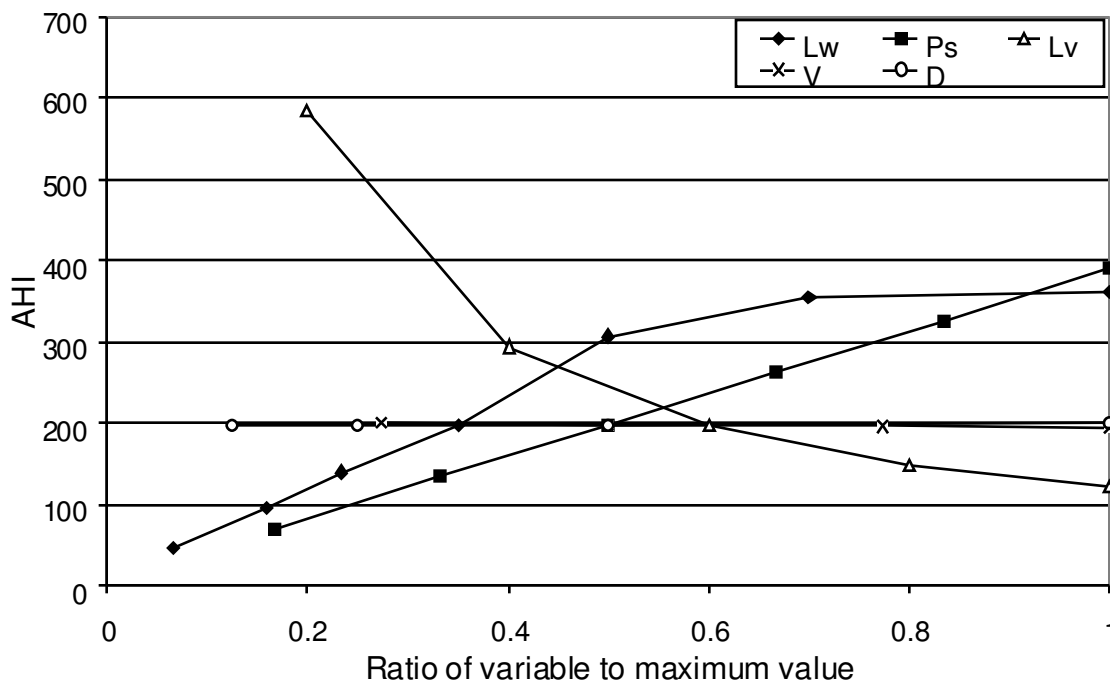
Figure 4.2   Avalanche Hazard Index sensitivity, with the ratio of variable to maximum value, on the X axis and Avalanche Hazard Index (AHI) on the Y axis.

The length of waiting queue L_w increases the AHI at an approximately constant rate up to a threshold of 0.7 (1050m). At this threshold, all of the safe waiting distances are utilized by the queue of waiting traffic and all possible queues extend into an avalanche path. Small increases thereafter are the result of the wider or adjoining avalanche paths being completely filled by waiting vehicles. The queue length is directly proportional to the time traffic is waiting, and the length of each vehicle on the road. Queue length can therefore be decreased through regular road patrols which reduce the waiting time. There is a strong linear increase in the AHI with P_s for the complete range tested. P_s values used have been derived from data from Rogers Pass, and may need to be adjusted for the Milford Road. This study will not endeavour to check the P_s range for the Milford Road. As the length of road a vehicle occupies L_v, decreases the AHI increases sharply. This simply enumerates how many elements are at risk in any avalanche path as shorter vehicles will mean more vehicles will fit into an avalanche path. While this means that having only bus traffic will lower the calculated AHI, it may not lower the actual risk as the AHI does not account for the number of people in a vehicle. Reductions in risk could

be expected if the same numbers of people were all travelling on buses, rather than individual cars, as the bus queue would be shorter, reducing the probability of the queue extending into an adjacent avalanche path. Changing values of average speed V, and stopping distance D, result in very slight changes of AHI. As average speed V increases, the AHI decreases very slightly, as moving vehicles are exposed to the hazard for a shorter period of time. As stopping distance D, increases the AHI increases slightly, as moving vehicles that cannot stop in time for an avalanche will be caught by that avalanche. Both variables only affect the P_m part of the AHI equation, not the P_w part, so are responsible for only very small changes in the overall AHI. The AHI is most strongly influenced by parameters that affect the P_w component.

4.3.2 Probability of Death to an Individual Results

Using the modified equations 4.10 and 4.11, of Wilhelm(1998) and Margreth et al.(2003) and the new weightings, the PDI of the controlled and theoretically uncontrolled avalanche regime on the Milford Road for the present (2002) situation has been calculated. Both of these analyses have been undertaken using the same input parameters:

$C:B =$ 0.86 : 0.14 (URS, 2004)

$\beta_B =$ 30 (estimated, Wilkins pers. comm., 2004)

$\beta_C =$ 1.6 (Margreth et al., 2003)

$V =$ 40 kmh^{-1} (Fitzharris and Owens, 1980)

$\lambda_{i3} =$ 0.05 (Schaerer, 1989)

$\lambda_{i4} =$ 0.25 (Schaerer, 1989)

$\lambda_{i5} =$ 0.5

Based on the database of all avalanche occurrences on an open road (Appendix I) and using the above parameters, the current controlled avalanche regime was calculated to have a PDI of 5.4 x 10^{-5} for a commuter with 2 passes per day and 1.6 x 10^{-4} for a member of the road crew with 6 passes per day. While the PDI for a daily commuter on the Milford Road, such as helicopter pilots, bus drivers and fishermen, will be the same

as for a tourist on any given day, if annualised a tourist will have a significantly lower PDI than the daily commuters. The intention of this analysis is to calculate the PDI for the most at risk public group of the population. The collective risk was calculated at 0.058 deaths per year. This must be viewed as an absolute maximum on the controlled Milford Road, as the speed of traffic is often greater than 40 kmh^{-1} and the current road operators are very aware of times of increasing hazard while the road is open, and use mitigating strategies as appropriate e.g. convoys. Weir(1998) calculated much higher PDI equivalents at approximately ten times the risk associated with normal road travel, or equivalent to activities such as white-water rafting.

Using the estimated frequencies of avalanche occurrence and size from Fitzharris and Owens(1980) (Appendix II), and the above parameters, the theoretically uncontrolled avalanche regime was calculated to have a PDI of 6.8×10^{-4} for a commuter with 2 passes per day and 2.1×10^{-3} for a member of the road crew with 6 passes per day. The collective risk was calculated at 0.726 deaths per year. This suggests that the Transit New Zealand Milford Road Avalanche Programme is responsible for the reduction of at least one order of magnitude in the PDI.

Using the theoretically uncontrolled avalanche regime, the following parameters were varied: the ratio of cars to buses $C:B$, number of passengers per bus β_B number of passengers per car β_C, and speed of the vehicles V. Only one parameter was changed at a time, leaving the remaining parameters unchanged, thereby allowing the examination of the sensitivity of the PDI of a commuter. The parameters were graphed against PDI as a ratio of the maximum parameter tested (Figure 4.3), where:

$C:B =$ 1.0 : 0.0 to 0.7 : 0.3 (no buses to over double the proportion of buses)

$\beta_B =$ 20 to 40 (half full to almost completely full)

$\beta_C =$ 1 to 4 (single occupancy to almost full)

$V =$ 20 to 100 kmh^{-1} (minimum and maximum road speed)
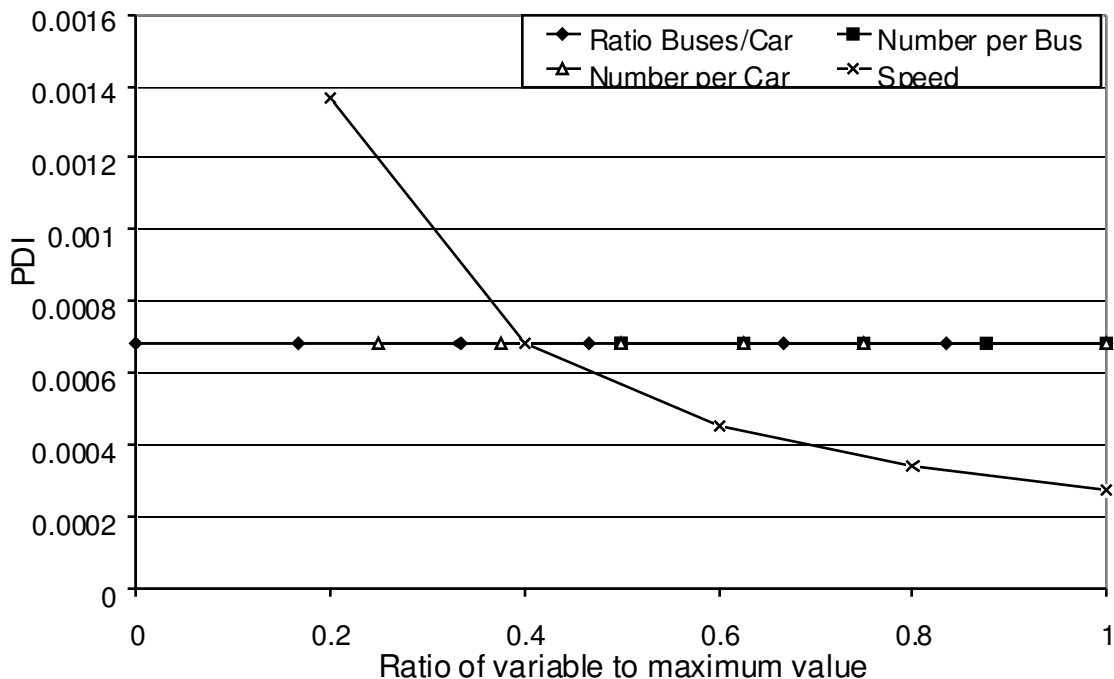
Figure 4.3.   Commuter PDI sensitivity, with the ratio of variable to maximum value, on the X axis and PDI on the Y axis.

The PDI is completely unaffected by the changes in the ratio of cars to buses C:B, number of passengers per bus β_B number of passengers per car β_C. This is because the risk to an individual remains the same regardless of whether they are in a bus or car, or the number of people in that vehicle with them. The speed of the vehicles V, does strongly affect the PDI. As the speed increases the PDI decreases, as faster moving vehicles are exposed to the hazard for a shorter period of time.

As shown in Figure 4.4, the collective risk increases rapidly at a linear rate as the ratio of cars to buses C:B, reaches a minimum of 0.70 : 0.30 cars to buses. This is simply due to the higher number of people in a bus, and therefore greater consequences if hit by an avalanche. Likewise, as the number of people in each bus β_B, and car β_C, increases, so too does the collective risk. As with the PDI, the collective risk decreases as the speed of the vehicles V, increases. Increasing the speed of the vehicles will reduce both the PDI and collective risk deduced from avalanche risk, but will most likely increase the risks from other sources, e.g. road accidents.
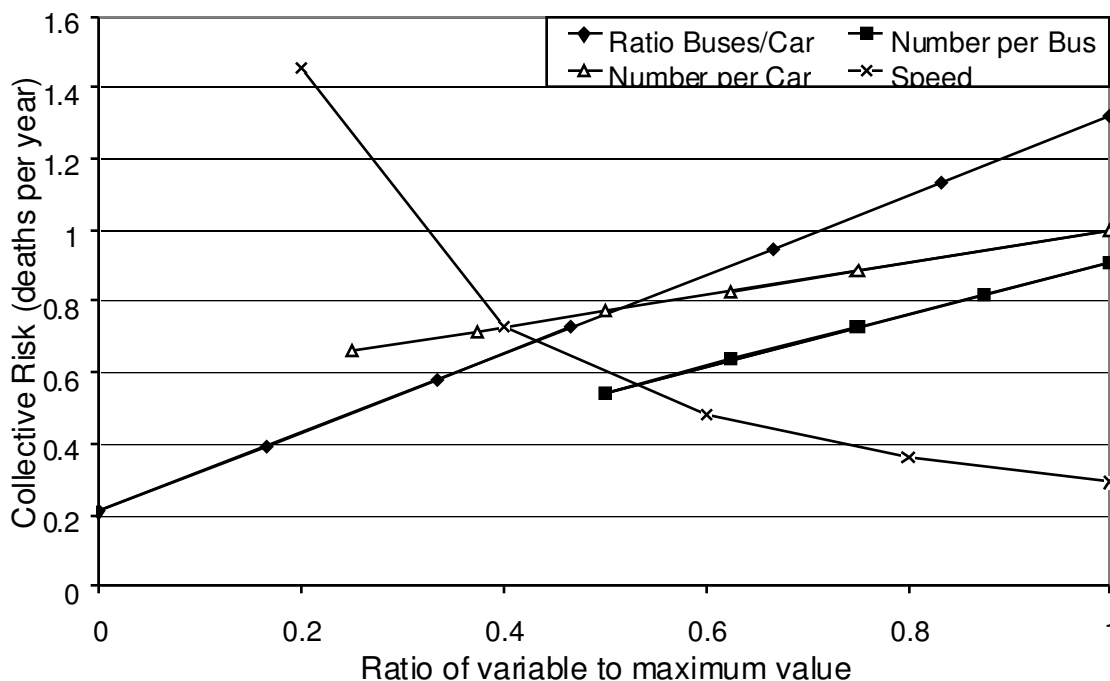
Figure 4.4   Collective risk sensitivity, with the ratio of variable to maximum value, on the X axis and collective risk on the Y axis.

The probability of death for each avalanche type λ_{ij} has also been varied in the range from:

$\lambda_{i3} =$ 0.075 to 0.05

$\lambda_{i4} =$ 0.17 to 0.42

$\lambda_{i5} =$ 0.2 to 0.5

PDI for commuters and road crew, and collective risk did change as a result of these modifications, but remained within the same orders of magnitude.

4.3.3 Comparison of estimated AHI and observed frequencies

The above calculations of AHI and PDI on a theoretically uncontrolled Milford Road have used the estimated frequencies of avalanche occurrence and size from Fitzharris and Owens(1980). While Chapter Three has shown there to be a marginally significant upwards trend in artificial avalanche occurrences, there is still an opportunity to compare

the estimates of Fitzharris and Owens(1980) to the database of avalanche occurrences. This comparison will verify whether the estimates of AHI and PDI on a theoretically uncontrolled Milford Road are realistic.

Avalanche size can be approximately associated with the different avalanche types, where size 5 equates to plunging avalanches, size 4.5 and 4 with deep snow avalanches, and size 3.5 with light snow avalanches. Using the database of avalanche occurrences the reliability of the estimates of frequency and magnitude by Fitzharris and Owens(1980) can now be examined for a selection of significant avalanche paths (Table 4.5).

Table 4.5   Comparison of AHI frequency estimates (Fitzharris and Owens, 1980) with number of avalanches and calculated observed frequencies from the avalanche database for eight selected avalanche paths.

Path (1980AHI)	Plung-ing Size 5			Deep snow Size 4 and 4.5			Light snow Size 3.5		
	Estimated frequency	Number of avalanches	Observed frequency	Estimated frequency	Number of avalanches	Observed frequency	Estimated frequency	Number of avalanches	Observed frequency
Murrels	0.04	1	0.06	0.10	3	0.17	0.20	5	0.28
Cleddau	0.04	2	0.11	0.10	11	0.61	0.00	8	0.44
Loop One	0.33	0	0.00	0.10	2	0.11	0.00	7	0.39
Moir	0.00	2	0.11	0.10	8	0.44	0.20	13	0.72
Gullivers Peak	0.04	2	0.11	0.10	3	0.17	0.07	0	0.00
McPherson	*	8	0.44	*	9	0.50	*	7	0.39
East Homer	0.33	5	0.28	1.00	17	0.94	2.00	23	1.28
Raspberry	0.10	4	0.22	0.50	24	1.33	1.00	21	1.17
Average [#]	0.13	2.3	0.13	0.29	9.7	0.54	0.50	11	0.61

*Not included in Fitzharris and Owens(1980)

[#]Averages do not include the McPherson Path

In Table 4.5, estimated frequency is from Fitzharris and Owens(1980), and the number of avalanches is the total number of avalanches on a given path in the time period 1985 to 2002. Observed frequency is calculated by dividing the number of occurrences by the 18 year record length. Table 4.5 shows that all of the estimates made by Fitzharris and Owens(1980), except for East Homer, are lower than the observed frequencies. This is

most likely because of the enhanced artificial control regime on the Milford Road, resulting in more avalanches being released than under a natural, uncontrolled, avalanche regime. The McPherson avalanche path was not recorded by Fitzharris and Owens(1980) as it was not considered that it would runout over the road. However, the observed frequencies suggest that it is a significant path, because large plunging avalanches can affect the road. Because of the short record used for the comparison, some variations for paths are expected; therefore the average frequencies for estimated and observed for the three size classes are also calculated. If the McPherson path is ignored, comparisons of the estimated and observed frequencies show that they are about the same for plunging avalanches at approximately 0.13, and slightly lower for deep snow and light snow avalanches, with 0.29 estimated compared with 0.54 observed, and 0.5 estimated compared with 0.61 observed, respectively.

The comparison between estimated frequency and observed frequency for avalanche type and avalanche path suggests that the original estimates by Fitzharris and Owens(1980) have underestimated the frequencies. However, this underestimation is to be expected as the avalanche programme has increased the frequency of avalanches, mainly through artificial release, as highlighted by the marginally significant increasing trend in artificial avalanches (Chapter Three). The estimated frequencies of Fitzharris and Owens(1980) are lower than the observed frequencies, and are therefore considered to more closely approximate a natural avalanche regime than the database record, which includes all of the control work. Therefore, these values are considered to be the best approximation of an uncontrolled or natural avalanche regime on the Milford Road.

4.3.4 Length of Record

When comparing the estimated frequencies (Fitzharris and Owens, 1980) with observed frequencies, long return period values occurring in a small sample must be considered. This can be expressed as a probability of one or more exceedences during a specific interval, as a function of the interval and the return period according to the equation (Tomlinson, 1980):

$$P = 1 - (1 - 1/R)^I$$

Where:

R = Return period in years

I = Length of record or interval in years

Considering that the record length used for comparison is 18 years, the probability of containing a 1 in R year event can be seen in Table 4.6.

Table 4.6   Probability of having included a 1 in R year event in the 18 year record available for the Milford Road.

Event	Probability
1 in 20 year event	0.60
1 in 50 year event	0.30
1 in 100 year event	0.17

This suggests further caution in the comparison of estimated with observed frequencies, especially when considering a short database record length. Therefore, the author is satisfied that while the estimates of frequency and magnitude by Fitzharris and Owens(1980) are lower than the observed frequencies, they are appropriate to be used as an approximation on an uncontrolled avalanche regime on the Milford Road.

4.3.5 Risk evaluation and comparison

Having determined the level of risk currently experienced on the Milford Road in terms of the AHI, PDI and collective risk, this can now be compared to other roads around the world, and to other acceptable risks for natural and man made hazards.

Using the equations of Schaerer(1989) the AHI on the Milford Road can be compared to that of Rogers Pass, B.C., Canada. Table 4.7 shows the comparison of AHI before any

control, after structural control (not including artillery), and the residual AHI for the Milford Road and Rogers Pass.

Table 4.7   AHI before and after control for Rogers Pass and the Milford Road.

Road	Endangered road (km)	Number of avalanche paths	T (vehicle d^{-1})	AHI – with no control	AHI – after structural control	AHI – after structural control, standardised to T = 1000	AHI - residual, standardised to T = 1000	AHI - residual
Rogers Pass, 1974 (Avalanche Task Force, 1974)	36	65	905	335	174	192	?	?
Rogers Pass, 1987 (Schaerer, 1989)	36	65	1700	1004	235	138	8.8	<15
Rogers Pass, 1992 (Stethem et al., 1995)	36	130	2300	850	214	93	15.2	<35
Milford, 2002 (This study)	29	50	381	186	186	488	7.3	<2.8

While the AHI has been modified since its inception and the method used by Stethem et al.(1995) for Rogers Pass is not clearly outlined, these values can still be used for the basis of a conservative comparison. *T* has been standardised to 1000 for all roads to permit comparison of the effect of the physical attributes of the avalanche paths, and therefore not just highlight the difference in traffic volumes. When the AHI after structural control is considered, based on a *T* = 1000, the Milford Road has a significantly higher AHI than the historical values for Rogers Pass (Table 4.7). It is interesting to note that per 1000 vehicles the AHI, after structural control, has decreased at Rogers Pass, clearly showing the effect of increasing the number of structures on the road. The Milford Road currently has no structures to mitigate the effect of an avalanche. When the residual AHI is considered, again based on *T* = 1000, the Milford Road has a much lower AHI than the historical values for Rodgers Pass.

Using Table 4.7, the effectiveness of the management and forecasting practices (following structural control) of each avalanche programme can also be compared.. The

AHI after structural control compared to the residual AHI is reduced by 179 or 84% on the 1992 Rogers Pass, compared to 183 or 98% on the present (2002) Milford Road. However, when comparing the uncontrolled AHI, Rogers Pass clearly has a much more serious avalanche problem with a very high AHI, especially for the 1987 calculation.

As stated earlier, Schaerer(1989) showed that people can accept an AHI of 1, and reducing this value would usually require control measures that are economically not justified, or would demand unacceptably long traffic delays. The calculations in Table 4.7 all show the residual AHI to exceed 1, suggesting that, according to the criterion of Schaerer(1989), the AHI is unacceptable on all these roads. However, the true AHI on these roads is lower than the calculated AHI, as the theoretical frequency of encounters has been found to be far greater than the observed number (Schaerer, 1989), and current road operators are aware of times of increasing hazard while the road is open, and will use mitigating strategies to reduce the hazard.

Using the equations of Wilhelm(1998) and Margreth et al.(2003), the collective risk on the Milford Road can be compared to several pass roads in Switzerland. While a direct comparison of the Milford Road will not be entirely equivalent (as the modified PDI calculations use higher probabilities of death for an avalanche), it will provide a basis for conservative comparison. When the initial collective risk is considered, based on a $T =$ 1000, the Milford Road is subject to significantly higher risk than three main pass roads in Switzerland; Flüela, Lukmanier and the Gotthard (Table 4.8). T has been standardised to 1000 for all roads to permit comparison of the effect of the physical attributes of the avalanche paths, rather than highlighting the difference in traffic volumes. When the residual risk is considered, again based on $T = 1000$, the Milford Road has only marginally higher risks than the Flüela and Lukmanier pass roads. When this is compared to the relative accessibility of the roads, the Milford Road is seldom closed more than 20 days year^{-1}, while the Flüela (between 1964 and 1971) was closed a minimum of 95 days year^{-1}, and the Lukmanier (between 1965 and 1997) was closed a minimum of 68 days year^{-1} (Margreth et al., 2003). The residual collective risk on the Milford Road, as controlled by the avalanche programme, is only 8% of the initial collective risk. This is

significantly less than 19% for the Flüela and 14-25% for the Lukmanier, which is controlled by artificial release on the northern side. The Gotthard however, has a very low residual collective risk, at only 2% of the initial collective risk, which reflects the long winter closures (> 142 days year^{-1}), thereby almost eliminating all risk.

Table 4.8   Collective risk before and after control. Modified from Margreth et al.(2003).

Road	Affected road length (km)	Endangered road (km)	Number of avalanche paths	T (vehicle d^{-1})	Closed days (d year^{-1})	Initial collective risk (deaths year^{-1})	Initial collective risk, T = 1000	Residual collective risk (deaths year^{-1})	Residual collective risk, T = 1000
Flüela	19.3	10.1	47	1000	> 95	0.70	0.70	0.13	0.13
Lukmanier	25	13.6	94	1000	> 68	0.51	0.51	0.07-0.13	0.07-0.13
Gotthard	24	15.7	55	6000	> 142	5.54	0.92	0.11	0.02
Milford	29	29	50	381	< 20	0.73	1.92	0.058	0.15

Wilhelm(1999 [in] Margreth et al., 2003) suggests that a driver on a public road with a low probability of avoiding an avalanche should have a PDI lower than $1x10^{-5}$. This is compared to a PDI of $8.3x10^{-5}$ for a traffic accident in Switzerland (Margreth et al., 2003). NGI(2003) suggests that an avalanche encounter should be viewed as an 'obligatory' or involuntary risk, and as such should have a 1:10 ratio of the traffic accident rate. In Norway, the traffic accident rate is approximately 400 for a total population of 4 million, so the avalanche rate corresponds to approximately 1 per 100,000 inhabitants or $1x10^{-5}$. New Zealand in 2002, with a similar population of 3,939,100 and road traffic fatalities of 404 (Land Transport Safety Authority, 2003) had a PDI for road traffic fatalities of $1.03x10^{-4}$, similar to that of Norway. Applying the approach taken by NGI(2003) suggests that the Milford Road should have a PDI from avalanche risk no greater than $1.03x10^{-5}$. The risk analysis provides a higher number at $5.4 x 10^{-5}$ for a commuter with 2 passes, based on the assumptions listed. However, the

acceptable PDI from a hazard, other than driving, on a road in New Zealand may have a higher tolerable limit, than in Norway.

To permit the comparison of avalanche risk in terms of PDI with risks from other hazards, the waiting traffic component that the equations of Wilhelm(1998) and Margreth et al.(2003) neglect, must be considered. Therefore, to allow for comparison with other hazards, equations 4.10 and 4.11 have been modified using parts of equation 4.5, to account for moving and waiting traffic for collective risk:

$$CR_w = \frac{\beta}{24} \sum_{j=3}^{5} \lambda_j \sum_{i=1}^{n} \left(\frac{T.L_{ij}}{R_{ij}.V} + P_s \frac{N_{wi+1j}.d_{i+1j}}{R_{i+1j}} \right) \qquad (4.12)$$

and individual risk:

$$IR_w = \frac{z}{24} \sum_{j=3}^{5} \lambda_j \sum_{i=1}^{n} \left(\frac{T.L_{ij}}{R_{ij}.V} + P_s \frac{N_{wi+1j}.d_{i+1j}}{R_{i+1j}} \right) \qquad (4.13)$$

where:
d_{i+1j} = length of time waiting vehicles are exposed to an avalanche in the adjacent path (hours)

When using the previously stated parameters and a value of 2 hour for d_{i+1j} is used, inclusion of the waiting traffic component increases the calculated individual and collective risk significantly as shown in Table 4.9.

Table 4.9   Collective risk and individual risk (deaths year[-1]) including waiting traffic and not including waiting traffic, for a commuter and a member of the road crew on the controlled and theoretically uncontrolled Milford Road using 2002 traffic values.

	CR	CRw	IR Commuter	IRw Commuter	IR Road crew	IRw Road crew
Uncontrolled Milford Road	0.726	20.23	6.8×10^4	1.9×10^2	2.1×10^3	5.7×10^2
Controlled Milford Road	0.058	0.76	5.4×10^5	7.1×10^4	1.6×10^4	2.1×10^3

The values calculated in Table 4.9 must be viewed as an absolute maximum on the controlled Milford Road, as the speed of traffic is often greater than 40 kmh[-1] and the current road operators are very aware of, and have measures in place to ensure safe practices during times of increasing hazard while the road is open, to minimise the length of time waiting traffic is exposed to an avalanche path. In this analysis two hours has been used as the exposure time for waiting traffic to highlight the impact of including waiting traffic into these equations. In reality, the whole queue will not be exposed for the same period of time, unless all the vehicles arrive simultaneously. As with the AHI, in the opinion of the author, because of the control measures in place, the true risk on the controlled Milford Road is closer to 0.5 to 0.35 of the calculated value, which results in approximately 0.27 deaths year[-1] for the collective risk, 2.5×10^{-4} for individual risk for a commuter and 7.5×10^{-4} for individual risk for a member of the road crew.

Suggested guidelines for individual risk in terms of PDI have been published by several organisations. In Iceland, new legislation for hazard zoning for residential areas has suggested that the upper limit of acceptable risk is 0.2×10^{-4} (Arnalds et al., 2004). In British Columbia, dam failure fatality probabilities must not exceed 1×10^{-4}, which is based upon the concept that the risk to an individual from a dam failure should not exceed the individual natural death risk run by the safest population group (Hoek, 2000). The Australian Geomechanics Society (AGS) has suggested 1×10^{-4} for natural slopes and 1×10^{-5} for engineered slopes for landslides (AGS, 2000). Nielsen et al.(1994) suggested that the annual probability of fatality of 1×10^{-4} also defined the boundary between

voluntary (restricted access to workers) and involuntary (general public) risk on dam sites. These results all suggest that the individual risk to a commuter on the controlled Milford Road, when accounting for waiting traffic, is unacceptably high when compared to the risk of other hazards. Therefore, to lower the level of risk on the Milford Road, it is imperative that stationary traffic should be avoided in the avalanche zone at all costs. In practice the author believes this to be the case already, with large areas of no stopping zones along the avalanche area, and large fines imposed on vehicles without snow chains (thereby reducing the likelihood of unintentional stops). Furthermore, while the individual and collective risk enumerated in deaths year^{-1} may still seem high, Schaerer(1989) noted that the theoretical frequency of encounters has been found to be far greater than the observed number, providing the example of Kootenay Pass, where the expected encounter frequency was six vehicles year^{-1} between 1965 and 1984, but on average only 1.9 vehicles year^{-1} were actually hit during this period.

4.4   Conclusion

Risk evaluation in terms of the AHI and PDI has been undertaken on the Milford Road for the present avalanche risk on the highway. This has been compared to the risk of a theoretical, uncontrolled avalanche regime, but with traffic at 2002 levels. The AHI analysis shows the theoretical uncontrolled AHI to be very high, with an AHI of 186.3. The avalanche programme's control reduces the present avalanche risk to approximately 0.97 to 1.38. The residual AHI for the Milford Road is significantly lower than that for Rogers Pass, even when standardised for $T = 1000$. In terms of calculated residual AHI, the Milford Road may have an unacceptable level of risk, but this is reduced to an acceptable level in practice. Sensitivity analysis of the assumptions made for the calculation of AHI show that the length of a waiting queue, the probability of a second avalanche in an adjacent path, and the length of road a vehicle occupies to affect the AHI strongly.

The modified Wilhelm(1998) and Margreth et al.(2003) PDI analysis shows the theoretically uncontrolled PDI to be very high at 6.8×10^{-4} for commuters and 2.1×10^{-3} for

a member of the road crew, and completely unacceptable. The avalanche programme's control reduces the PDI for avalanche risk to 5.4 x 10^{-5}, which is higher than the suggested PDI for avalanche risk on roads in Switzerland and Norway, but may still be acceptable in New Zealand because of a higher acceptance level for individual risk as calculated from traffic fatalities. Collective avalanche risk on the Milford Road also shows the theoretically uncontrolled risk to be very high, and unacceptable. The controlled collective risk is about the same, but slightly higher than similar roads in Switzerland, but the Milford Road is far more accessible, because of fewer closed days. Sensitivity analysis of the assumptions made for the calculation of PDI show that the speed of a vehicle is the only parameter that affects PDI, while all parameters tested affect the collective risk.

A new equation for PDI which calculated the risk posed to waiting traffic was formulated and results showed that the calculated avalanche risk on the controlled, present day Milford Road is too high, and unacceptable when compared to other risks. In practice the real risk posed from avalanche is considered to be significantly lower, and acceptable, because of the mitigating strategies used to reduce the potential exposure of waiting vehicles. To maintain this acceptable level of risk with increasing traffic volumes, continued improvement in the understanding of avalanching is required to maintain an effective avalanche programme.

5.0 Statistical forecasting of avalanche activity

5.1 Introduction

This chapter has been modified from the manuscript Hendrikx et al.(2005). It describes the statistical analysis of meteorological variables using classification trees to determine, and potentially forecast, significant avalanche activity on the Milford Road. In previous work, a diverse range of quantitative methods have been used to develop ways of forecasting various measures of avalanche activity (Föhn, 1998). Early work of Perla(1970) investigated the meteorological and snow parameter thresholds associated with avalanching in two North American areas. Regression analysis was used to predict avalanche activity by Judson and Erickson(1973). Subsequently, the multivariate techniques of discriminant function analysis (Judson and Erickson, 1973; Bois et al., 1975; Bovis, 1977, and Föhn et al., 1977; McGregor, 1989; McClung and Tweedy, 1993) and more recently canonical discriminant analysis (Floyer and McClung, 2003) have been applied to distinguish avalanche and non-avalanche days. The multivariate analyses rely on normality assumptions (Buser, 1983; McGregor, 1989) and Buser(1983, 1989) promoted the nearest neighbour method as a non-parametric approach to forecasting avalanches by identifying days from past records with similar conditions. A variant to the nearest neighbour approach using expert systems was developed by Schweizer and Föhn(1996). Unfortunately, the nearest neighbour approach requires a very large database of weather, snowpack and avalanche occurrences. Other non-parametric methods which have been used are classification and regression trees (Davis and Elder, 1994; Davis et al., 1996, 1999). This method has proven to work on smaller data sets, and the interpretations of complex interactions are clearer and often more easily understood than other model constructions (Davis et al., 1999), making them ideal for operational forecasting.

These approaches to avalanche occurrence prediction have identified a large number of predictor variables. Meteorological variables are the most common with some measure of precipitation (new snow depth or snow water equivalent) common to all studies referred to above. Wind speed is also common in most though not all (e.g. Floyer and McClung, 2003). Combined precipitation and wind variables have also recently been found to be useful (Davis et al., 1999). Where wet and dry avalanches have been distinguished, temperature and radiation variables are important predictors (Bois et al., 1975; Bovis, 1977; Föhn et al., 1977; McGregor, 1989; McClung and Tweedy, 1993). Snowpack variables have been used less often though some approaches (e.g. Schweizer et al., 1998; Schweizer et al., 2003) focus on this aspect. Other studies have included direct or indirect measures of snowpack conditions such as new snow density (Davis and Elder, 1994), rammsonde or foot penetration (Bois et al., 1975; Föhn et al., 1977; McClung and Tweedy, 1993; Floyer and McClung, 2003) and vapour pressure gradient, an indirect measure of surface snow quality (Davis et al., 1999). As noted by Föhn(1998), it is difficult to compare prediction success rates between different approaches. However, for studies based on avalanche and non-avalanche days, and providing that approximately equal numbers of each category are used in the analysis, correct classifications of 80% or better are considered to be useful for forecasting. The number of predictor variables used by different authors is also a consideration. Most multivariate models include at least three variables (e.g. Judson and Erickson, 1973) while some have as many as seven (Bois et al., 1975).

As noted in Chapter Three, observations show that avalanches on the Milford Road tend to be predominantly direct action avalanches, as the majority occur during or shortly following a storm cycle (Conway et al., 2000). This is also observed in the examination of available fracture line profiles, where the weakness is most often found to be in the new snow. Climax avalanches do occur, but far less frequently, and predominantly towards the end of the avalanche season. In common with other maritime mountainous areas (e.g. Floyer and McClung, 2003), there is a lack of distinct wet and dry avalanche seasons. On the Milford Road, Fitzharris and Owens(1980) noted that wet avalanches can occur from July to November, while dry avalanches can occur from May to November.

Rain can occur to high levels at any time during the winter, but occurs less frequently in July and August. Rain on snow events have been recognised to cause widespread avalanching in many different areas (Conway and Raymond, 1993), but have been given special attention on the Milford Road with the development of a lysimeter to enable the measurement of percolation to the base of the snowpack (Carran et al., 2000).

When considering the direct action avalanche regime experienced on the Milford Road and the previous work pertaining to statistical avalanche forecasting, there is a clear need to investigate the potential of applying these techniques to the Milford Road. Therefore, the main objective of this chapter is to identify the meteorological variables responsible for avalanching in the extreme maritime climate of the Milford Road region. Specifically, the main aim is to create a forecasting classification tree using remotely measured meteorological variables as predictors of a significant avalanche day in this direct action avalanche environment.

5.2   Classification Tree Methods

Classification trees provide a data mining or an exploratory data analysis method which can be used to study the relationships between a dependent measure, and a large number of possible predictor variables. A full discussion of classification and regression trees (C&RT) is given by Breiman et al.(1993).

Classification trees have a number of distinct advantages over other statistical techniques for classifying, grouping or discriminating within large data sets. They provide insight into the predictive structure of the data, are non-parametric and seem largely insensitive to underlying distributions of the data (Breiman et al., 1993). Outliers are isolated into a node, and do not have any effect on the splitting of the subsequent tree. The interpretations of complex interactions are clearer and often more easily understood than other model constructions (Davis et al., 1999). Furthermore, they are not based on a probabilistic model. There is no probability level or confidence interval associated with predictions derived from using classification trees to classify a new set of data. The

confidence of the results produced by a given model is based on its historical accuracy. For all of these reasons, classification trees have been used by other researchers for both predictive (Rosenthal et al., 2002) and exploratory data analysis (Davis and Elder, 1994; Davis et al., 1996, 1999; Schweizer and Jamieson, 2003) in relation to avalanche activity.

5.2.1 Meteorological data

Meteorological variables are available from two automated weather stations (AWS), Mt Belle at 1600 m a.s.l., at approximate starting zone elevations, and East Homer at 900 m a.s.l., located in the valley below, at road level (Figure 2.2 and Table 5.1). Unfortunately, the Mt Belle AWS is located in an exposed ridge location and snow depth data can be misleading beyond a threshold depth. However, Conway et al.(2002) found that using the East Homer AWS results in reliable estimates of precipitation in the starting zones. The complete data set for Mt Belle AWS spans an 18 year period from 1985 to 2002, with hourly observations starting from 1989. The East Homer AWS has hourly meteorological observations from 1993 onwards. Therefore, when considering only hourly meteorological observations and data availability at both AWS sites, the data set was reduced to a 10 year period from 1993 to 2002.

Table 5.1   Hourly observations of meteorological variables collected from Mt Belle AWS at the lower starting zone elevation and East Homer AWS at road level elevation

Mt. Belle AWS at starting zones, 1600 m	East Homer AWS at road level, 900 m
Air Temperature (°C)	Air Temperature (°C)
Snow Depth (m)	Snow Depth (m)
Hourly Precipitation (mm)	Hourly Precipitation (mm)
Wind Speed (kmh^{-1})	Air Pressure (hPa)
Wind Direction (degree)	

As shown in Table 5.1, five potentially relevant meteorological variables were available from the Mt Belle AWS and four were available from the East Homer AWS. From these nine variables, 48 direct, accumulated and derived parameters were generated for the analysis (Table 5.2).

Table 5.2   48 direct, accumulated and derived meteorological parameters used in the analysis that were obtained from the variables collected at Mt Belle and East Homer AWS. XX in the symbols refers to the time period (12, 24 or 72 hours) preceding the mean time of avalanche occurrence over which the variable is calculated

Mt Belle AWS	Symbol	Time
Average Air Temperature	TempAvXX	12, 24, 72
Maximum Air Temperature	TempMaxXX	12, 24, 72
Minimum Air Temperature	TempMinXX	12, 24, 72
Average Snow Depth	SnowDAvXX	12, 24, 72
Average Wind Speed	WspdAvXX	12, 24, 72
Vector Wind Speed	Vector uXX	12, 24, 72
Vector Wind Direction	Vector dXX	12, 24, 72
East Homer AWS	**Symbol**	**Time**
Average Air Pressure	AirPAveXX	12, 24, 72
Average Air Temperature	TAveXX_EH	12, 24, 72
Maximum Air Temperature	TMaxXX_EH	12, 24, 72
Minimum Air Temperature	TMinXX_EH	12, 24, 72
Average Snow Depth	SDAveXX_EH	12, 24, 72
Maximum Hourly Precipitation	PTMaxXX_EH	12, 24, 72
Sum of Hourly Precipitation	PTSUMXX_EH	12, 24, 72
Combined Mt Belle and East Homer	**Symbol**	**Time**
Wind Drift 1	XXhSumPPT*WSpdAve_NTemp	12, 24, 72
Wind Drift 2	XXhSumPPT*WSpdAve_Temp	12, 24, 72

The choice of selecting these parameters was based on previous work and predictability of the parameters in terms of regional weather forecasting. Average, maximum and minimum air temperatures were obtained for 12, 24 and 72 hour periods preceding avalanche occurrence. Average air pressure and average snow depth for the same periods were also considered. Following previous studies (Judson and Erickson, 1973; Bois et al.,

1975; Bovis, 1977; Föhn, et al., 1977), wind speeds were averaged and sums of precipitation used, a proxy for snowfall, for 12, 24 and 72 hour periods. Maximum hourly precipitation was also included to examine the case of high intensity storms preceding avalanche occurrence. Several previous studies have used a snow drift parameter (Judson and Erickson, 1973; Föhn et al., 1977; Davis et al, 1996; 1999). In this study the snow drift parameter (Wind Drift 1) was defined as the product of the sum of hourly precipitation and the average wind speed to the fourth power as previously used by Davis et al.,(1999) and based on the work of Pomeroy(1988) for situations with unlimited snow availability. However, in maritime climate areas such as the Milford Road region, rain to high elevations and periods of strong surface snowmelt may often significantly restrict snow transport. While development of a robust model to predict snow drift dependent on air temperature and snow surface is beyond the scope of this study, as a first approach a second wind drift parameter (Wind Drift 2) was created that attempted to account for some of these cases. The same expression was used as before, but for periods where the average air temperature for the time period of interest exceeded 1.5°C at Mt Belle AWS, the snow drift value was set to zero.

5.2.2 Avalanche days

Previous studies of avalanche forecasting have used a range of indices of avalanche activity. In some cases, levels of predicted hazard have been compared to measures of local or regional stability (Judson and King, 1985; Elder and Armstrong, 1987; Schweizer and Föhn, 1996; Schweizer et al., 2003). Other investigations have used the number of avalanche events (Judson and Erickson, 1973; Davis and Elder, 1994), the sum of avalanche sizes (Davis and Elder, 1994; Davis et al., 1996, 1999) or the sum of avalanche sizes converted to avalanche mass (Schweizer et al., 1998). Most commonly, some measure of an avalanche day has been used (Judson and Erickson, 1973; Bois et al., 1974; Föhn et al., 1977; Buser, 1983, 1989; McGregor, 1989; Floyer and McClung, 2003) and this is most appropriate for use in classification tree analysis. Some studies, for example McClung and Tweedy(1993), have used threshold sizes or threshold avalanche activity indices expressed as the sum of avalanche sizes to indicate avalanche days, while

Floyer and McClung(2003) used potentially hazardous threshold sizes for individual paths for this purpose. For this study, the definition of an avalanche day was based on the potential effects on the highway by combining a threshold size and an avalanche activity measure as follows:

Avalanche Day = Maximum Avalanche Size Class $\geq$ 2.5, OR Sum of Size Class $\geq$ 10

This definition of avalanche day ensures that all significant avalanche activity is included in the model, as large individual avalanches are considered as are periods of widespread smaller instabilities. The ten year period considered from 1993 to 2002 inclusive, contained 1842 individual avalanche occurrences. Of these avalanches, 769 were natural and 1073 were artificially triggered. Using the definition of an avalanche day 148 individual days were recorded as avalanche days in the 10 year data set.

A further set of 148 non-avalanche days was randomly selected from the remaining days without avalanches. These days were selected between 30 May and 20 December, the maximum temporal extent of avalanching from historical data and were distributed such that there were an equal number of non-avalanche days and avalanche days in each year. This was done to ensure that non-avalanche days selected were not over represented in winters with limited avalanching. The 47 previously coded below-the-threshold non-avalanche days were then added to this set to give totals of 195 non-avalanche days and 148 avalanche days. The inclusion of the 47 below-the-threshold non-avalanche days presents a tough 'test' for a statistical model as the sets are not as clear cut as they might have been had these been omitted.

Several studies have distinguished dry and wet avalanches. However, as noted by Floyer and McClung(2003), there is poor discrimination between these types of avalanches in maritime climates, especially when determined from avalanche deposits, so this was not used here. Natural and artificially triggered avalanches have also been distinguished in previous investigations either because of incomplete coverage of control (e.g. Föhn et al., 1977) or because control was restricted to fine weather days (e.g. Floyer and McClung,

2003). This was not implemented in this study because control work is usually undertaken reasonably uniformly over the most significant paths immediately after storms, and as the avalanches on the Milford Road tend to be mostly direct action, it is not considered that the influence of artificial release will affect the analysis. Furthermore, the aim is to create an operational forecasting tool, so it must be workable under the current avalanche regime, which includes regular artificial release.

5.2.3 Combining avalanche and meteorological data

The date and time from the avalanche day was used to obtain the 48 meteorological parameters in Table 5.2. All parameters were extracted for the 12, 24 and 72 hour period preceding the mean avalanche occurrence time, where the mean occurrence time was calculated from the mean of all avalanches on a day e.g. if there were two avalanches in a day, one at 0600 and one at 1200, then the mean avalanche occurrence time was 0900. Non-avalanche days had a fixed mean avalanche occurrence time of 1200. The 48 meteorological parameters were extracted for all of the 343 cases. Previous work has gone to great lengths to back shift data into the time of avalanche occurrence (Davis et al., 1996, 1999). This was not carried out for this data set as the occurrence time, occasionally estimated, was used for natural avalanches and artificial avalanches are predominantly released at the first break during, or shortly after a storm. It is thought that the majority of the avalanches are recorded to within an hour or two of the actual time of occurrence.

5.3.4 Classification tree analysis

Using STATISTICA (StatSoft, 2003) a classification tree was generated for an avalanche day as the result is a categorical value namely, yes or no, where yes means that the given day is an avalanche day. Using the 48 parameters, the classification tree was permitted to grow, recursively splitting data into increasingly homogeneous nodes by minimising a Gini index of diversity deviation to define node impurity. The Gini index is the sum of

products of all pairs of class proportions for classes present at a given node (Breiman et al., 1993). The maximum value is attained when class sizes at the node are equal, and reaches a value of zero when only one class is present at the node. The tree was allowed to grow to its maximum extent, T_{max}, until there was only one class in each node. This tree, T_{max} was considered to be an over-fit classification tree, allowing examination of all avalanche days. This type of over-fit tree has been used as an exploratory tool in previous classification tree work (Davis et al., 1996, 1999; Elder and Davis, 2000; Rosenthal, et al., 2002). Because it overfits values, such a tree is of very limited use for forecasting when applied to a new data set.

To determine the optimal level of classification for forecasting, a procedure which involved cross validation as outlined by Breiman et al.(1993) was employed. This procedure, which consisted of subjecting T_{max} to 10-fold cross validation for estimating accuracy for data sets, is recommended where the learning sample is too small to have the test sample taken from it, or no test sample is available. The purpose of this cross validation is to determine the "best" sized tree for use as a predictive tool. This "best" tree will be a descendant from the original T_{max} tree, using only the splits that provide maximum correct classification, or minimum misclassification. Cross validation is achieved by repeating the tree growing analysis 10 times with different randomly drawn samples from the analysis data. This is repeated for every tree size starting at the root of the tree, and applying it to the prediction of observations from randomly selected testing samples drawn from the original analysis data This results in a number of sub trees being generated from T_{max} and for each sub-tree, the average accuracy for cross validated predicted classification is calculated. Misclassification incurs a cost, in this case one per incorrect case, the total misclassification cost for each tree can be expressed as a cross validated (CV) cost. Breiman et al. (1993) suggests that the "best" tree is the smallest sized (least complex tree, as measured using the re-substitution cost) whose CV costs do not differ appreciably from the minimum CV costs. They proposed the one standard error (SE) rule that states that the "best" tree is the smallest sized tree whose CV costs do not exceed the minimum CV costs plus one times the standard error of the CV costs for the minimum CV costs tree (Breiman et al., 1993). Using this rule helps to avoid over fitting

or under fitting of the data for predictive purposes. While this method is acknowledged as not being foolproof, it does remove the subjectivity involved in the selection. It has been found that using the one SE rule leads to conservative estimates of predictive accuracy (Breiman et al., 1993). This rule was used to determine the best tree for the prediction of avalanche days.

5.3   Classification Tree Results

The over fit classification tree T_{max} split the 343 case data set into pure homogeneous nodes of avalanche and non-avalanche days in only 44 nodes. This tree was then subjected to 10-fold cross validation to determine the best tree for the predictive, forecasting application. The CV and re-substitution cost sequence associated with the various alternative trees can be seen in Figure 5.3. Tree 8 has the lowest CV cost at 0.221 with a standard error of 0.023. By applying the one SE rule, and finding the least complex tree within one times the standard error of the tree with minimum CV cost, the best tree is found to be Tree 9, with a CV cost of 0.242.
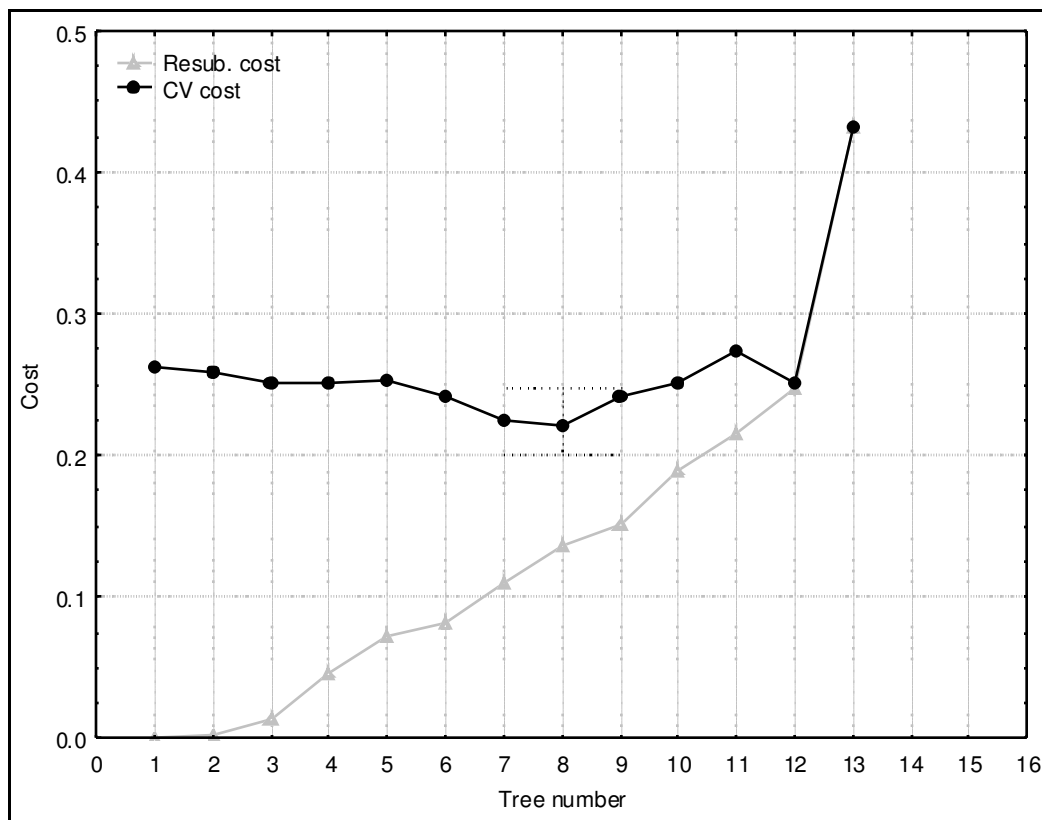
Figure 5.3   Cost sequence for the classification trees analysis created for avalanche day
showing Tree 8 with the lowest CV cost (circles). The dotted error bar
indicates the SE for Tree 8 and identifies Tree 9 as the best tree for
forecasting

Tree 9 (the entire tree in Figure 5.4) has six terminal nodes resulting from five splits. The
first split from the root node (ID=1) is determined using the temperature dependent 72
hour wind drift 2 parameter (72hSumPPT*WSpdAve_Temp). This splits the 343 mostly
non-avalanche days, into 167 mostly avalanche days (ID=3) above ≈ 863000, and 176
mostly non-avalanche days below (ID=2). The 176 mostly non-avalanche days are split
on the basis of the 72 hour averaged wind speed at Mt Belle, with 17 as mostly avalanche
days (ID=4) below 3.96 kmh^{-1} and 159 as mostly non-avalanche days above this (ID=5).
The 167 mostly avalanche days (ID=3) are split on the basis of 12 hour averaged air
pressure at East Homer, with 142 mostly avalanche days below 1010.23 hPa and 25
mostly non-avalanche days above this. The 142 mostly avalanche days (ID=42) are split
on the basis of the 72 hour maximum air temperature at Mt Belle, with 97 mostly
avalanche days below 2.9°C and 45 mostly non-avalanche days above this. The 45

mostly non-avalanche days (ID=45) are split on the basis of 72 hour averaged snow depth at Mt Belle, with 21 mostly non-avalanche days below 1.95m and 24 mostly avalanche days above this.
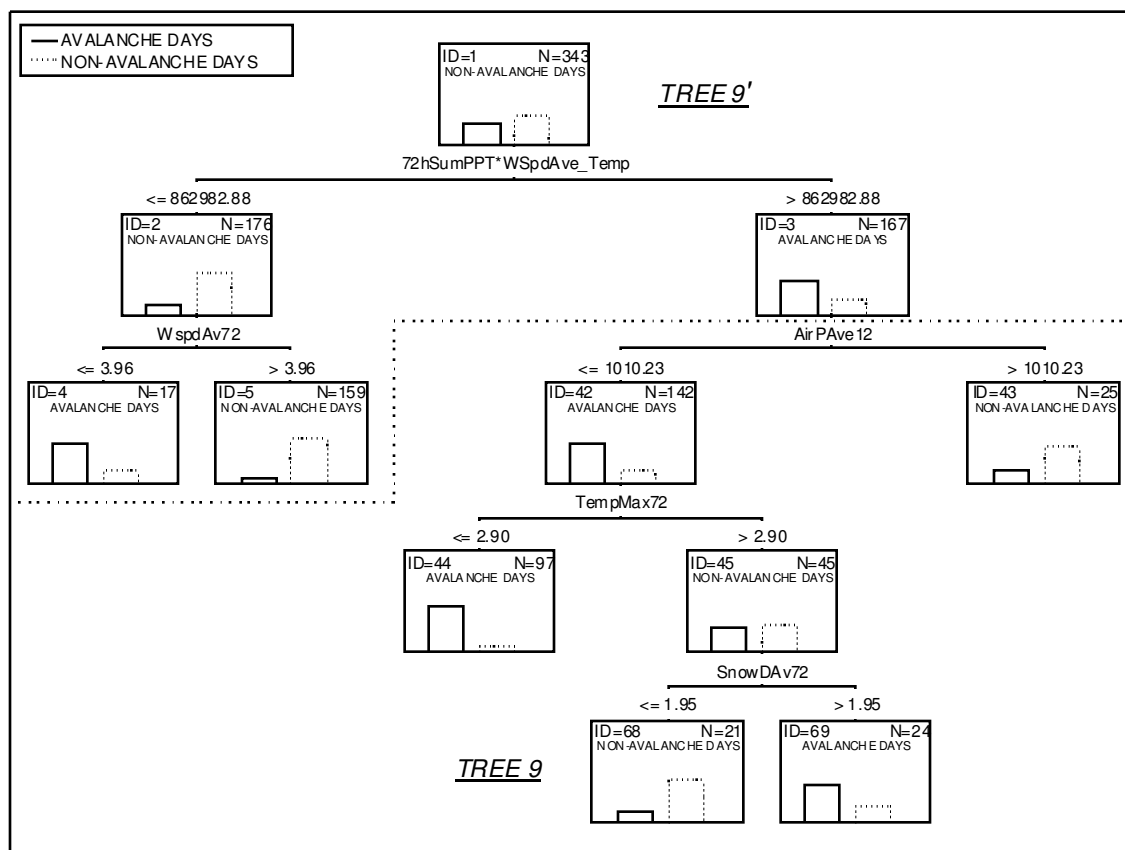
Figure 5.4   Avalanche day classification tree analysis following 10-fold cross validation showing the full tree, Tree 9 and the reduced tree, above the dotted horizontal line, Tree 9'. Variable names used are as in Table 5.2.

The classification matrix for tree 9 (Table 5.3) gives an overall probability of detection (POD) of 85%, with 291 of the 343 cases correctly identified. The rate of correct POD for avalanche days is lower at 79% with 117 of the 148 cases correctly identified. The remaining 31 cases (21% of observed avalanche days), were incorrectly predicted as non-avalanche days, i.e. false negatives. These false negative days are potentially more significant, or dangerous for operational purposes than the 21 false alarm or false positive cases. To lower the number of false negative cases, the misclassification cost was changed to penalise the analysis more for incorrectly classifying observed avalanche days

as non-avalanche days. Initially, the misclassification costs were set at one for both types of misclassification. In the second analysis, a misclassification cost of two for false negatives is introduced and a misclassification cost of one for false positives is maintained. This resulted in a smaller classification tree, Tree 9', consisting of the nodes ID=1 to ID=5 from Tree 9 (Figure 5.4). The classification matrix for this tree (Table 5.4) gives an overall lower POD of 78%, with 267 of the 343 cases correctly identified. However, the rate of correct POD for avalanche days is higher at 86% with 128 of the 148 cases correctly identified, thereby lowering the number of false negatives from 31 to 20. As a consequence of raising the misclassification cost for the false negative case, the model is now more conservative resulting in an increase of false positives or false alarm cases from 21 to 56 in Tree 9'.

Table 5.3   Classification matrix for Tree 9, with observed cases in columns and the predicted cases in rows. The total number of observed avalanche day, and non-avalanche day cases are in bold at the bottom of the columns

N=343		Observed	
		YES	NO
Predicted	YES	117	21
	NO	31	174
		148	**195**

Table 5.4   Classification matrix for Tree 9', with observed cases in columns, and the predicted cases in rows. The total number of observed avalanche day, and non-avalanche day cases are in bold at the bottom of the columns. Misclassification costs are shown in brackets, and have been set higher for the false negative cases.

N=343		Observed	
		YES	NO
Predicted	YES	128 (0)	56 (1)
	NO	20 (2)	139 (0)
		148	**195**

5.4 Discussion

Classification tree methods have been applied to a range of avalanche data sets (Davis et al., 1996, 1999; Elder and Davis, 2000; Rosenthal et al., 2002; Schweizer and Jamieson, 2003). However, to the author's knowledge there has been no study that has successfully applied this cross validation technique for estimating forecasting accuracy. Previous work has either used classification trees for exploratory purposes (Davis et al., 1996; 1999), or tested against data sets for a new season (Rosenthal et al., 2002).

The 10-fold cross validated classification tree results in statistically very high correct classification rates. These rates are very encouraging, should the method be as conservative as Breiman et al.(1993) suggests it is using the one SE rule. Furthermore, the estimated overall POD of Tree 9 of 85% exceeds the desired 80% performance limit suggested by Föhn(1998) for models not taking into account physical snow cover processes and rupture criteria. It is suggested that the main reason the classification rates are so high is due to the direct action avalanche regime experienced on the Milford Road and the inclusive definition for the avalanche day parameter.

The use of classification trees as an exploratory tool to gain better understanding of the processes operating is clearly illustrated in Tree 9. On examination of the splitting criteria one can observe some splits that are obviously linked to a range of physical processes. The first split, based on the 72 hour temperature dependent wind drift 2 parameter, clearly splits the dataset into mostly avalanche and non-avalanche days. The avalanche days below this splitting value (as seen in ID=2) represent the avalanche days with light winds, and heavy snow, as the wind is the fourth power in the wind drift parameter. The following split on this node using the 72 hour averaged wind speed further reinforces this concept, with the majority of the remaining avalanche days occurring at very light wind speeds, below 3.96 kmh^{-1}.

The split at node three (ID=3) based on the 12 hour averaged air pressure is interesting as it is the only variable used in the classification tree that is not over a 72 hour period. As the majority of the avalanche days occur below the splitting criterion on air pressure, short durations of lower air pressure must be important to the avalanche formation process, i.e. the centre of a low, or the passing of a trough. This comes as no surprise as these are often also periods of high precipitation intensity. Below this one can see the role of the maximum air temperatures, with the vast majority of remaining avalanche days occurring below a maximum of 2.9°C. The final node (ID=45) provides some insight to a threshold snow depth for avalanches occurring with high maximum temperatures, most likely to be the thaw events. This depth of 1.95m does not seem unreasonable as field observation suggests that at least 1.5m of snow is required to cover ground roughness.

Some of the important parameters defining the splits in the classification tree have been noted by previous studies. The importance of the wind drift parameter was highlighted by Davis et al.(1996, 1999) as was the 3 day precipitation (included in the wind drift 1 and wind drift 2 parameters) by Bakkehoi(1987) for direct action avalanches in Norway. However, the 12 hour air pressure, or anything analogous to this, has not been commented on in previous works, and may reflect the nature of the maritime climate with rapidly moving synoptic weather systems, in which the Milford Road is located.

While the exploratory nature of classification trees is appealing, the impact of changing the misclassification cost for false negative cases also needs to be considered for operational forecasting purposes. While the overall POD for the second tree (Tree 9') is lower at 78%, the rate of correct POD for avalanche days is much higher, with the number of false negatives lower. Unfortunately, as a consequence of modifying the false negative misclassification cost of the analysis, the number of false positives or false alarms has also increased with Tree 9'. Arguably however, it is the ability to be able to predict avalanche days, rather than non-avalanche days that is a more important measure of the success of any operational model. Tree 9' while much smaller and providing less exploratory insight, does reinforce the importance of wind and precipitation in this maritime climate as discussed by Sturman and Wanner(2001) and Sturman and Tapper(1996) for the general climate of the Southern Alps. These parameters are considered to provide the fundamental controls on avalanche forecasting in this maritime climate.

Finally, it is proposed that Tree 9' would be more suitable for conservative forecasting purposes as it is more sensitive to the case of false negatives. However, if the interest is in providing further insight into the process operating Tree 9 is better suited. Therefore, as a logical next step, a new season's data should be compared to the statistical predictive accuracy for both Tree 9 and Tree 9'. This would permit the examination of which tree has the highest operationally correct POD and thereby determine which tree would be best suited for future forecasting.

5.5   Conclusion

This study has successfully trained and 10-fold cross validated two classification trees to identify avalanche days based on meteorological parameters for the Milford Road. Using an extensive database of meteorological parameters and avalanche occurrences from the Transit New Zealand Milford Road Avalanche Programme, the relationship between storm and avalanche activity in this extreme climatic region has been described and

statistically explored. Two 10-fold cross validated classification trees were created, and suggested for use in forecasting. The classification tree with highest accuracy of 85% predicted avalanche days less well at 79%. An alternative tree using only wind speed and wind speed and precipitation combined in a temperature sensitive wind drift parameter resulted in a lower overall accuracy of 78%, but permitted a higher rate of correct prediction for avalanche days at 86%. These parameters are considered to be the fundamental controls on avalanche forecasting in this maritime climate. The more conservative tree also reduced the number of false negative cases (observed as avalanche days, but predicted as non-avalanche days) from 31 to 20 at a cost of increasing the false positive or false alarm rate.

6.0 Visualisation and examination of avalanche activity in a GIS

6.1 Introduction

This chapter has been modified from the manuscript Hendrikx et al.(2004). It examines topographical and meteorological controls on avalanche occurrence and links these variables in a Geographic Information System (GIS) which in turn allows for the visualisation of the spatial distribution of avalanche occurrence under a range of different scenarios.

In discussing the fundamentals of avalanche forecasting, LaChapelle(1980), McClung and Schaerer(1993) and McClung(2002b) all noted that there is a need to improve methods of data storage and analysis for the purpose of maintaining institutional memory. A GIS would facilitate this need for the Milford Road and also provide for the visualisation of the temporal and spatial effect of weather events on avalanches. Maintaining this institutional memory is an integral part in succession planning and provides the necessary background for avalanche hazard management and forecasting (LaChapelle, 1980; McClung and Schaerer, 1993; McClung, 2002a, 2002b).

Advances in GIS technologies and high resolution Digital Elevation Models (DEM) have the potential to contribute to several components of avalanche forecasting, visualisation and control. A GIS can assist in modelling avalanche formation processes such as snow accumulation and snowdrift, provide a spatially based inventory of avalanche events and associated control, allow visualisation of this data, and allow automated processes for avalanche terrain mapping. Bolognesi et al.(1996) presented the idea of using a GIS to describe starting zones to assist in hazard mapping and provide input for avalanche hazard forecasting. However, it is only in recent studies that attempts have been made to

automate the process of identifying avalanche paths and thereby the avalanche hazard (Gruber and Haefner, 1995; Tracy, 2001; Maggionni et al., 2002; Ghinoi, 2003). Maggionni et al.(2002) used specific terrain parameters to predict avalanche occurrence frequency from an extensive database from around Davos, Switzerland. Using a GIS as a tool for visualisation is becoming more readily accepted as a common method to display avalanche hazard as shown through the work of Leuthold et al.(1996), Stoffel et al.(1998), Gruber(2001), McCollister et al.(2002; 2003), and Purves et al.(2003). Purves et al.(2003) further extended this idea by allowing a forecaster to query the available data using a nearest neighbour approach as a basis for hypothesis testing. McCollister et al.(2003) also incorporated a nearest neighbour approach within a GIS to visualise predicted avalanche probabilities. A probabilistic method allowed McCollister to examine the spatial relationship of avalanche occurrences under various meteorological conditions and to express the result as a probability of occurrence. Patterns were found at the slide path scale, but no patterns were found when grouped by aspect, suggesting local topography is more important when relating wind direction to avalanche activity.

Earlier work on the Milford Road by Petrie(1984) examining the spatial distribution of avalanching, considered 16 large events and related these to synoptic weather records. Three main processes for large avalanches were distinguished, rain on snow, snow overloading and thaw events. Rain on snow was found to be associated with a northwesterly airstream on the western limb of an anticyclone to the east of the South Island. Snow overloading events were associated with a series of southerly fronts, often followed by a depression moving southwards and thaw events were associated with a slow moving intense anticyclone crossing the South Island. Petrie(1984) also found slopes with northeast aspects had the greatest amount of lee slope loading, as they are subject to loading from a wider range of common wind directions.

With this background in mind, the aims of this chapter are threefold:

❋ To describe a GIS that links information on the spatial extent of avalanche occurrences, photos, meteorological data, DEM and high resolution aerial photographs

❋ To show how the use of this GIS for hypothesis testing, through querying a range of temporal, spatial and meteorological parameters will lead to a better qualitative understanding of the spatial distribution of avalanche occurrences and thereby maintain institutional memory

❋ To quantify the effect of topography and meteorological parameters on the spatial distribution of avalanche occurrences on the Milford Road

6.2   Information and approaches

The broad approach taken was to create a GIS that links the spatial information on avalanche occurrences with the meteorological data and display this on a high resolution DEM. The avalanche and meteorological information comes from the Transit New Zealand Milford Road Avalanche Programme as described in Section 2.7.

6.2.1 Avalanche Data

As noted in Chapter Two the Transit New Zealand Milford Road Avalanche Programme stores information on avalanche occurrences in a variety of forms. Since 1985 a consistent and accurate avalanche database has been maintained. This database containing all standard avalanche observation information is complemented with a selection of photographs showing spatial extent of avalanching, with the extent manually drawn on a base photograph of the avalanche path in question. Unfortunately, neither the database nor the photographs individually provide a complete data set on spatial extent of avalanching. Out of the 2805 avalanche events, approximately 1500 have images and 1400 have information about avalanche width. Generally, larger avalanches have been

recorded to higher a standard than smaller avalanches. However, all avalanches on record have information on size and path name. Therefore, using the information available in the database on width, depth and extent of cover over the road, in combination with the photographs, representative outlines for avalanche occurrences, at 0.5 Canadian size class intervals(McClung and Schaerer, 1993), were created. This was done mainly because of data constraints, but also to allow all avalanche occurrences to be graphically displayed, despite their varying data quality. Representative avalanche outlines were calibrated and drawn within ESRI's(1999) ArcGIS for each size on each path from available photos and database information. In total there are 75 avalanche paths, where zones in a path are considered as a separate path. These representative outlines were then used to describe the spatial extent of all avalanches of that size on that particular path, resulting in a maximum of 11 different outlines for each of the 75 avalanche paths This method obviously makes the assumption that there is a positive relationship between avalanche class size and spatial extent as shown by Keylock et al.(1999). Examination of the data set suggested that this was a reasonable assumption, though the author readily acknowledges that an individual avalanche of a particular size may well exceed the representative outline of that size. What this method lacks in precision, it gains in being able to qualify the data while also facilitating the examination of spatial patterns from a dataset that previously was only being stored in a database form showing no spatial information.

Each of the representative avalanche outlines were then duplicated for each avalanche occurrence and coded with the unique identifier from the avalanche database. The code enabled a spatial representation to be connected to the avalanche database, to associated meteorological data, and where available, an avalanche occurrence photo.

6.2.2 Meteorological Data

To examine the effect of meteorological parameters on the spatial distribution of avalanche occurrences, the outlines of avalanche extent were connected to the appropriate meteorological data. Meteorological data was selected from Mt Belle and East Homer

AWS which both record standard meteorological parameters (Figure 2.2 and Table 5.1). The previous 72 hours weather data from these two weather stations was then selected for each avalanche occurrence as described in section 5.2.1. Only the preceding 72 hour meteorological data was extracted as earlier work has shown this environment to be a predominantly direct action avalanche regime with the majority of avalanching occur during or shortly after a storm (Conway et al., 2000; Hendrikx et al., 2005). For this analysis only the 72 hour vector averaged wind direction and speed from Mt Belle AWS have been considered. As noted in Chapter Five, Mt Belle is located at starting zone elevation, on an exposed ridge, but below the mean mountain top height. This suggests that while Mt Belle may be indicative of wind speeds in the starting zones, it may do less well for the general synoptic wind direction across the region. Wind directions recorded at Mt Belle are likely to reflect wind funnelling by local topography.

Parameters other than wind direction and wind speed can be queried but these have not been used in these analyses. This was undertaken as a first approach, to clearly differentiate between the documented two major storm directions, northwest and south. Using only the 72 hour vector averaged wind direction and speed does mean that only storms of 72 hours duration or longer are examined and shorter storms with variable wind directions will be excluded. Using the available hourly data resulted in a data set of 2237 avalanches occurrences on 299 individual avalanche days.

6.2.3 Topographic Data

Detailed topographic data is required for the representation of the avalanche information. A 25m DEM is available from Land Information New Zealand (LINZ) for all of New Zealand and is derived from vector contour and spot height point data contained in the Infomap 260 series 1:50,000 scale topographic database. The DEM has a positional accuracy of ± 22m from its actual position for 90% of the ungeneralised features (Land Information New Zealand, 2005). Unfortunately, further specific information regarding the accuracy of the data in the Milford Road region is not available.

In order to obtain a more accurate alternative, an ASTER (Advanced Spaceborne Thermal Emission and Reflection Radiometer) image was obtained for the area, from which a DEM could be constructed. ASTER is an imaging instrument flying on Terra, a satellite launched in December 1999 as part of NASA's Earth Observing System (Abrams et al., 2002). ASTER's along-track stereo sensor allows for photogrammetric DEM generation using the vertical and aft tilted telescopes (Figure 6.1).
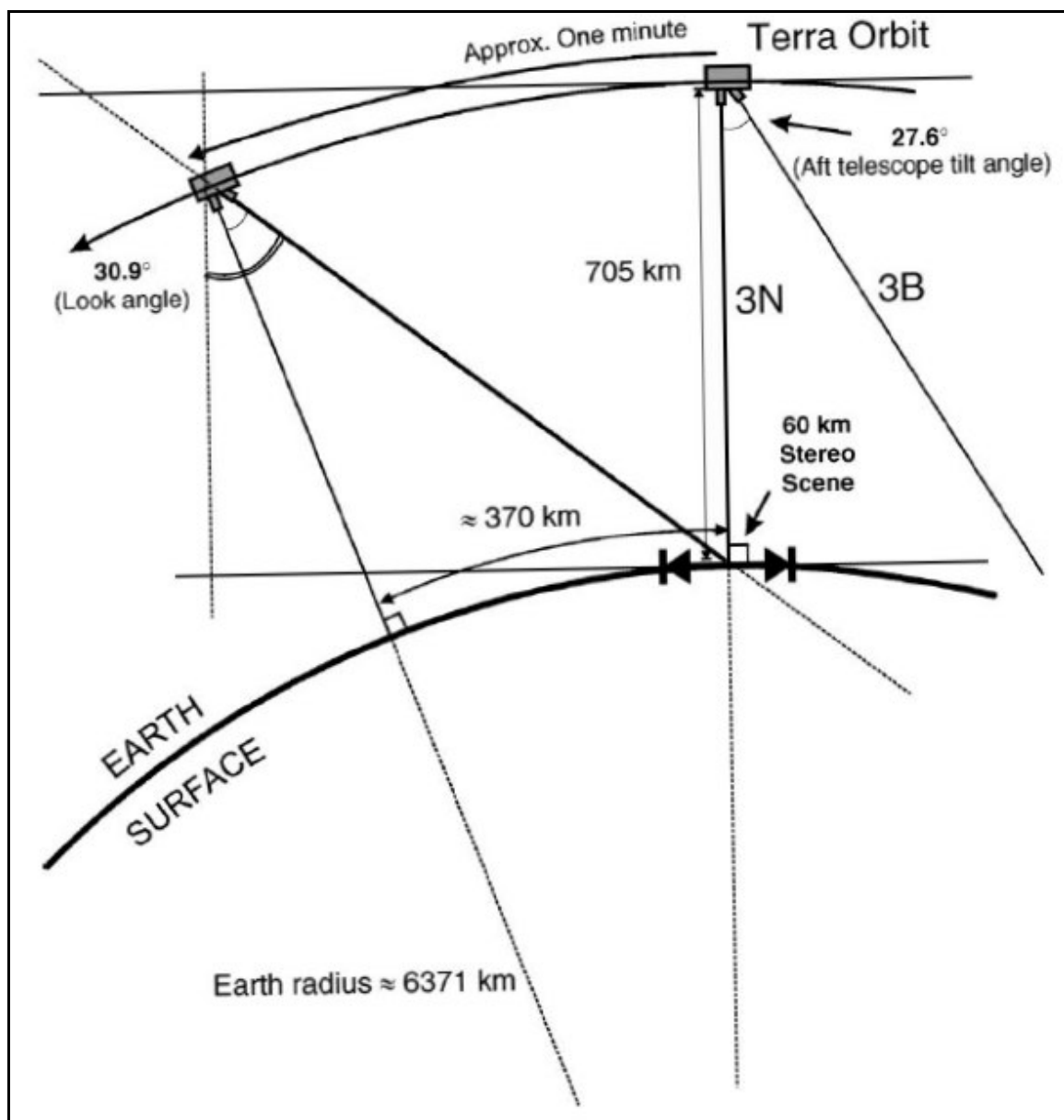
Figure 6.1   Diagram of the imaging arrangement for ASTER along track stereo.
               (Source: Hirano et al., 2003, p.358)

An ASTER satellite image was obtained from NASA that included the Milford Road and surrounding area (Figure 6.2). The L1A ASTER image was acquired on 27/01/2002, centred at -44.93°latitude, 168.08° Longitude, Granuale: SC:AST_L1A.003:2005904706. Field work using differentially correctable GPS was completed in February 2003 to obtain ground control points for the ASTER satellite Image. ERDAS Imagine v8.3 (Leica Geosystems, 2003) was used to create a second order polynomial model against which the GPS points could be compared. This comparison was undertaken to quantify the deviation of each GPS point relative to a best-fit model used to rectify the image. Erroneous points with high error values were reconsidered and on occasion relocated. Previous studies suggested that this method could potentially provide data for the creation of a DEM of a resolution equal to or greater than 7m (Welch et al., 1998; Lang and Welch, 1999; Abrams and Welch, 2001).
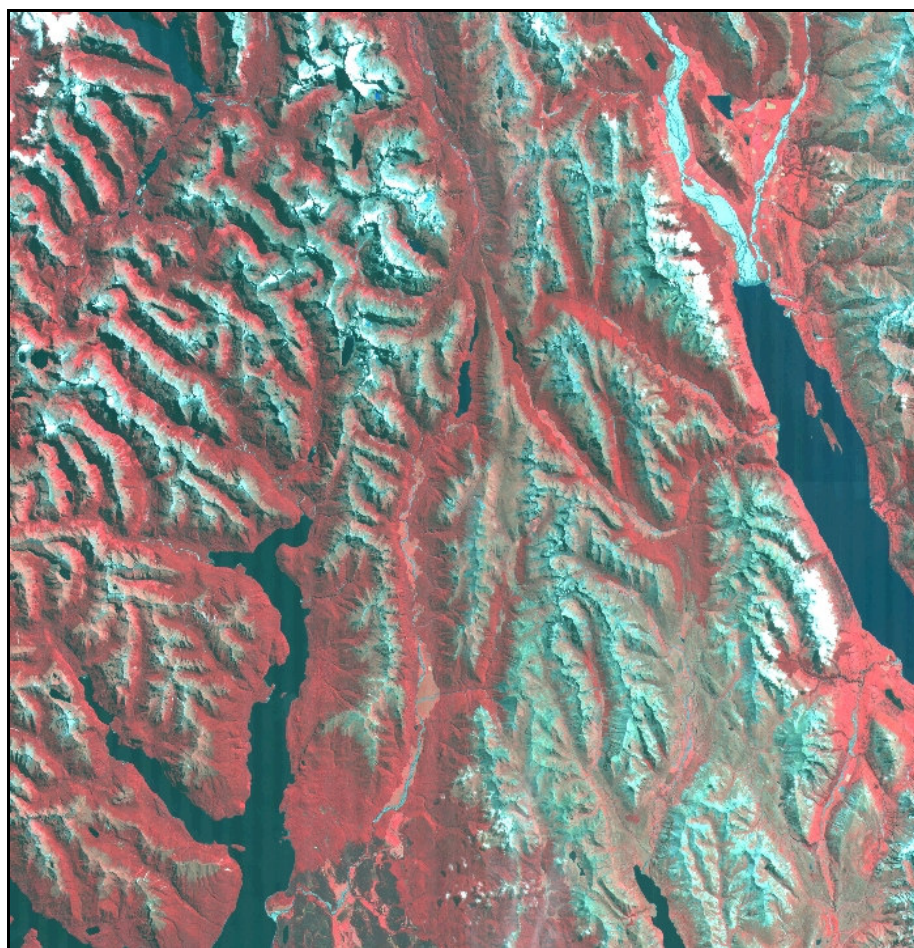
Figure 6.2   L1A ASTER image used for the Milford Road region with Milford Sound (Top left), Lake Te Anau (Bottom left) and Lake Wakatipu (Centre right)

Unfortunately, after having obtained high quality ground control points, and submitting this data to NASA via an online request form, the resulting DEM was unsatisfactory. The DEM had many significant "holes" in the surface because of the steep terrain and shadowing resulting in missing data from the 3B signal, and loss of the stereo pair (Figure 6.3). The DEM also had a disappointing low spatial resolution of 30m, compared to that of 25m for the LINZ DEM. Comparisons with the LINZ 25m DEM showed significant differences, with up to 1000m in elevation between the two DEMs at points on attenuated ridge lines.
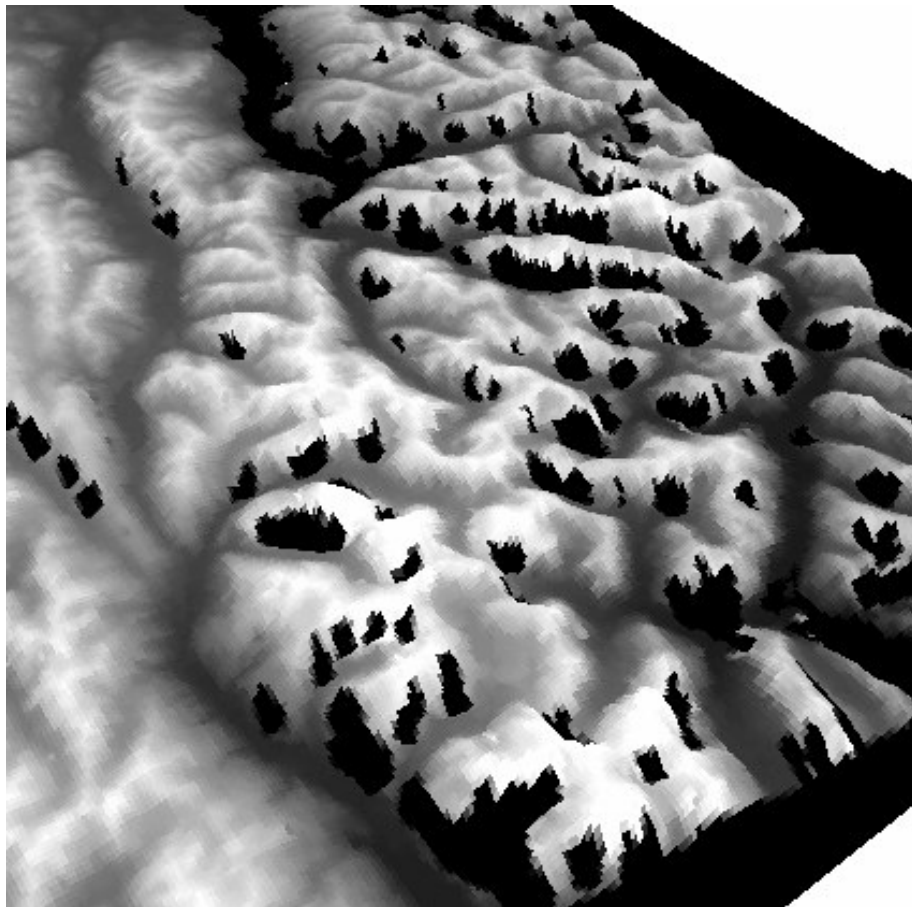
Figure 6.3   ASTER DEM created from ground control points and L1A ASTER image, note the large holes in the DEM. Milford Sound (Bottom right), Lake Te Anau (Top Left)

Recent work with ASTER DEMs has shown similar results in steep alpine areas, with individual maximum errors in elevation of up to 500m and a Root Mean Square (RMS) error of ± 60m (Kääb, 2002; Kääb et al., 2003). Hirano et al.(2003) calculated a maximum of ± 50m RMS error in less steep terrain, and Vignon et al. (2003) calculated a RMS error of ± 22, with individual maximum errors of 58m. However, Cuartero et al.(2004) and Gonçalves and Oliveria(2004), working in rolling terrain, concurred with Abrams(2000) estimates that the ASTER DEMs will have an absolute accuracy of between 15-30m RMS error, calculating an RMS error of ± 15m.

With the LINZ 25m DEM being of insufficient accuracy, and the ASTER DEM providing no improvement, it was decided to pursue a third option for DEM production, digital photogrammetry. This DEM was produced using automatic and interactive photogrammetric terrain modelling processes. The aerial photography used was acquired on 15 December 1988, has a nominal scale of 1:50,000 and was taken with a 152mm focal length lens metric aerial camera with a negative size of 23cm by 23cm. The film was scanned using a ZI Imaging Photoscan 2001, with a spot size of 14μm. The photogrammetric processing was undertaken using Socet Set photogrammetric software (BAE Systems, 2003). A DEM with a grid spacing of 3m was generated using the automatic terrain extract module of the software, using hierarchical image matching algorithms to locate conjugate points in stereo overlaps between photos. Interactive terrain editing tools were then used by an experienced photogrammetrist at Aerial Mapping New Zealand Ltd. to edit the DEM where the automatic terrain extraction had not been successful. Particular attention was paid to the ridge lines and outcrops to ensure that they were well represented by the terrain model. In open ground, the DEM is estimated to have a relative accuracy of ±3m RMS error, with an absolute accuracy of ±5m RMS error. The representative outlines of avalanche occurrences were then drawn in the GIS on this high resolution DEM and associated aerial photograph. An aspect grid was created from the 5m DEM and this was used to determine average aspect of the avalanche occurrences and avalanche paths into 8 discrete aspect classes.

6.2.4 Outline of the GIS

The three data components previously discussed, avalanche outlines, meteorological data and the 5m DEM and associated aerial photograph, were joined in the GIS to create a relational spatial database (Figure 6.4). In the GIS used (ESRI, 1999), queries are facilitated under a standard "select-by-attributes" command, using Boolean language allowing searches of the entire database and associated linked tables. On return of the search criterion, the linked tables can also be viewed and further queried. Examples of search criteria include: path name, location, aspect, trigger, size, time range and multiple meteorological parameters.
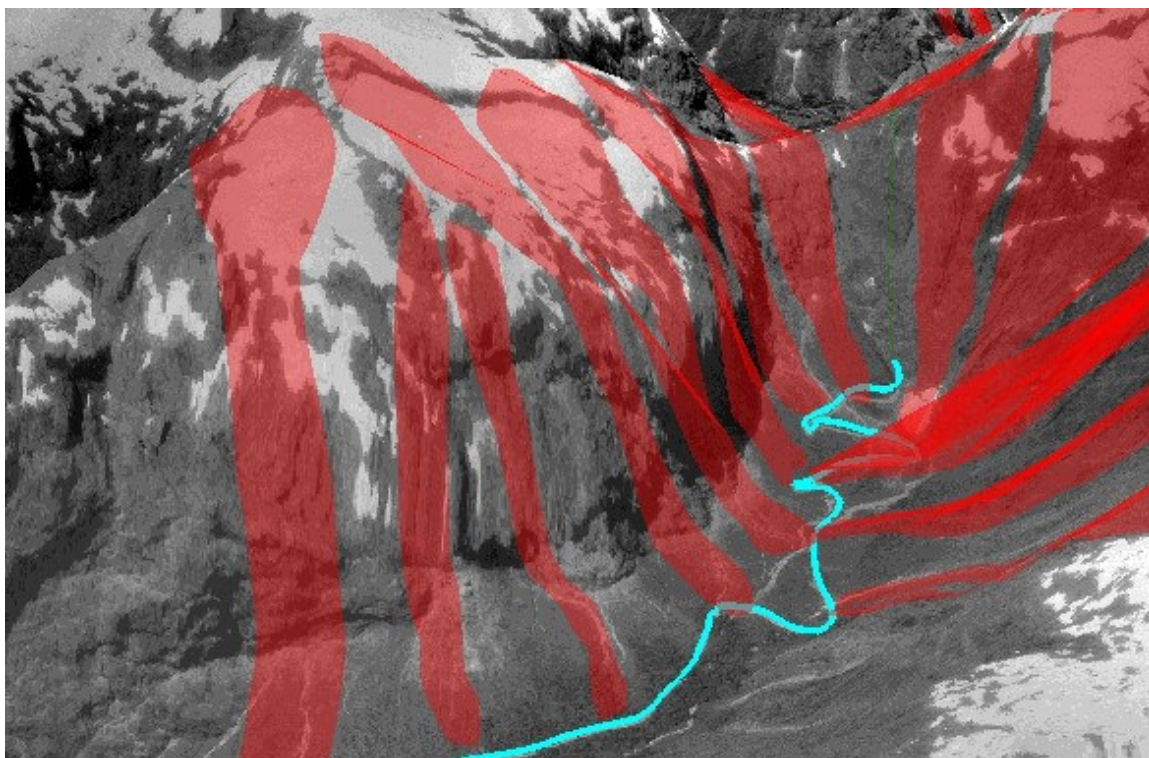
Figure 6.4   3D view of the western side of the Homer Tunnel, showing multiple avalanche paths (Red), the Milford Road (Cyan), and the aerial photograph overlaid on the DEM

The GIS allows a forecaster to specify any range of parameters and visualise the resulting spatial distribution. For example, one can query a particular time period, to see which paths avalanched during a storm, and then see the associated meteorological parameters.

One can also examine the complete history of just a single path, a particular month or the entire record for the whole area. The system can also be used for hypothesis testing of scenarios and as a teaching tool for new forecasters. For instance if an approaching storm is forecast to have a given wind speed and direction with a certain amount of precipitation, the forecaster can query the meteorological data for similar conditions and view all of the resultant avalanche occurrences. These avalanche occurrences can then be further queried, for example, to only consider avalanche paths that have already been controlled, or to restrict the query to occurrences with a similar snow depth. The end result of any query is displayed on the high resolution aerial photograph in plan view. The number of occurrences on each path for any given scenario can be then colour coded from transparent (no occurrences) to light yellow (few occurrences) to red (many occurrences). While this approach does not provide a probability of avalanche occurrence on a path, it allows a forecaster to obtain a qualitative understanding of where avalanches have occurred under similar conditions in the past.

6.2.5 Visualisation of storm direction effects on avalanche activity

Using the GIS, a qualitative analysis can be undertaken to examine the effect of meteorological parameters on the spatial distribution of avalanche occurrences. Two dominant storm types were selected, southerly and northwesterly storms. These were selected as previous work (Petrie, 1984) and anecdotal evidence from forecasters suggested that they both show characteristic meteorological trends and therefore may result in different avalanche occurrence locations. The southerly storm is usually colder, has lighter winds and less precipitation than the northwesterly storm. A southerly storm will often bring snow down to road level and deposit light dry snow in the starting zones, whereas a northwesterly storm will regularly bring rain or heavy wet snow to the starting zones, especially in spring. These two storm directions are related to the synoptic types SW and T, which have been shown in Chapter Three to have a positive correlation with avalanche occurrences. The difference between synoptic chart wind direction indicators and ground level wind direction as recorded at Mt Belle can be explained by a number of

reasons including, the frictional effects over mountains and resultant deflection of the wind direction, and the funnelling of wind by local topography.

For this analysis, all days with a 72 hour vector averaged wind direction between and including 134° to 225° were considered as a southerly storm, irrespective of wind speed. This resulted in only 19 avalanche days being selected, with 99 avalanche occurrences. As the majority of the data set contained days with northwest wind, a tighter constraint was placed on the selection of northwest storm days. With the intention of observing the effect of lee slope loading, a light to moderate wind speed threshold was selected. The selected days for northwest storms were days with a 72 hour vector averaged wind direction between and including 270° to 360°, with 72 hour vector averaged wind speeds between and including 20 to 30 kmh^{-1}. This resulted in 53 avalanche days being selected, with 408 avalanches occurrences. Using the colour coding system built into the GIS, the resultant pattern of avalanche occurrences permitted a qualitative examination of the spatial extent of all avalanche occurrences by path in relation to the two storms.

6.2.6 Topographic controls on avalanche occurrence

While a qualitative analysis of avalanche occurrences provides some insight into the spatial distribution of avalanches, the data base may be queried to provide information for quantitative comparisons, for example by calculating the ratio of number of avalanche occurrences on a given aspect to the number of paths of that aspect. As a first approach, aspect was chosen as the topographic variable to be examined, as slope, elevation and morphology of the starting zones were considered to be less variable. Aspect, while only being one component of topography that may explain the spatial distribution, has been used previously to examine avalanche occurrence relationships (Petrie, 1984; Maggioni et al., 2002; McCollister et al., 2002; Ghinoi, 2003; McCollister et al., 2003). Additional analysis could consider elevation, slope or morphology, as a singular or compound query. However, for this analysis only aspect was considered to highlight how this method can be applied.

Avalanche paths and avalanche occurrences where classified into the 8 cardinal points of the compass and an Excess Ratio (ER) was calculated as shown in equation 6.1. The ER describes the relationship between the number of avalanche occurrences and the number of avalanche paths for a given aspect class. A ratio greater than zero indicates that there are relatively more avalanche occurrences on a given aspect than the number of avalanche paths would suggest, whereas a ratio less than zero means that avalanche occurrences on the given aspect are relatively less frequent.

$$ER_a = \left(\frac{\Phi_a \left/ \sum_{i=1}^{8} \Phi_i \right.}{\Lambda_a \left/ \sum_{i=1}^{8} \Lambda_i \right.} \right) - 1 \qquad (6.1)$$

Where: Φ = Number of avalanche occurrences

    Λ = Number of avalanche paths

    i = Index for aspect class (e.g. north, northeast, east… etc.)

    a = Index for aspect of interest

6.2.7 The influence of the avalanche size

To further examine the relationship between avalanche occurrence and topography, all avalanche occurrences were classified into size groupings. Avalanche class size was divided into 5 groups: class sizes 1 to 1.5; 2 to 2.5; 3 to 3.5; 4 to 4.5 and size 5. Each of the size groups was then further classed in the 8 aspect classes and expressed in terms of the ER as shown in equation 6.1, where Φ is the number of size X avalanche occurrences, and Λ is the number of all avalanche occurrences. The ER has the same interpretation as previously noted except that it is expressed for the five size classes indicated.

6.2.8 The influence of storm direction

The ER was also applied to the two storm directions from section 6.2.5 to quantify the trends observed in the qualitative analysis. Both of the storm directions specified in the GIS analysis, northwesterly and southerly, had their avalanche occurrences classed into the 8 aspect classes and expressed in terms of the ER as shown in equation 6.1, where Φ is the number of avalanche occurrences for the storm direction, and Λ is the number of all avalanche occurrences. The ER has the same interpretation as previously noted.

6.3 Results and Discussion

This section will discuss the qualitative and quantitative results of the various analysis undertaken using the GIS.

6.3.1 GIS visualisation of storm direction

Using the GIS, the spatial distribution of avalanche occurrences classified by avalanche path for both southerly and northwesterly storms was qualitatively examined. Figure 6.5 shows the result of the query, where all avalanches resulting from winds from the south are considered. The southerly storm shows low values of avalanche occurrences on avalanche paths with a southerly aspect and higher values on avalanche paths with northwest, north and northeast aspects. This shows the effect of lee and cross slope loading and windward scour of these aspects under southerly wind directions. Southerly storms are often colder than northwesterly storms and deposit drier snow to low elevations, allowing wind redistribution to occur more easily. As seen in Figure 6.5 a discrepancy to this pattern exists with high values of avalanche occurrences on two paths with a southeast aspect (circled). The reason for this discrepancy is unclear, but may be attributed to the effect of local topography causing cross loading, or they could be unrelated to topography, resulting from heavy precipitation with very light southerly winds.
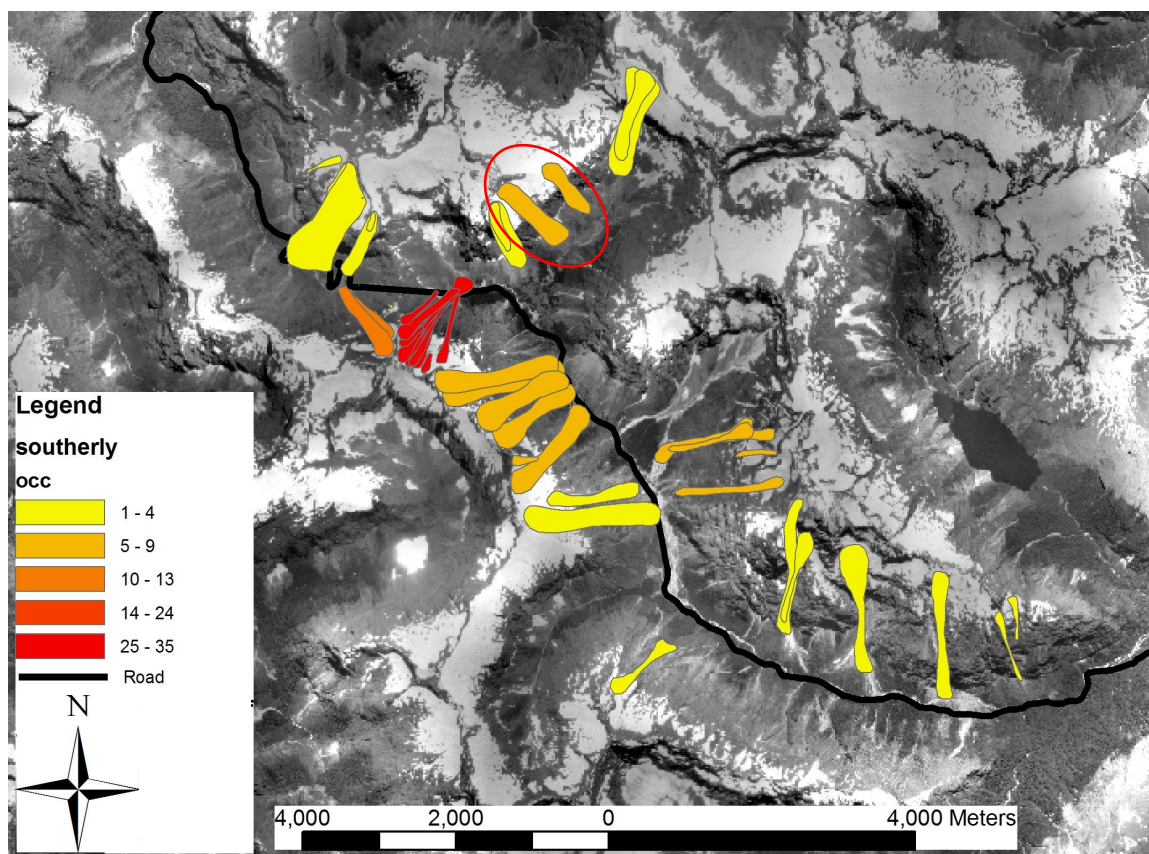
Figure 6.5   Qualitative GIS analysis of a southerly storm, showing cross and lee slope
loading on northwest, north and northeast aspects. Two notable
discrepancies to this pattern, on a south east aspect, are circled.

Figure 6.6 shows the result of the query to select all avalanches resulting from winds
from the northwesterly direction with a speed of between 20 and 30 kmh^{-1}. The
northwesterly storm analysis shows high values of avalanche occurrences on paths with
southwest, northeast and east and southeast aspects. The effect of lee and cross slope
loading is again noticeable, but the effect of windward scour is less clear, with high
avalanche occurrences also present on avalanche paths with northwest aspects. This can
be attributed to the warmer nature of the northwesterly storms. Northwest winds will
often be warm and lead to rain to high elevations, making a consolidated snowpack
which is difficult to entrain by wind. The inclusion of a temperature threshold to define
the extent or presence of wind drift, as used in Chapter Five where only days with a 72

hour mean air temperature below 1.5°C at Mt Belle were considered, revealed only very minor differences, with slightly more lee slope and less windward activity.
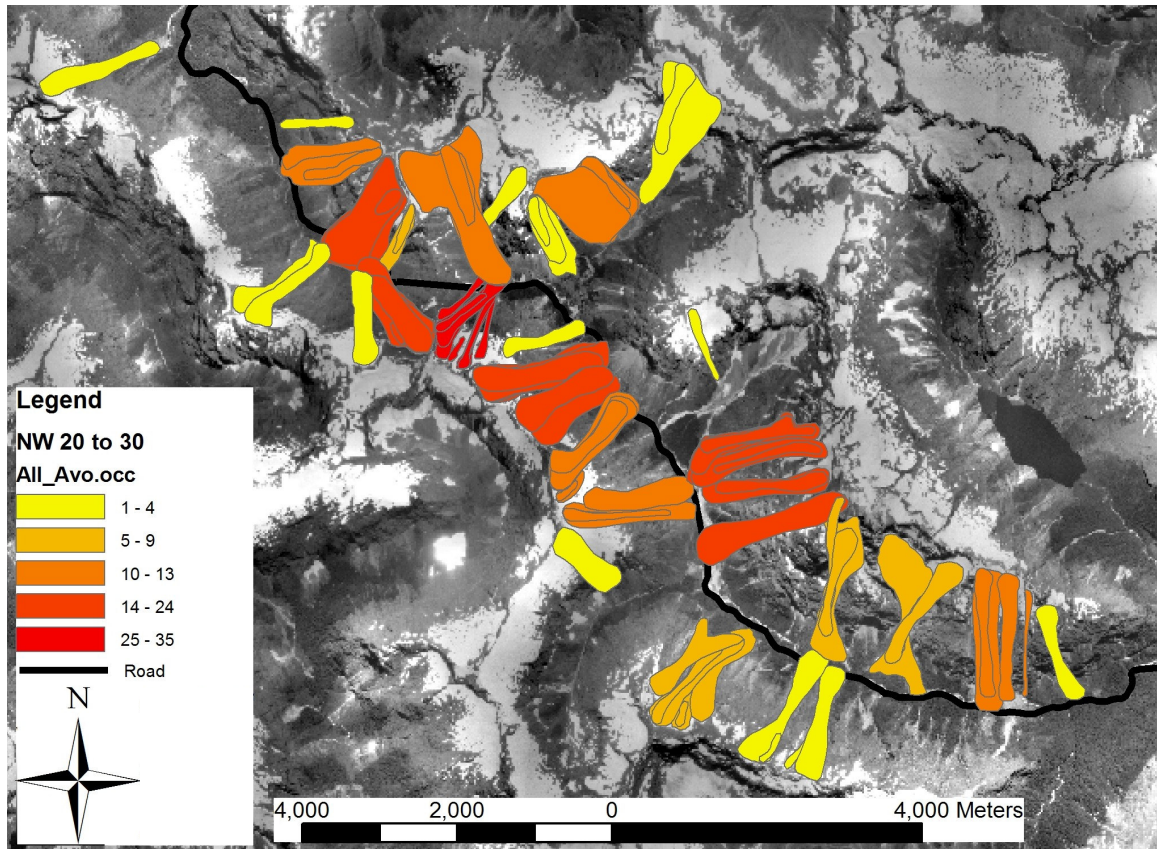
Figure 6.6   Qualitative GIS analysis of a northwesterly storm, showing cross and lee slope loading on southwest, northeast and east and southeast aspects.

As shown in these examples, the qualitative GIS analysis, while not providing a probability of avalanche occurrence as McCollister et al.(2002, 2003) does, allows a forecaster to obtain an improved qualitative understanding of where avalanches have occurred under similar conditions in the past. It also succeeds in working as a tool to allow easy querying of the database thereby permitting hypothesis testing, visualisation and aids in maintenance of the institutional memory.

6.3.2 Avalanche paths and avalanche occurrences by aspect

While the GIS permits qualitative analyses, the ER permits the quantitative examination of topographic controls. Figure 6.7, shows that avalanche paths are most frequent on north, northeast, south and southeast aspects and slightly less frequent on east aspects. They are much less frequent on southwest, west and especially northwest slopes. This distribution of avalanche paths in relation to aspect is mostly explained by the general southeast to northwest alignment of the Hollyford and Cleaddau Valley systems.
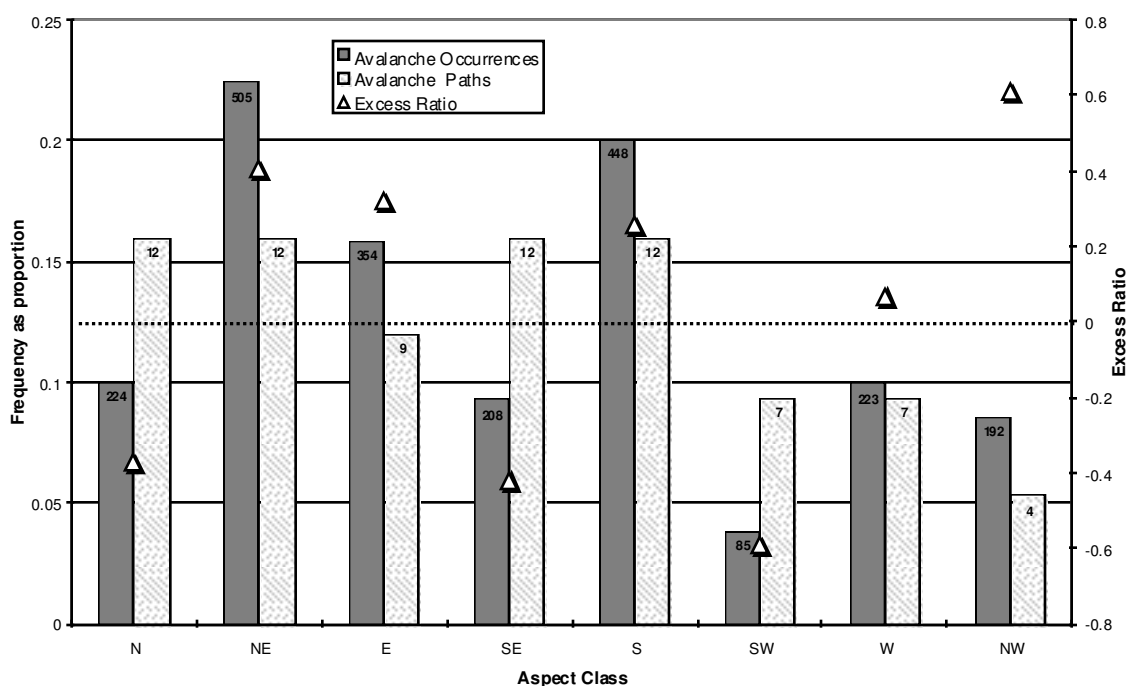
Figure 6.7   Frequency of avalanche paths and occurrences by aspect expressed as proportions and the ER. Absolute values for number of occurrences and paths are shown at the top of the columns

Avalanche occurrences are most frequent on northeast (0.22) followed by south (0.2) and east (0.16) aspects. Avalanche occurrences are least frequent on southwest (0.04) aspects, and have low frequencies on northwest (0.09), southeast (0.09), west (0.10) and north (0.10) aspects. The ER, for avalanche occurrences relative to avalanche paths as calculated for the north aspect, using equation 6.1, is shown in a worked example below in equation 6.2.

$$ER_N = \left(\frac{242/2237}{12/75}\right) - 1 \quad = \quad -0.37 \qquad (6.2)$$

The ER is greatest on northwest (0.61) followed by northeast (0.40) and east (0.32) aspects. The lowest ER is on southwest (-0.59) followed by southeast (-0.42) and north (-0.37) aspects (Figure 6.7). The high ER on the northeast aspect is consistent with the work of Petrie(1984) who suggested that this aspect is subject to loading from a wider range of common wind directions but the high ER for the northwest aspect is somewhat unexpected as the northwest wind is the predominant storm wind direction and one might expect to observe the effects of lee slope loading increasing the ER on southeast and southwest slopes. However, a closer look at the individual avalanche paths with northwest and northeast aspects reveals that they are also the paths that are frequently bombed for artificial release. The low ER on southwest and southeast aspects can be attributed to the fact that many of these avalanche paths do not affect the road directly or are obscured from view from the road, possibly leading to a lower rate of recording, especially of smaller events. Because of the lack of clear outcomes of this analysis, the influence of avalanche size was examined.

6.3.3 Avalanche size by aspect

In figure 6.8 the ER values for avalanche size classes are graphed for each aspect class. While size 5 avalanches only contribute approximately 2% of the total avalanche occurrences (Figure 3.7), they show some interesting trends when examined in terms of their ER. The high ER for size 5 avalanches on the southeast (2.07) and southwest (1.69) aspects shows that there are relatively more size 5 avalanches on these aspects, than the number of avalanche occurrences would suggest. This is consistent with the predominant wind direction being from the northwest, resulting in lee and cross slope loading. It is interesting to note the opposite effect for avalanches on northeast and northwest aspects, which is probably because of the effect of wind scour reducing the number of size 5 avalanches on these aspects. A contributing factor to the high ER is that the dominant

avalanche paths in these aspects do not affect road safety possibly leading to a lower level of active management and therefore a greater chance to accumulate sufficient snow to form size 5 avalanches. The suggestion of limited management on theses aspects is further supported by the low ER for size 1 and 1.5 avalanches on the southeast and southwest aspects (Figure 6.8), possibly representing under recording, because of low relevance to road safety management.
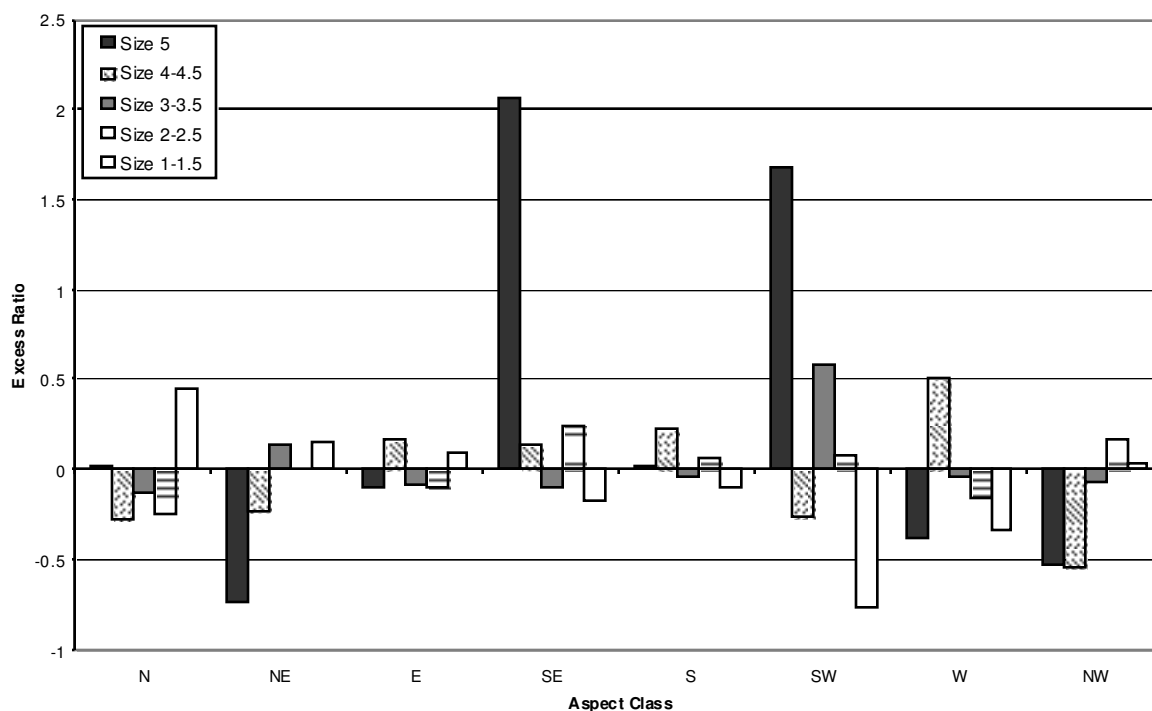
Figure 6.8   The ER for 5 size classes by aspect

6.3.4 Avalanche aspect by typical weather events

Having used the ER to examine the relationships between avalanche path and avalanche occurrence, and by avalanche size, it was applied to the two storm directions qualitatively examined using the GIS. Figure 6.9 shows that for the southerly storm the ER is low on the south (-0.47) and southwest (-0.35) aspects, while a high ER is on the northwest (0.41) and northeast (0.26) aspects. This clearly shows the effect of lee slope loading and

windward scour on these aspects under southerly wind directions. As shown in the GIS analysis, the SE aspect is somewhat anomalous.
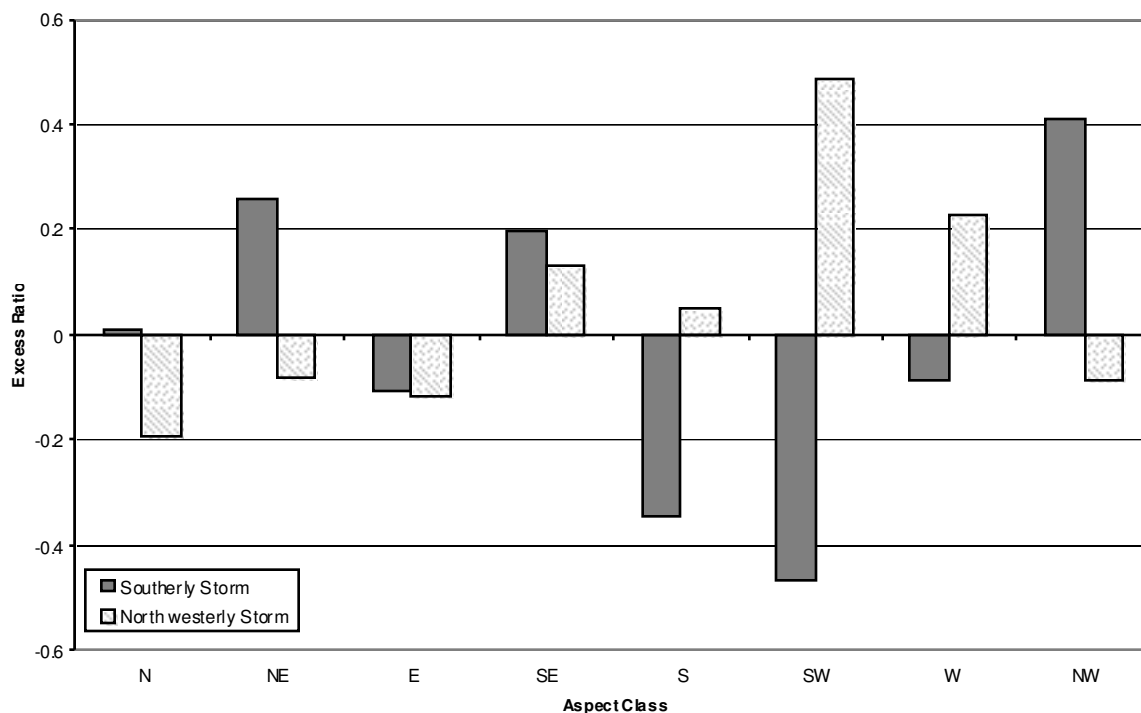
Figure 6.9   ER for two storm directions, northwest and south by aspect class

The northwest storm conditions result in a high ER on southwest (0.48) and west (0.23) aspects and a low ER on the north (-0.19) aspect (Figure 6.9). The effect of lee slope and cross slope loading is also clearly seen in the northwest storm with high ER values in southwest and west aspects. The effect of windward scour is less clear, with only small deviations in the ER for north and northwest aspects. As noted earlier, this reduction in windward scour can be attributed to the difference in temperatures between the two different storms, and resultant wind drift potential of the snow. It is encouraging to note that the patterns clearly observed in the qualitative GIS analysis of the two storm directions are mirrored by the quantitative ER analysis.

These analyses, quantitative and qualitative, are all completed using aspect and various subsets of the avalanche occurrence or avalanche path datasets. While the spatial relationships at sub aspect scale has not been considered, as McCollister et al.(2003) did,

at the slide path scale, some clear patterns in avalanche occurrences by aspect can be seen. While the analysis provided some unexpected results, for example a greater proportion of avalanche occurrence on windward slopes than expected, further refinements on the basis of size and storm characteristics do show clear aspect effects. This clear aspect relationship is thought to be due to two reasons, firstly, the majority of avalanches occur during or shortly after a storm, which is a reflection of the maritime snow climate, and storms predominantly come from two main directions, south and northwest. Secondly, in comparison to the work of McCollister et al.(2003), the Milford Road has avalanches when considered by area, at a scale one order of magnitude greater. This has led to an averaging affect by aspect, therefore not exhibiting the effect of local scale topography to the same extent.

6.4   Conclusion

This chapter has provided a description of the GIS, explaining the various data components available for query and analysis. This has highlighted how the GIS permits rapid access to a range of related meteorological, photographic, and topographic information for avalanche occurrences, which had previously had been stored separately, or in non-electronic formats. Examples have been shown how this GIS can be used for hypothesis testing and visualisation, to obtain a qualitative understanding of the spatial distribution of avalanche occurrence for specific time periods and under specific meteorological conditions. While not providing a numerical or probabilistic result to the question of whether there will be avalanches or not, it allows the forecaster to easily review and query the avalanche database, thereby contributing to the maintenance of the institutional memory of the programme.

An ER was used to investigate the aspect control of avalanches in relation to all avalanche occurrences and the aspect distribution of avalanche paths for two characteristic meteorological conditions and a range of avalanche sizes. The analysis based on all avalanche occurrences relative to avalanche paths revealed some unexpected results; however the refinements on the basis of size and storm characteristics do show

clear aspect effects, which are consistent with previous work (Petrie, 1984). The greatest ER is found for size 5 avalanches on southeast aspects, highlighting the importance of lee slope loading under northwesterly winds for large avalanches. The analysis by meteorological conditions also shows similar results, but with a lower ER. Southerly storms show clear aspect relationships, related to snow transportation. Northwesterly storms show much less scour on windward slopes but equal amounts of lee loading as southerly storms, mainly because of the warmer nature of these storms. The observed relationships with aspect and avalanche occurrence under specific storm directions is attributed to the maritime climate of the region, resulting in direct action avalanching and the size of starting zones resulting in averaging of aspect across the large slopes.

7.0 Conclusion

7.1   Summary of main findings

Many different aspects of snow, hazard and avalanching on the Milford Road, Fiordland have been examined in this thesis. This chapter provides a summary of the main research findings, listed below, comments on the implications of these findings, and makes recommendations for future research.

7.1.1 Snow and avalanche regime

❋ Graphical and statistical analysis of the snow depths showed that large variability exists both inter-annually and intra-annually, with a coefficient of variation of 36% for annual snow depths, significantly lower than that of previous work from a small number of sites east of the main divide in New Zealand.

❋ A marginally significant increasing trend of 4.6 avalanches year^{-1} in artificial avalanche occurrence was found and related to an increasing level of avalanche control.

❋ Analysis of inter-annual variations showed that snow depth and artificial avalanche occurrence showed a positive relationship, indicating that years with greater snow depth receive more active control.

❋ Average annual snow depth and total number of avalanche occurrences were found to have highly significant negative correlation coefficients with the frequency of synoptic types that produce clear settled weather and highly

significant positive correlation coefficients with synoptic types that bring strong wind, cold air and precipitation.

❀ Avalanche occurrences were found to have highly significant positive correlations with Trenberth indices that measure the strength of the airflow from the westerly quarter.

7.1.2 Avalanche risk evaluation

❀ Traffic flow was found to be increasing annually, significantly in the shoulder seasons, and have a distinctly tidal traffic flow, all of which affected the avalanche hazard.

❀ For 2002 traffic flows, the avalanche programme reduced the avalanche hazard index (AHI) from 186 to less that 3 and by at least one order of magnitude in terms of the two approaches to probability of death to individuals (PDI) analyses.

❀ The collective risk on the Milford Road as calculated by the equations of Wilhelm(1998) and Margreth et al.(2003) is slightly higher than similar roads in Switzerland, but the Milford Road is far more accessible with many fewer closed days.

❀ The residual AHI for the Milford Road is significantly lower than for Rogers Pass, Canada, even when standardised for traffic volumes of 1000.

❀ Sensitivity analysis of the assumptions made for the calculation of AHI and PDI showed that the length of a waiting queue, the probability of a second avalanche in an adjacent path, and the length of road a vehicle occupies affect the AHI strongly, while the speed of a vehicle is the only parameter to affect PDI, and all parameters tested affect collective risk.

❋ Estimated frequencies by Fitzharris and Owens(1980) were found to underestimate the observed frequencies of avalanches and were considered the best approximation of an uncontrolled or natural avalanche regime on the Milford Road.

❋ New equations for PDI which account for waiting traffic result in calculated values which are higher than those posed by other hazards, and are considered unacceptable. In practice, the real risk is considered to be lower and acceptable.

7.1.3 Statistical forecasting of avalanche activity

❋ Using different misclassification costs, two 10-fold cross validated classification trees were successfully trained to identify avalanche days based on meteorological parameters.

❋ The first classification tree was generated using equal misclassification costs and had an overall accuracy of 85%, but predicted avalanche days less well at 79%.

❋ The second classification tree was generated using a higher misclassification cost for false negatives and used only wind speed and precipitation and wind speed combined in a temperature sensitive wind drift parameter to obtain overall accuracy of 78%, with correct prediction for avalanche days of 86%.

❋ Wind speed and precipitation are considered to be the fundamental controls on avalanche forecasting in this maritime climate.

7.1.4 Visualisation and examination of avalanche activity in a GIS

❋ The GIS permitted rapid access to a range of related meteorological, photographic, and topographic information for all avalanche occurrences.

❋ Visualisation and hypothesis testing in the GIS has provided a means to improve qualitative understanding of the spatial distribution of avalanche occurrence under specified scenarios.

❋ The GIS has the potential to contribute to the maintenance of the institutional memory of the avalanche programme.

❋ Using an excess ratio (ER) based on aspect, avalanche occurrences were found to be significantly less on avalanche paths that do not affect the road.

❋ For size 5 avalanches the greatest ER was found on southeast aspects, highlighting the importance of lee slope loading under northwesterly winds for large avalanches.

❋ The ER analysis for southerly storms showed clear aspect relationships, related to snow transportation. Northwesterly storms show much less scour on windward slopes but equal amounts of lee loading as southerly storms.

7.2 Implications of the main findings

As seen above, the main findings of this thesis cover a multitude of ideas and concepts regarding the snow and avalanche regime in a maritime climate, hazard assessment, and visualisation of avalanche information. This thesis has enhanced the general understanding of avalanching, especially in a maritime climate, and specifically in relation to the Milford Road. While the thesis has dealt with these ideas in separate

chapters for format and structure, they are inseparably linked. These linkages already made within the chapters will be elaborated upon, and their limitations will be considered.

The study of the year-to-year snow and avalanche regime highlighted that while there was a positive relationship between snow depths and avalanche occurrences, stronger correlations were found with atmospheric circulations. The highly significant correlations between avalanche occurrences and Trenberth indices measuring airflow from the westerly quarter, and synoptic types also with airflow from the westerly quarter clearly showed the influence of weather from this direction on avalanche occurrences. Weather from this quarter, and the aforementioned synoptic types are associated with strong winds and precipitation, the two parameters that are considered to be fundamental controls on avalanche forecasting in this maritime climate according to the classification tree analysis. The classification tree analysis also uncovered 12 hour averaged air pressure as a significant classifier, which is supported by the significant synoptic types, as they are often fast moving and have a trough of low pressure. Furthermore, the strong relationship between the avalanche occurrences and the synoptic types, associated with storm incidence, further supports the direct action avalanche regime of this maritime climate.

The analysis of the avalanche regime revealed that there was a marginally significant increasing trend in artificial avalanche occurrences, which is mirrored by increasing traffic volumes and pressures to maintain road access in winter. Analysis of the risk on the road highlights that while the traffic volumes have increased markedly, the avalanche hazard, expressed in terms of AHI and PDI is similar to or significantly lower than similar roads elsewhere around the world, despite being closed on fewer occasions. The risk analysis suggested that to maintain current level of managed risk, future management of the road must be increased to match increasing traffic flow. This is reflected in the recent work undertaken for a scoping exercise for an extension to the Homer tunnel, aimed at eliminating risk from the East Homer and McPherson avalanche paths (URS, 2004). It is also considered that implementation of both forecasting based on classification trees and the incorporation of the GIS will aid future hazard management.

This thesis bases many of the main findings upon the database of avalanche occurrences and associated meteorological and snow data. It is encouraging that a relatively short time series of snow depth and avalanche occurrence has yielded positive results compared to other studies. Despite this, caution must be urged with the extrapolation of these results, as only a relatively short time period has been considered, and most of this was confined to a phase of the Interdecadal Pacific Oscillation (IPO) with a high frequency of El Niño years.

While the data in the database are of exceptional quality and consistency, especially when compared to that of other data sets in New Zealand, they are still imperfect. This is primarily because the data has been collected by an operational avalanche programme, which ultimately is most concerned with the day-to-day safety of the road users. This is further compounded by problems relating to accuracy and completeness (especially in the early parts of the record), and variation in data quality and quantity brought about by changes in forecasters and instrumentation. These concerns about the data length and quality have implications for all results sections of this thesis.

7.3   Recommendations for future work

Among the many suggested recommendations for future work, and of foremost concern is the continuation and improvement of data collection. While this has steadily been occurring with the continued upgrading and improvement of the AWS network and improved recording standards and methods by forecasters, it will remain an ongoing challenge to maintain high data quality and integrity regardless of operational demands. One of the shortcomings of the database is the consistent lack of distinction between wet and dry avalanches despite the fact that early observations (Smith, 1947) indicated that this distinction was significant. This is partly attributed to the climatic setting, where because of the friction and heat generated during the avalanche movement, differences between wet and dry avalanches are not apparent from the avalanche debris. More emphasis should be made on the recording of the moisture content of avalanche events,

through careful observations while in motion, or increased effort in obtaining crown wall profiles. Uncertainties also exist with regard to the exact timing of natural avalanche occurrences during storms. New techniques (Scott and Lance, 2002) have been developed for remotely recording the time of avalanche occurrence and these should be pursued for the Milford Road.

Integration with new technologies also opens potential avenues for future work in the operational collection and storage of avalanche occurrence information. With the development of compact and robust hand held 'palm pilot' type computers, future forecaster could record spatial avalanche occurrence data directly on screen, and upload this directly into a GIS. Furthermore, any additional information such as digital photographs or movies could then also be up-loaded to this palm pilot and added to the GIS.

Improved estimates of return periods using more detailed dendrochronology would greatly improve the accuracy of the estimates of risk, by lengthening the total record of avalanche occurrences. When areas of mature forest are destroyed by avalanches, it should be standard practice to retrieve complete discs with appropriate markings regarding orientation such that dating of historical events may be enabled.

Aside from collecting new data, and integrating new methods to do so, there are excellent opportunities to more closely examine the relationship between avalanche occurrences and snow depths with atmospheric circulation at different time scales. Correlation between daily snow fall or avalanche occurrences with synoptic type may lead to type casting particular synoptic types in terms of avalanche activity and snowfall. Additionally, should it eventually be possible to forecast year-to-year variations of the frequency of synoptic types or circulation indices, it may be possible to better prepare for large avalanche winters. Other measures of atmospheric circulation such as anomalies at the 500mb or 700mb level, or sea surface temperature anomalies around New Zealand may also provide good correlations and lead to opportunities for prediction of snow depths or avalanche intensity for a given season. The relationship between avalanche

occurrences or at the least snow depth and end of summer snow line for a local glacier (Clare et al., 2002) may lead to reconstruction of historical snow depths back to 1977, thereby permitting further examination of relationships with atmospheric circulations beyond the current record length.

In terms of risk analysis, as the database improves in quantity and quality, it may be possible to calculate a value for the probability of a subsequent avalanche in an adjacent or other part of the same path, specifically for the Milford Road. As well as estimating the potential impact of avalanches on loss of life, the risk analysis can also be used for the determination of a cost benefit ratio for the building of future protection structures on the Milford Road. Similarly, the cost of building a structure can then also be compared to updated daily economic losses for New Zealand and Fiordland from road closure.

Implementation and refinement of the selected classification tree for operational purposes would verify or negate the cross validation technique used to create the model. Testing with a new season's data would highlight if the technique is in fact conservative, as Breiman et al.(1993) suggest it is, or optimistic. Further development of a wind drift parameter is also suggested, to better parameterise the conditions that restrict wind drift in a maritime climate. This may involve a field study to determine the boundary conditions for wind drift in this environment. Rain on snow also needs to be better parametrised in the wind drift model, as it is known to cause avalanches, but is reduced to zero at present because of the temperature dependence. These, as well as other studies could be accommodated at the newly built Crosscut Hut, which is already being used for operational snowpack studies. Additional snow pack studies could examine the influence of weak layers resulting from snow metamorphism or from changes within storms, and the results of these studies will contribute to future development of analytical approaches to forecasting such as the SNOSS programme.

Further development of the GIS is also recommended, with endless opportunities available to store, visualise and examine data here within. Operationally, the development of a user-friendly interface within the GIS is considered to be of utmost importance to

ensure forecasters utilise this tool. The interface should permit the forecaster to query the database of avalanche occurrence by either searching a particular date range, group of paths, and or range of meteorological conditions, and the resultant query should be visualised in the GIS. Access to linked data, such as photographs, movies or snow profiles will then be achieved through selecting avalanche occurrences or avalanche paths. Once the GIS is established, there are further opportunities to fully integrate the GIS into daily forecasting, with the implementation of additional factors such as visualisation of lee slope loading, or detailed information on bomb placement for artificial control. Future research work with the GIS could pursue more detailed examination of the spatial distribution of avalanche occurrences, with other topographic factors, or the type casting of particular storm cycles with avalanche occurrences.

References

Abrams, M., 2000. The Advanced Spaceborne Thermal Emission and Reflection Radiometer (ASTER): data products for the high spatial resolution imager on NASA's Terra platform. *International Journal of Remote Sensing*, 21(5), 847-859.

Abrams, H.J., Hook, S.J. and Ramachandra, B., 2002. *Aster Users Handbook, Version 2*. Jet Propulsion Laboratory, NASA, California, USA, 135 pp

Abrams, H.J. and Welch, R., 2001. *Aster DEM release notes*. Jet Propulsion Laboratory, NASA, California, USA, 2 pp

Anderson, H.J., 1990. *Men of the Milford Road*. Craig Printing, Invercargill, New Zealand, 236 pp.

Armstrong, B.R., 1981. A quantitative analysis of avalanche hazard on U.S. Highway 550, southwestern Colorado. Paper presented at the *Western Snow Conference*, 49, 95-104.

Arnalds, Þ, Jónasson, K. and Sirgurdsson, S., 2004. Avalanche hazard zoning in Iceland based on individual risk. *Annals of Glaciology*, 38, 285-290.

Ashby, G., 2002. Development of a Risk Management Strategy for Part of State Highway 73 in the South Island of New Zealand. Paper presented at the *New Zealand Society for Risk Management Conference*.

Australian Bureau of Meteorology, 2005. *S.O.I. Archives - 1876 to Present,* website (http://www.bom.gov.au/climate/current/soihtm1.shtml)

Australian Geomechanics Society Sub-committee on Landslide Risk Assessment, 2000. Landslide risk management concepts and guidelines. *Journal and News of the AGS*, 35, No. 1.

Avalanche Task Force, 1974. *Report on findings and recommendations, Appendix II*. British Columbia Department of Highways, Victoria, B.C., Canada.

BAE Systems, 2003. *Socet Set*, Version 5.1., [software]. http://www.socetset.com/

Bakkehoi, S., 1987. Snow avalanche prediction using probabilistic method. [In] Salm, B., and Gubler, H., (Editors), *Avalanche Formation. Movements and Effects*. I.A.H.S. Publication 162, 557-569.

Bednorz, E., 2002. Snow cover in western Poland and macro-scale circulation conditions. *International Journal of Climatology*, 22(5), 533-541.

Beniston, M., 1997: Variations of snow depth and duration in the Swiss Alps over the last 50 years: links to changes in large-scale climatic forcings. *Climatic Change*, 36, 281-300

Beniston, M., Keller, F. and Goyette, S., 2003a. Snow pack in the Swiss Alps under changing climatic conditions: an empirical approach for climate impacts studies. *Theoretical and Applied Climatology*, 74, 19-31.

Beniston, M., Keller, F., Koffi, B. and Goyette, S., 2003b. Estimates of snow accumulation and volume in the Swiss Alps under changing climatic conditions. *Theoretical and Applied Climatology*, 74, 125-140.

Berger, C.L., Lupo, A.R., Browning, P., Bodner, M., Chambers, M.D. and Rayburn, C.C., 2002. A climatology of northwest Missouri snowfall events: Long-term trends and interannual variability. *Physical Geography*, 23, 427-448.

Birkeland, K.W. and Mock, C.J., 2001. The major snow avalanche cycle of February 1986 in the western United States. *Natural Hazards*, 24, 75-95.

Birkeland, K.W., Mock, C.J. and Shinker, J.J., 2001. Avalanche extremes and atmospheric circulation patterns. *Annals of Glaciology*, 32, 135-140.

Bois, P., Obled, C. and Good, W., 1975. Multivariate data analysis as a tool for day-to-day avalanche forecast. Paper presented at *International Symposium on Snow Mechanics*, I.A.H.S. Publication 114, Grindelwald, Switzerland, 391–403.

Bolognesi, R., Denuelle M. and Dexter L., 1996. Avalanche Forecasting with GIS. Paper presented at *International Snow Science Workshop*, Banff, Canada, 11-13.

Bovis, M.J., 1977. Statistical forecasting of snow avalanches, San Juan Mountains, southern Colorado, USA. *Journal of Glaciology*, 18(78), 87–99.

Breiman, L., Friedman, J. H., Olshen, R. A. and Stone, C. J., 1993. *Classification and regression trees*. Chapman & Hall, New York, USA, 358pp.

Briggs, N., 1997. *Determination of avalanche starting zones and runout distances. An application of GIS*. Unpublished Masters Thesis, University of Canterbury, Christchurch, New Zealand, 97 pp.

Brown, R.D. and Braaten, R.O., 1998. Spatial and temporal variability of Canadian monthly snow depths, 1946-1995. *Atmosphere-Ocean*, 36, 37-54.

Burrows, C.J., 1976. Exceptional snowstorms in the South Island High Country. *Tusock Grassland and Mountain Lands Institute Review*, 32, 43–47.

Buser, O., 1983. Avalanche forecast with the method of nearest neighbours: An interactive approach. *Cold Regions Science and Technology*, 8(2), 155-163.

Buser, O., 1989. Two years experience of operational avalanche forecasting using nearest neighbours method. *Annals of Glaciology*, 13, 31-34.

Carran, A., 2002. *Avalanche Contract Administrator*, Works Infrastructure, Te Anau, New Zealand, personal communication. (September, 2002).

Carran, W., Hall, S., Kendall, C., Carran, A. and Conway, H., 2000. Snow Temperature and Water Outflow During Rain and Melt; Milford Highway, New Zealand. Paper presented at *International Snow Science Workshop*, Big Sky, Montana, 173-177.

Changnon S.A., 1999. Impacts of 1997-98 El Nino-generated weather in the United States. *Bulletin of the American Meteorological Society*, 80(9), 1819-1827.

Chinn, T.J., 1981. Snowfall variations, hazards and snow melt. [In] *Mountain Lands Workshop, Water and Soil Science Centre, Christchurch*. Ministry of Works and Development Report No. WS 525, Ministry of Works and Development for the National Water and Soil Conservation Organization, Wellington, New Zealand, 1–21.

Chinn T.J., 1991. *Glacier inventory of New Zealand* (unpublished). Institute of Geological and Nuclear Sciences, Wellington, New Zealand.

Chinn, T.J., 1996. New Zealand glacier responses to climate change of the past century. *New Zealand Journal of Geology and Geophysics*, 39, 15-428.

Chinn, T.J., 1999. New Zealand glacier response to climate change of the past 2 decades. *Global and Planetary Change*, 22(1-4), 155-168.

Chinn, T.J., Winkler, S., Salinger, M.J. and Haakensen, N., 2005. Recent glacier advances in Norway and New Zealand: A comparison of their glaciological and meteorological causes. *Geografiska Annaler,* 87A(1), 141-157.

Chinn T.J. and Whitehouse I.E., 1980. Glacier snow line variations in the Southern Alps, New Zealand. [In] *World Glacier Inventory, Proceedings of the Riederalp Workshop*, September, 1978. International Association of Hydrological Sciences Publication 126, IAHS, Wallingford, England, 219–228.

Clare, G. R., Fitzharris, B.B., Chinn, T.J. and Salinger, M.J., 2002. Interannual variation in end-of-summer snowlines of the Southern Alps of New Zealand, and relationships with Southern Hemisphere atmospheric circulation and sea surface temperature patterns. *International Journal of Climatology*, 22(1), 107-120.

Clark, M.P., Serreze, M.C. and Robinson, D.A., 1999. Atmosphere controls on Eurasian snow extent. *International Journal of Climatology*, 19, 27–40.

Conway, B.H., 1977. *Snow Avalanches and Beech Trees*. Unpublished Masters Thesis, University of Canterbury, Christchurch, New Zealand, 212 pp.

Conway, H., Carran, W. and Carran, A., 2000. The Timing, Size and Impact of Avalanches on the Milford Highway, New Zealand. Paper presented at *International Snow Science Workshop*, Big Sky, Montana, 167-172.

Conway, H., Carran, W. and Carran, A., 2002. Estimating Avalanche Runout on the Milford Road, New Zealand. Paper presented at *International Snow Science Workshop*, Pentiction, B.C. Canada.

Conway, H. and Raymond, C.F., 1993. Snow stability during rain. *Journal of Glaciology*, 39(133), 635-642.

Conway, H. and Wilbour, C., 1999. Evolution of snow slope stability during storms. *Cold Regions Science and Technology*, 30(1-3), 67-77.

Corti, S., Molteni, F. and Brankovic, 2000. Predictability of snow-depth anomalies over Eurasia and associated circulation patterns. *Quarterly Journal of the Royal Meteorological Society*, 26(562), 241-262.

Cuartero, A., Felicísimo, A.M. and Ariza, F.J., 2004. Accuracy of DEM generation from TERRA-ASTER stereo data. Paper presented at *XXth International Society for Photogrammetry and Remote Sensing and Spatial Information Sciences Congress*, Istanbul, Turkey, Commission VI papers, Vol. XXXV, part B4.

Davis, R.E. and Elder, K., 1994. Application of classification and regression trees: selection of avalanche indices at Mammoth Mountain. Paper presented at *International Snow Science Workshop*, Snowbird, Utah, USA, 285-294.

Davis, R.E., Elder, K., Howlett, D. and Bouzaglou, E., 1996. Analysis of weather and avalanche records from Alta, Utah and Mammoth Mountain, California using

classification trees. Paper presented at *International Snow Science Workshop*, Revelstoke, BC, Canada, 14-18.

Davis, R.E., Elder, K., Howlett, D. and Bouzaglou, E., 1999. Relating storm and weather factors to dry slab avalanche activity at Alta, Utah, and Mammoth Mountain, California, using classification and regression trees. *Cold Regions Science and Technology*, 30, 79-89.

de Lautour, S.M.A., 1999. Seasonal snow storage in hydro catchments and atmospheric circulation patterns. Unpublished Masters Thesis, University of Otago, Dunedin, New Zealand, 165 pp

Department of Conservation, 2002. *Fiordland National Park Management Plan Draft.* Southland Conservancy Conservation Management Planning Series No. 11. Department of Conservation, Invercargill, New Zealand, 228 pp.

Dingwall, P.R., Fitzharris, B.B. and Owens, I.F., 1989. Natural hazards and visitor safety in New Zealand's national parks. *New Zealand Geographer,* 45(1), 68-79.

Ede, J., 1988. *The Mountain Men of Milford*. Caxton press Christchurch, New Zealand. 164 pp.

Elder, K. and Armstrong, B. R., 1987. A quantitative approach for verifying avalanche hazard ratings. [In] Salm, B., and Gubler, H., (Editors), *Avalanche Formation. Movements and Effects*. I.A.H.S. Publication 162, 593-603.

Elder, K. and Davis, R.E., 2000. Decision trees predicting avalanche response: Tools for training? Paper presented at *International Snow Science Workshop*, Big Sky, Montana, USA, 140-141.

ESRI., 1999. *ArcGIS,* Version 8.3., [software]. http://www.esri.com

Falarz, M., 2004. Variability and trends in the duration and depth of snow cover in Poland in the 20th century. *International Journal of Climatology*, 24, 1713-1727.

Fitzharris, B.B., 1979. Meteorological influences on Avalanches. [In] *Snow Avalanches, A review with Special Reference to New Zealand*. NZMSC, Avalanche committee report No.1., Wellington, New Zealand.

Fitzharris, B.B., 1987. A climatology of major avalanche winters in western Canada. *Atmosphere–Ocean*, 25, 115–136.

Fitzharris, B.B. and Bakkehøi, S., 1986. A synoptic climatology of major avalanche winters in Norway. *Journal of Climatology*, 6, 431–446.

Fitzharris, B.B., Chinn, T.J. and Lamont, G.N. 1997. Glacier mass balance fluctuations and atmospheric circulation patterns over the Southern Alps, New Zealand. *International Journal of Climatology,* 17, 745–63.

Fitzharris, B.B. and Garr, C.E. 1995. Simulation of past variability in seasonal snow in the Southern Alps, New Zealand. *Annals of Glaciology,* 21, 377–382.

Fitzharris, B.B. and McAlevey, B.P., 1999. Remote sensing of seasonal snow cover in the mountains of New Zealand using satellite imagery. *Geocarto International*, 14(3), 33-42.

Fitzharris, B.B., Lawson, W. and Owens, I.F., 1999. Research on glaciers and snow in New Zealand. *Progress in Physical Geography*, 23(4), 469–500.

Fitzharris, B.B. and Owens, I.F., 1980. *Avalanche atlas of the Milford Road; an Assessment of the Hazard to Traffic*. New Zealand Mountain Safety Council, Avalanche committee Report No. 4, 79 pp.

Fitzharris, B.B. and Owens, I.F., 1984. Avalanche tarns. *Journal of Glaciology,* 30(106), 308-312.

Floyer, J.A. and McClung, D.M., 2003 Numerical avalanche prediction: Bear Pass, British Columbia, Canada. *Cold Regions Science and Technology*, 37(3), 333-342.

Föhn, P.M.B., 1992. Climatic change, snow-cover and avalanches. [In] Boer, M and Koster, E., (Editors), *Greenhouse impact on cold climate ecosystems and landscapes*. Catena, Supplement, 22, 11-21.

Föhn, P.M.B., 1998. An overview of avalanche forecasting models and methods. [In] Hestnes, E., (Editor), *25 years of snow avalanche research*, Voss, Norway, 12-16 May 1998. NGI Publication. Norwegian Geotechnical Institute, Oslo, Norway, 19-27.

Föhn, P.M.B., 1999. *Peer Review of the Operational Avalanche Safety procedures used by Civil Works Otago/Southland, New Zealand along the State Highway 94 "Milford Road"*. Unpublished Report for Mr. Don Lyon, Area Engineer Southland, Transit New Zealand.

Föhn, P., Good, W., Bois, P. and Obled, C., 1977. Evaluation and comparison of statistical and conventional methods of forecasting avalanche hazard. *Journal of Glaciology*, 19(81), 375-387.

Frei, A. and Robinson, D.A., 1999. Northern Hemisphere snow extent: Regional variability 1972-1994. *International Journal of Climatology*, 19, 1535-1560.

Furdada, G., Martí, G., Oller, P., García, C., Mases, M. and Vilaplana, J.M., 1995. Avalanche mapping and related G.I.S. applications in the Catalan Pyrenees. *Surveys in Geophysics*, 16, 681-693.

Garr, C.E. and Fitzharris, B.B., 1996. Using seasonal snow to forecast inflows into South Island hydro lakes. pp 63-67. [In] *Prospects and needs for climate forecasting : proceedings of a workshop / sponsored by the New Zealand Climate Committee*. Miscellaneous series / The Royal Society of New Zealand, 34, pp117.

Geocarto International, 1999. *New Zealand: South Island, Lake Pukaki* (Space Shuttle Atlantis), [image], 14(3), 96.

Ghinoi, A., 2003. *A new contribution to the assessment of snow avalanche susceptibility: Applications in Tyrol (Austria) and in Alta Val Badia (Dolomites, Italy)*.

Unpublished Doctoral Thesis, University of Modena and Reggio Emilia, Italy, 282 pp.

Glazovskaya, T.G., 1998. Global distribution of snow avalanches and changing activity in the Northern Hemisphere due to climate change. *Annals of Glaciology*, 26, 337-342.

Glazovskaya, T.G. and Seliverstov, G., 1998. Long-term forecasting of changes of snowiness and avalanche activity in the world due to the global warming. [In] Hestnes, E., (Editor), *25 years of snow avalanche research*, Voss, Norway, 12-16 May 1998. NGI Publication, Norwegian Geotechnical Institute, Oslo, Norway, (203), 113-116.

Gonçalves, J.A. and Oliveira, A.M., 2004. Accuracy analysis of DEMS derived from ASTER imagery. Paper presented at *XXth International Society for Photogrammetry and Remote Sensing and Spatial Information Sciences Congress*, Istanbul, Turkey,, Commission III papers, Vol. XXXV, part B3.

Gordon, N. D., 1985. The Southern Oscillation: A New Zealand perspective. *Journal of the Royal Society of New Zealand*, 15(2), 137-155.

Griffiths, G.A. and McSaveney, M.J., 1983. Distribution of mean annual precipitation across some steepland regions of New Zealand. *New Zealand Journal of Science*, 26, 197–209.

Gruber, U., 2001. Using GIS for avalanche hazard mapping in Switzerland. Paper presented at *ESRI*, *21st ESRI International User Conference*, *2001*. http://www.esri.com/library/userconf/proc01/professional/abstract/a964.html (May 25, 2002).

Gruber, U. and Haefner, H., 1995. Avalanche hazard mapping with satellite data and a digital elevation model. *Applied Geography*, 15(2), 99-113.

Grundstein, A., 2003. A synoptic-scale climate analysis of anomalous snow water equivalent over the northern great plains of the USA. *International Journal of Climatology*, 23, 871-886.

Grundstein, A. and Leathers, D.J., 1998. A case study of the synoptic patterns influencing midwinter snowmelt across the northern Great Plains. *Hydrological Processes*, 12, 2293-2305.

Harrison, W., 1986. Seasonal accumulation and loss of snow from a block mountain catchment in Central Otago. *Journal of Hydrology (New Zealand)*, 25, 1–17.

Hartley, S. and Keables, M.J., 1998. Synoptic associations of winter climate and snowfall variability in New England, USA, 1950-1992. *International Journal of Climatology*, 18, 281-298.

Hendrikx, J., Owens, I., Carran, W. and Carran, A., 2004. Overview of the spatial distribution of avalanche activity in relation to meteorological and topographic variables in an extreme maritime environment. Paper presented at *International Snow Science Workshop*, Jackson Hole, Wyoming, USA.

Hendrikx, J., Owens, I., Carran, W. and Carran, A., 2005. Avalanche activity in an extreme maritime climate: The application of classification trees for forecasting. *Cold Regions Science and Technology*, 43, 104-116.

Heydenrych, C., Salinger, M.J. and Renwick, J., 2001. *Climate and Severe Fire Seasons*, client report prepared for the National Rural Fire Authority, AK00125, 117 pp.

Hirano, A., Welch, R. and Lang, H., 2003. Mapping from ASTER stereo image data: DEM validation and accuracy assessment. *ISPRS Journal of Photogrammetry and Remote Sensing*, 57, 356-370.

Hoek, E., 2000. *Practical Rock Engineering – course notes by Evert Hoek*. A.A.Balkema Publishers, Rotterdam, Netherlands, 313 pp.

Hooker, B.L. and Fitzharris, B.B., 1999. The correlation between climatic parameters and the retreat and advance of Franz Josef Glacier, New Zealand. *Global and Planetary Change*, 22(1-4), 39-48.

Hurrell, J.W.,1995. Decadal Trends in the North Atlantic Oscillation: Regional Temperatures and Precipitation. *Science*, 269, 676-679.

Irwin, D., MacQueen, W. and Owens, I., 2002. *Avalanche Accidents in Aotearoa – New Zealand*. Mountain Safety Council, Wellington, 153 pp.

Irwin, D. and Owens, I., 2004. A history of avalanche accidents in Aotearoa – New Zealand. Paper presented at *International Snow Science Workshop*, Jackson Hole, Wyoming, USA.

Judson, A. and Erickson, B.J., 1973. *Predicting avalanche intensity from weather data: A statistical analysis, U.S. Rocky Mountain Forest and Range Experiment Station, Fort Collins, Colorado*. U.S. Forest Service research paper, RM-112, 12 pp.

Judson, A. and King, R., 1985. An index of regional snowpack stability based on natural slab avalanches. *Journal of Glaciology*, 31(108), 67-73.

Kääb, A., 2002. Monitoring high-mountain terrain deformation from repeated air-and spaceborne optical data: examples using digital aerial imagery and ASTER data. *ISPRS Journal of Photogrammetry & Remote Sensing*, 57, 39-52.

Kääb, A., Huggel, C., Paul, F., Wessels, R., Raup, B., Kieffer, H. and Kargel, J., 2003. Glacier monitoring from ASTER imagery: accuracy and applications. Paper presented at *European Association of Remote Sensing Laboratories Workshop*, LIS-SIG, Berne, Switzerland, 43-53.

Kelly, M.R., 1992. *The variability of seasonal snow cover in North West Otago*. Unpublished Masters of Applied Science Thesis, Lincoln University, Lincoln, New Zealand, 138 pp.

Kerr, T., 2005. *Snow storage modelling in the Lake Pukaki catchment, New Zealand: An investigation of enhancements to the SnowSim model*. Unpublished Masters of Science thesis, University of Canterbury, Christchurch, New Zealand, 151 pp.

Kerr, G.N., Taylor, C.N., Kerr, I.G.C. and Fitzgerald, K., 1990. *A study of the issues and options for the future of Fiordland*. Unpublished report for the fiordland promotion association. Centre for Resource Management, Lincoln University.

Keylock, C.L., McClung, D.M. and Magnússon, M., 1999. Avalanche risk mapping by simulation. *Journal of Glaciology*, 45(150), 303-314.

Kidson, J.W., 2000. An analysis of New Zealand synoptic types and their use in defining weather regimes. *International Journal of Climatology*, 20, 299-316.

Kidson, J.W. and Renwick, J.A., 2002. Patterns of convection in the tropical pacific and their influence on New Zealand weather. *International .Journal of Climatology*, 22, 151-174.

Kristensen, K., Harbitz, C.B. and Harbitz, A., 2003. Road Traffic and avalanches – methods for risk evaluation and risk management. *Surveys in Geophysics*, 24, 603-616.

LaChapelle, E. R. 1966. Avalanche forecasting: a modern synthesis. *International Association of Hydrological Sciences*, Publication 69, 350-356.

LaChapelle, E.R., 1979. *An Assessment of avalanche problems in New Zealand*. New Zealand Mountain Safety Council Avalanche Committee, Report No. 2, 53 pp.

LaChapelle, E.R., 1980. The fundamental process in conventional avalanche forecasting. *Journal of Glaciology*, 26(94), 75-84.

Lamont, G.N., Chinn, T.J. and Fitzharris, B.B., 1999. Slopes of glacier ELAs in the Southern Alps of New Zealand in relation to atmospheric circulation patterns. *Global and Planetary Change*, 22(1-4), 209-219

Land Information New Zealand, 1994. *Milford* [map]*, 1:50,000, Topographic Map 260-D40 1*[st] *Edition*, Land Information New Zealand, Wellington.

Land Information New Zealand, 1995. *Eglinton* [map]*, 1:50,000, Topographic Map 260-D41 1*[st] *Edition*, Land Information New Zealand, Wellington.

Land Information New Zealand, 2005. *Land Information New Zealand*, webpage. http://www.linz.govt.nz/rcs/linz/pub/web/root/home/index.jsp, (15 December, 2002).

Land Transport Safety Authority, 2003. *Motor Vehicle Crashes in New Zealand, 2002*. Strategy Division, Land Transport Safety Authority, Wellington, New Zealand.

Lang, H.R. and Welch, R., 1999. *Algorithm theoretical basis document for Aster digital elevation models (Standard product AST14)*, *Version 3.0*. Jet Propulsion Laboratory, NASA, California, USA, 69 pp

Laternser, M. and Schneebeli, M., 2002. Temporal trend and spatial distribution of avalanche activity during the last 50 years in Switzerland. *Natural Hazards*, 27, 201-230.

Laternser, M. and Schneebeli, M., 2003. Long-term snow climate trends of the Swiss Alps (1931-99). *International Journal of Climatology*, 23(7), 733-750.

Lee, S., Klein, A. and Over, T., 2004. Effect of the El Niño-southern oscillation on the temperature, precipitation, snow water equivalent and resulting streamflow in the Upper Rio Grande river basin. *Hydrological Processes*, 18, 1053-1071.

Leica Geosystems, 2003. *ERDAS Imagine*, Version 8.3., [software]. http://www.gis.leica-geosystems.com/default.asp

Leuthold, H., Allgöwer, B. and Meister, R., 1996. Visualization and Analysis of the Swiss Avalanche Bulletin using GIS. Paper presented at *International Snow Science Workshop*, Banff, Canada, 35-40.

López-Moreno, J. I., 2005. Recent Variations of Snowpack Depth in the Central Spanish Pyrenee. *Arctic, Antarctic, and Alpine Research*, 37(2), 253-260.

Maggioni, M., Gruber, U. and Stoffel, A., 2002. Definition and characterisation of potential avalanche release areas. Paper presented at *22nd ESRI International User Conference,* http://gis.esri.com/library/userconf/proc02/pap1161/p1161.html (15 October, 2002).

Margreth, S., Stoffel, L. and Wilhelm, C., 2003. Winter opening of high alpine pass roads—analysis and case studies from the Swiss Alps. *Cold Regions Science and Technology*, 37, 467–482

Marti, G., Mases, M., Oller, P., Marturia, J., Artiolo, J.P. and Pignone, R., 1997. The avalanche cadastre management using G.I.S. in the Catalan Pyrenees. [In]: Berastegui, X., Puigdefabregas, C., Jungwirth, F., Schmid, H., Artiolo, J.P. and Pignone, R., (eds.), *Proceedings of the Second congress on Regional geological cartography and information systems*. Barcelona, Spain, Institute of Cartography Catalunya, pp. 205-210.

Martin, E., Giraud, G., Lejeune, Y. and Boudart, G., 2001. Impact of a climate change on avalanche hazard. *Annals of Glaciology*, 32, 163-167.

McClung, D.M., 2002a. The Elements of Applied Avalanche Forecasting Part I: The Human Issues. *Natural Hazards*, 25, 111-129.

McClung, D.M., 2002b. The Elements of Applied Avalanche Forecasting Part II: The Physical Issues and the Rules of Applied Avalanche Forecasting. *Natural Hazards*, 25, 131-146.

McClung, D.M. and Schaerer P.A., 1993. *The Avalanche handbook*. The Mountaineers, Seattle, USA, 271 pp.

McClung, D.M. and Tweedy, J., 1993. Characteristics of avalanching: Kootenay Pass, British Columbia, Canada. *Journal of Glaciology*, 39(132), 316-322.

McCollister, C., Birkeland, K., Hansen K. and Comey, R., 2002. A probabilistic technique for exploring multi-scale spatial patterns in historical avalanche data by combining GIS and meteorological nearest neighbors with an example from the Jackson Hole Ski Area, Wyoming. Paper presented at *International Snow Science Workshop*, Pentiction, B.C. Canada.

McCollister, C., Birkeland, K., Hansen, K., Aspinall, R. and Comey, R., 2003. Exploring multi-scale spatial patterns in historical avalanche data, Jackson Hole Mountain Resort, Wyoming. *Cold Regions Science and Technology*, 37, 299-313

McGinnis, D.L., 2000. Synoptic controls on the upper Colorado River basin snowfall. *International Journal of Climatology,* 20, 131-149.

McGregor, G.R., 1989. Snow avalanche forecasting by discriminant function analysis. *Weather and Climate*, 9, 3-14.

McLauchlan, H.J., 1995. *An assessment of the velocities, impact pressure and other related effects of the avalanches on the Milford Road, Fiordland, New Zealand.* Unpublished Masters Thesis, University of Canterbury, Christchurch, New Zealand, 195 pp.

Ministry of Tourism, 2005. *Overview of the Tourism Industry*, webpage. www.tourism.govt.nz/ (10 February, 2005)

Mock, C. J., 1995. Avalanche climatology of the continental zone in the southern Rocky Mountains. *Physical Geography*, 16, 165–187.

Mock, C.J. and Birkeland, K.W., 2000. Snow Avalanche Climatology of the Western United States Mountain Ranges. *Bulletin of the American Meteorological Society*, 81(10), 2367-2392.

Moore, R.D. and McKendry, I.G., 1996. Spring snowpack anomaly patterns and winter climatic variability, British Columbia, Canada. *Water Resources research*, 32(3), 623-632.

Moore, R. D. and Prowse, T. D., 1988. Snow hydrology of the Waimakariri catchment, South Island, New Zealand. *Journal of Hydrology (New Zealand)*, 27, 44-68.

Morinaga, Y., Tian, S. and Shinoda, M., 2003. Winter snow anomaly and atmospheric circulation in Mongolia. *International Journal of Climatology*, 23(13), 1627-1636.

Morris, J.Y. and O'Loughlin, C.L., 1965. Snow investigations in the Craigieburn Range. *Journal of Hydrology (New Zealand),* 4, 2–16.

Neale, A.A. and Thompson, G.H., 1977, *Meteorological conditions accompanying heavy snow falls in southern New Zealand*. New Zealand Metrological Service Technical Information circular 155. Meteorological Service, Wellington, New Zealand.

Neale, S.M. and Fitzharris, B.B., 1997. Energy balance and synoptic climatology of a melting snowpack in the Southern Alps, New Zealand. *International Journal of Climatology*, 17, 1595–609.

New Zealand Meteorological Service, 1984. *The climate and weather of Southland*. Miscellaneous publication, 115(15), New Zealand Meteorological Service, Wellington, New Zealand, 50 pp.

Nielsen, N.M., Hartford, D.N.D. and MacDonald, T.F., 1994. Selection of tolerable risk criteria for dam safety decision making. Paper presented at the *1994 Canadian Dam Safety Conference, Winnipeg, Manitoba.* BiTech Publishers, Vancouver, Canada, 355-369.

NIWA, 2003. *National Institute of Water & Atmospheric Research,* webpage http://www.niwa.co.nz/edu/resources/climate/ (20 January, 2005)

Norwegian Geotechnical Institute (NGI), 2003. *Road traffic and avalanches – methods for risk evaluation and risk management*. NGI report no. 20001289-4, Oslo, Norway, 33 pp.

O'Loughlin, C.L., 1969. *Further snow investigations in the Craigieburn Range.* Unpublished protection Forestry Report, 52, 48 pp.

Owens, I.F., 2002. *Associate Professor*, Geography Department, University of Canterbury, Christchurch, New Zealand, personal communication. (September, 2002).

Owens, I.F. and Fitzharris, B.B., 1985. *Avalanche atlas of the Milford Track and assessment of the hazard to walkers.* New Zealand Mountain Safety Council Avalanche Committee, Report No. 8, 77 pp.

Owens, I.F. and Fitzharris, B.B., 1989. Assessing avalanche risk levels on walking tracks in Fiordland, New Zealand. *Annals of Glaciology,* 13, 231-236.

Patten, J.M., Smith, S.R. and O'Brien, J.J., 2003. Impacts of ENSO on Snowfall frequencies in the United States. *Weather and Forecasting*, 18, 965-980.

Perla, R.I., 1970. On contributory factors in avalanche hazard evaluation. *Canadian Geotechnical Journal*, 7(4), 414-419.

Petrie, M.H., 1984. *Meteorological conditions associated with large avalanche events on the Milford Road.* Unpublished Postgraduate Diploma Dissertation, University of Otago, Dunedin, New Zealand, 214 pp.

Pomeroy, J.W., 1988. *Wind Transport of Snow*. Unpublished Doctoral Thesis, University of Saskatchewan, Saskatoon, Canada, 226 pp.

Prowse, T.D., Owens, I.F. and McGregor, G.R., 1981. Adjustment to Avalanche Hazard in New Zealand. *New Zealand Geographer*, 37(1): 25-31.

Purves, R.S., Morrison, K.W., Moss G. and Wright, D.S.B., 2003. Nearest neighbours for avalanche forecasting in Scotland – development, verification and optimisation of a model. *Cold Regions Science and Technology*, 37, 343-355.

Renwick, J.A., Hurst, R.J. and Kidson, J.W. 1998. 'Climatic influences on the survival of southern Gemfish (Rexea Solandri, Gempylidae) in New Zealand waters', *International Journal of Climatology*, 18, 1655–1667.

Rikiishi, K. and Sakakibara, J., 2004. Seasonal cycle of the snow coverage in the former Soviet Union and its relation with atmospheric circulation. *Annals of Glaciology*, 38, 106-114.

Rosenthal, W., Elder, K. and Davis, R.E., 2002. Operational Decision Tree Avalanche Forecasting. Paper presented at *International Snow Science Workshop*, Pentiction BC, Canada, 13-18.

Salinger, M.J., 1980a. New Zealand Climate: I. Precipitation Patterns. *Monthly Weather Review*, 108, 1892-1904.

Salinger, M.J., 1980b. New Zealand Climate: II. Temperature Patterns. *Monthly Weather Review*, 108, 1904-1912.

Salinger, M.J. and Mullan, A.B., 1999. New Zealand climate: temperature and precipitation variations and their links with atmospheric circulation 1930–1994. *International Journal of Climatology*, 19, 1049-1071.

Salinger, M.J., Renwick, J.A. and Mullan, A.B., 2001. Interdecadal Pacific Oscillation and South Pacific Climate. *International Journal of Climatology*, 21, 1705-1721.

Schaerer, P., 1989. The Avalanche Hazard Index. *Annals of Glaciology*, 13, 241-247.

Scherrer, S.C. and Appenzeller, C., 2003. Swiss alpine snow variability and its links to large scale flow patterns. Paper presented at *ICAM/MAP Brig (CH) Meeting 2003*.

Scherrer, S.C., Appenzeller, C. and Laternser, M., 2004. Trends in Swiss Alpine snow days: The role of local- and large-scale variability. *Geophysical Research Letters*, 31(L13215), 1-4.

Schneebeli, M., Laternser, M. and Ammann, W., 1997. Destructive snow avalanches and climate change in the Swiss Alps. *Eclogae Geologicae Helvetiae*, 90(3), 457-461.

Schweizer, J. and Föhn, P.M., 1996. Avalanche forecasting an expert system approach. *Journal of Glaciology*, 42(141), 318–332.

Schweizer, J. and Jamieson, B., 2003. Snowpack properties for snow profile analysis. *Cold Regions Science and Technology*, 37, 233-241.

Schweizer, J., Jamieson, J.B. and Skjonsberg, D., 1998. Avalanche forecasting for transportation corridor and backcountry in Glacier National Park (BC, Canada). In: E. Hestnes (Editor), *25 years of snow avalanche research*, Voss, Norway, 12-16 May 1998. NGI Publication. Norwegian Geotechnical Institute, Oslo, Norway, 238-244.

Schweizer, J., Kronholm, K. and Wiesinger, T., 2003. Verification of regional snowpack stability and avalanche danger. *Cold Regions Science and Technology*, 37(3), 277-288.

Scott, E.D. and Lance, C., 2002. Infrasonic Monitoring of Avalanche Activity. Paper presented at *International Snow Science Workshop*, Penticton, B.C., Canada.

Shrestha, A.B., Wake, C.P., Dibb, J.E. and Mayewski, P.A., 2000. Precipitation fluctuations in the Nepal Himalaya and its vicinity and relationship with some large scale climatological parameters. *International Journal of Climatology*, 20(3), 317-327.

Smith, H.W., 1947. Avalanches. *New Zealand Engineering*, 2(5): 491-496.

StatSoft Inc., 2003. *STATISTICA*, Version 6., [software]. http://www.statsoft.com

Stethem, C., Schaerer, P., Jamieson, B. and Edworthy, J., 1995. Five mountain parks highway avalanche study. Paper presented at *International Snow Science Workshop*, Snowbird, Utah, USA, 72-79.

Stoffel, A., Meister R. and Schweizer, J., 1998. Spatial characteristics of avalanche activity in an Alpine valley – a GIS approach. *Annals of Glaciology*, 26, 329-336.

Sturman, A.P. and Tapper, N.J. 1996. *The weather and climate of Australia and New Zealand*. Oxford University Press, Melbourne, Australia, 476 pp.

Sturman, A. and Wanner, H., 2001. A comparative Review of the Weather and Climate of the Southern Alps of New Zealand and the European Alps. *Mountain Research and Development*, 21(4), 359-369.

Tomlinson, A.I., 1980. *The frequency of high intensity rainfalls in New Zealand, Part 1*. Water and Soil Technical Publication No. 19, Water and Soil Division, Ministry of Works and Development, Christchurch, New Zealand.

Toppe, R., 1987. Terrain models - A tool for natural hazard mapping. *International Association of Hydrological Sciences,* 162, 629-638.

Tracy, L., 2001. Using GIS in Avalanche Hazard Management. Paper presented at *ESRI, 21st ESRI International User Conference, 2001* http://gis.esri.com/library/userconf/proc01/professional/papers/pap439/p439.htm (25 May, 2002).

Transit New Zealand, 2002. Annual Average Daily Traffic (AADT) data. http://www.transit.govt.nz/technical_information/view_manual.jsp?primary_key=29 (15 January, 2003)

Travers Morgan (NZ) Ltd., 1995. *Tourism benefits from sealing roads: User survey of the Milford Sound road*. Transit New Zealand Research Report No. 45 33pp.

Trenberth K.E., 1975. A quasi-biennial standing wave in the Southern Hemisphere and interrelations with sea surface temperature. *Quarterly Journal of the Royal Meteorological Society*, 101, 576-593.

Trenberth K.E., 1976. Fluctuations and trends in indices of the southern hemisphere circulation. *Quarterly Journal of the Royal Meteorological Society*, 102, 65-76.

Trenberth, K.E., 1977. Relationships between inflow to Clutha lakes, broad-scale atmospheric circulation parameters, and rainfall. *New Zealand Journal of Science*, 20, 63-71.

Tyson, P.D., Sturman, A.P., Fitzharris, B.B., Mason, S.J. and Owens, I.F., 1997. Circulation changes and teleconnections between glacial advances on the west coast of New Zealand and extended spells of drought years in South Africa. *International Journal of Climatology*, 17(14), 1499-1512.

URS, 2004. *Final draft scoping report for the SH94 Homer Tunnel east portal avalanche shed, Section 6.1 Traffic Statistics*. Unpublished draft report for Transit New Zealand, URS Report R001A3C, 6 pp.

Vignon, F., Arnaud, Y. and Kaser, G., 2003. Quantification of glacier volume change using topograhic and ASTER DEMs. Paper presented at *International Geoscience and Remote Sensing Symposium IGARSS'03*, Toulouse, France, 2605-2607.

Weir, P.L., 1998. Avalanche Risk Management – the Milford Road. [In] Elms, D. (ed.). *Owning the Future: Integrated Risk Management in Practice*. University of Canterbury Center for Advanced Engineering, Christchurch, New Zealand, pp. 275-292.

Welch, R., Jordan, T., Lang, H. and Murakami, H., 1998. ASTER as a source for topographic data in the late 1990's. *IEEE Transactions on Geoscience and Remote Sensing*, 36(4), 1282-1289.

Wilhelm, C., 1998. *Quantitative risk analysis for evaluation of avalanche protection projects*. Norwegian Geotechnical Institute Publication, Oslo, Norway, vol. 203, pp. 288–293.

Wilkins, I., 2004. *Avalanche Forecaster and UIAGM Mountain Guide*, Works Infrastructure, Te Anau, New Zealand, personal communication. (August, 2004).

Wood, B.L., 1960. *Fiord, Sheet 27 (1st Edition) Geological Map of New Zealand 1:250000* [map]. DSIR, Wellington, New Zealand.

World Heritage Convention, 1972. *Convention Concerning the Protection of the World Cultural and Natural Heritage*. Report presented at the General Conference of the United Nations Educational, Scientific and Cultural Organization meeting, 17 October to 21 November, Paris, France, 17pp.

Appendix I

Appendix I Estimated magnitudes and frequencies of avalanche occurrences on a controlled, open, Milford Road, based on 18 year database (1985-2002).

Path Name	from Hollyford turnoff (km)	(m)	S min (m)	S (m)	Powder snow (J1)		Light snow (J2)		Deep snow (J3)		Plunging/ Severe blast (J4)		Path Number
					1/F	L	1/F	L	1/F	L	1/F	L	
Turnoff	0.1	100	5000	5000									1
(Falls 1)	0.9	900	800	800									2
(Falls 2)	1.2	1200	300	300									3
(Falls 3)	1.3	1300	100	100									4
(Falls 4)	1.5	1500	200	200									5
Gates	2	2000	225	335			4.5	550					6
Camera 1	2.3	2300	25	135									7
Camera 2	2.4	2400	100	100									8
Camera 3	2.6	2600	200	200									9
(East Peak 1)	3.2	3200	600	600									10
East Peak 2	4	4000	800	800									11
(Christina 1)	4.6	4600	600	600									12
Windfall 1	4.6	4600	0	0									14
Christina 2	5	5000	375	385	18	50							13
Windfall 2	5	5000	-25	-15									15
Powerhouse 1	6	6000	1000	1000									16
Powerhouse 2	6.1	6100	100	100									17
Powerhouse 3	6.5	6500	400	400									18
(North Peak 1)	7.3	7300	800	800									20
Students Peak	7.6	7600	300	300									19
North Peak 2	7.9	7900	300	300									21
North Peak 3	8.1	8100	191	194.6			18	10					22
(Cirque Creek)	8.3	8300	191	194.6									23
Bakehouse	9.1	9100	725	755			18	150					24
Crosscut 1	9.3	9300	125	155									25
			300	300									

Appendix I   Continued

Path Name	from Hollyford turnoff (km)	(m)	S min (m)	S (m)	Powder snow (J1)		Light snow (J2)		Deep snow (J3)		Plunging/Severe blast (J4)		Path Number
					1/F	L	1/F	L	1/F	L	1/F	L	
Crosscut 2	9.6	9600	-75	-45									26
The Sinks	9.6	9600	425	455	18	25	18	150					28
Crosscut 3	10.1	10100	250	270									27
Raspberry Patch	10.4	10400	650	670			18	100					29
Forks	11.1	11100	750	770									30
Talbot	11.9	11900	450	510			9	100	18	100			31
Homer Tunnel	12.5	12500	-200	-120			9	200			18	100	32
Portal	12.5	12500	1500	1540			9	200					33
Homer Saddle	14.1	14100	150	170									34
Loop 1	14.3	14300	250	270			18	100					35
West Tunnel	14.6	14600	-600	-360									36
Moir	14.6	14600	-500	-260	4.5	50	18	1200					37
Gulliver 1	14.7	14700	400	400									38
Loop 2	15.1	15100	-25	105									39
Cleddau	15.4	15400	-325	-195	18	100	9	650					40
(Gulliver 2)	15.4	15400	200	200									41
Gulliver 3	15.6	15600	100	100									42
Gulliver 4	15.7	15700	-500	-180									43
Morels	16	16000	-500	-180			18	1600	18	10			44
Dip 1	16.3	16300	300	300									45
Dip 2	16.6	16600	700	700									46
Big Rock	17.3	17300	4600	4600									47
Schaerer	21.9	21900	600	600									48
Chasm	22.5	22500	6000	6000									49
Stables	28.5	28500	2500	2500									50
		31000											

Appendix II

Appendix II Estimated magnitudes and frequencies of avalanche occurrences on an uncontrolled, natural, Milford Road (Fitzharris and Owens, 1980)

Path Name	from Hollyford turnoff (km)	(m)	S min (m)	S (m)	Powder snow (j1)		Light snow (j2)		Deep snow (j3)		Plunging/ Severe blast (j4)		Path Number
					1/F	L	1/F	L	1/F	L	1/F	L	
Turnoff	0.1	100	5000	5010	15	20	50	20					1
(Falls 1)	0.9	900	775	785									2
(Falls 2)	1.2	1200	300	300									3
(Falls 3)	1.3	1300	100	100									4
(Falls 4)	1.5	1500	200	200									5
Gates	2	2000	250	350	2	300	2	200			30	500	6
Camera 1	2.3	2300	35	141	3	30							7
Camera 2	2.4	2400	70	82	3	30							8
Camera 3	2.6	2600	170	182	3	30							9
(East Peak 1)	3.2	3200	585	591									10
East Peak 2	4	4000	725	755	22	40	30	150					11
(Christina 1)	4.6	4600	525	555									12
Windfall 1	4.6	4600	-100	-60	5	200	10	200					14
Christina 2	5	5000	280	328	10	40	30	40					13
Windfall 2	5	5000	-120	-72	3	200	5	200	10	150			15
Powerhouse 1	6	6000	875	925	15	50			50	50			16
Powerhouse 2	6.1	6100	35	61	20	80			50	80			17
Powerhouse 3	6.5	6500	325	355			15	70	20	70			18
(North Peak 1)	7.3	7300	765	779									20
Students Peak	7.6	7600	-50	90	1	100	5	100			25	700	19
North Peak 2	7.9	7900	-80	72	1	50	3	60					21
North Peak 3	8.1	8100	140	164	1	50	3	60	25	60			22
(Cirque Creek)	8.3	8300	170	182									23
Bakehouse	9.1	9100	550	650	1	100	10	300	25	500			24
Crosscut 1	9.3	9300	-150	-10	50	200							25
			100	180									

Appendix II   Continued

Path Name	from Hollyford turnoff (km)	(m)	S min (m)	S (m)	Powder snow (f1)		Light snow (f2)		Deep snow (f3)		Plunging/Severe blast (f4)		Path Number
					1/F	L	1/F	L	1/F	L	1/F	L	
Crosscut 2	9.6	9600	-400	-240	50	200							26
The Sinks	9.6	9600	170	302	2	100	5	600	5	600			28
Crosscut 3	10.1	10100	-30	102	50	60							27
Raspberry Patch	10.4	10400	340	484	0.25	100	1	100	2	150	10	600	29
Forks	11.1	11100	685	731	1	50	15	120	50	50			30
Talbot	11.9	11900	395	477	5	110							31
Homer Tunnel	12.5	12500	-200	-120	0.2	200	0.5	200	1	200	3	300	32
Portal	12.5	12500	1530	1558	3	100	15	50					33
Homer Saddle	14.1	14100	80	128			10	20	10	40			34
Loop 1	14.3	14300	170	222	0.3	50	1	60	10	200	3	200	35
West Tunnel	14.6	14600	-50	-30	1	30	5	60	10	60			36
Moir	14.6	14600	60	76	1	20	5	40	10	40			37
Gulliver 1	14.7	14700	350	370	1	20	15	40					38
Loop 2	15.1	15100	240	264	1	30					10	60	39
Cleddau	15.4	15400	-60	-36	1	30			10	60	25	60	40
(Gulliver 2)	15.4	15400	145	167					10	60	25	60	41
Gulliver 3	15.6	15600	45	67	10	30	30	50					42
Gulliver 4	15.7	15700	230	258	10	30	30	60					43
Morels	16	16000	225	255	1	50	5	40	10	80	25	80	44
Dip 1	16.3	16300	245	267			30	70					45
Dip 2	16.6	16600	380	508			20	40					46
Big Rock	17.3	17300	4290	4414	1	50			30	600			47
Schaerer	21.9	21900	520	552	10	10	20	20					48
Chasm	22.5	22500	5820	5892			50	140					49
Stables	28.5	28500	2390	2434							15	220	50
		31000											